Cellular Mobile Radio Propagation Characteristics: Case Study of Globacom and Mobile Telecommunications Networks (MTN)

BY

SHITTU, Waliu Adisa

A Thesis submitted to the Electrical Engineering Department, Ahmadu Bello University, Zaria, in Partial Fulfillment of the Requirements for the award of the Degree of Master of Science (M.Sc.) in Electrical Engineering.

MARCH 2006

DECLARATION

I, SHITTU, Waliu Adisa, hereby declare that the work reported in this thesis is entirely my work and has not been submitted anywhere before for any form of degree whatsoever. All sources of knowledge used have been duly acknowledged by way of references.

……. **……..**
SHITTU, Waliu Adisa **Date**
MSC/ENG/36073/2002-2003

CERTIFICATION

This is to certify that this thesis titled: "**Cellular Mobile Radio Propagation Characteristics: Case Study of Globacom and Mobile Telecommunications Networks (MTN)**" meets the requirements governing the award of a Master of Science (M.Sc.) Degree in Electrical Engineering of Ahmadu Bello University and is approved for its contribution to knowledge and literary presentation.

……	**…….**
Prof. B.G. Bajoga	
Main Supervisor	**Date**
……	**…….**
Dr. D.D. Dajab	
Minor Supervisor	**Date**
……	**…….**
Prof. M.A. Gulma	
Head of Department	**Date**
……	**…….**
Prof. J. Umoh	
Dean, Postgraduate School	**Date**

DEDICATION

This thesis is dedicated to:

Medinah Adebukola Shittu,

Aishah Ar-Ramadhaan Shittu, and

Abdullahi Al-mubaarak Shittu

for their love, understanding and care during the course of this thesis.

ACKNOWLEDGEMENTS

I hereby acknowledge with gratitude the priceless and unquantifiable mercies, care and protection of the Almighty Allah (S.W.T) over me since the day I was born and through the period of this M.Sc. program. Without doubt, to Allah alone belongs the commencement and completion of a task. I, therefore thank Him for seeing me through this program albeit all odds.

I also acknowledge the efforts of my late father Mallam Shittu Alabi and my mother Madam Wuriwatu Arike Shittu for modeling me, through the special bounty of Allah from my tender age to what I am today. If any one thinks I am worth anything today, first and foremost, it is by the grace of Allah, then the efforts of my parents.

I am also greatly indebted to my supervisor, Professor B.G. Bajoga whose fatherly guidance, untiring efforts and wealth of experience has contributed in no small measures to the success of not only this thesis but also the entire M.Sc. programme. Your punctual attendance to lectures and prompt attention to reading this thesis is highly appreciated. May the Almighty Allah in His infinite mercies reciprocate your efforts with abundant blessings on you and your progeny, aamin.

My words of appreciation also go to Dr. P.F.U. Taylor for his contributions to this thesis and his painstaking demand that we always do things the right way. The contributions of the Head of the Department, Professor M.A. Gulma cannot go unmentioned. Your prompt treatment of my applications for various letters of introduction to other departments consulted in the course of this work is highly appreciated. Another lecturer whose contributions are deeply appreciated and worth mentioning is Dr. D.D. Dajab. May God Almighty be with you in all your endeavours.

My sincere gratitude also goes to Dr. and Mrs. M.O. Yusuf for their advice and support before the commencement of this programme and throughout the duration the programme lasted. Your contributions towards the successful completion of this thesis are also highly appreciated.

Certainly, this list of acknowledgement will be incomplete without mentioning the efforts of Mallams Abdullah Suleiman and Yunus Popoola who provided me with very useful information in the course of this work. Finally, the contributions of my very close friend, Mallam Abubakar Abdullahi Mas'ud and all other members of my class: Ma'aji, F.S., Abdu-Aguye, U.F., Bala, S., Ibrahim, D.A., Mohammed, Y.N., Mele, M.G. and Mu'azu, H.A. (Mrs.), are deeply appreciated. May Allah be with you all, aamin.

SHITTU, Waliu Adisa

ABUDEE, Zaria
March 2006

ABSTRACT

This thesis is on the study of Cellular Mobile Radio Signal Propagation Characteristics. Measurements of received signal powers were taken when the measuring device was moving outwards from some selected Base Stations along the Propagation paths, in outdoor environments (rural and urban). The variations of the signal in relation to distance away from the Base Stations were closely studied. The main propagation mechanisms of the radio signal such as direct propagation, reflection, and diffraction were considered. Effects of these mechanisms such as path loss, multipath propagation, and shadowing were investigated. In order to study these effects, two site-specific scenarios were chosen. The first scenario consisted of open/rural areas on some selected roads along which measurements were taken with a Cellular Mobile Network Analyser being moved away from the base stations. The second scenario comprised some selected buildings on Ahmadu Bello University (ABU) main campus. Here, multipath propagation and shadowing effects of the buildings were considered in order to study the characteristics of the received signal power levels. Using parameters of the base stations studied in this investigation in the Free-Space and Okumura/Hata models, values of received signal power and path loss obtained were found to fall short significantly from averaged values obtained from measurements. For scenario 1, the mean differences were +54.73 dBm and -42.81 dB for the received signal power and path loss respectively and the corresponding value for received signal power was +12.60 dBm, for scenario 2. These mean differences are too significant to be neglected. Thus, they constituted correction factors in the new proposed models which closely approximate measurement values. Finally, these new proposed models were coded using C programming language.

TABLE OF CONTENTS

Title

Title Page i

Declaration ii

Certification iii

Dedication iv

Acknowledgement v

Abstract vii

Table of Contents viii

List of Figures xii

List of Tables xiv

List of Abbreviations/Symbols xvii

CHAPTER ONE - GENERAL INTRODUCTION 1

1.1 Introduction 1

1.2 Problem Definition 3

1.3 Thesis Objectives 3

1.4 Motivation 3

1.5 Scope of Work 4

1.6 Frequency Spectrum and Their Typical Uses 4

1.7 Frequency Bands of the DCMR Systems 4

1.8 Literature Review 6

1.9 Thesis Outline 7

CHAPTER TWO – THEORETICAL BACKGROUND **8**

2.0 Introduction 8

2.1 Description of the DCMR System 8

2.1.1 Mobile Station 9

2.1.2 Base Station Subsystem 9

2.1.3 Network Subsystem 10

2.2 Call Routing 12

2.3 Choice of VHF and UHF Bands for DCMR Systems 14

2.4 Radio Link Properties 14

2.4.1 Free Space Propagation 15

2.4.2 Reflection 16

2.4.3 Diffraction 17

2.5 Radio and Propagation Channels 18

2.6 Signal Impairments 19

2.6.1 Path loss 19

2.6.2 Shadowing 19

2.6.3 Multipath Propagation 20

2.7 Propagation Models 20

2.7.1 Free-Space Path loss Model 21

2.7.2 Empirical Models 23

2.7.2.1 The Hata-Okumura Model 24

2.7.2.2 Walfisch-Ikegami Model 25

2.7.3 Deterministic Models 26

2.8 Uses of Propagation Models 28

CHAPTER THREE – METHODOLOGY 29

3.0 Introduction 29

3.1 Description of the Measurement Environments 29

3.1.1 First Scenario 29

3.1.2 Second Scenario 31

3.2 Experimental Set-up 33

3.2.1 First Scenario 33

3.2.2 Second Scenario 34

3.3 Prediction of Received Signal Power using Modified Two-Ray Model 35

3.4 Data bases used in the Second Scenario 37

3.4 Visibility Relations 37

3.5 Determination of the Ray Parameters 39

CHAPTER FOUR – ANALYSIS AND RESULTS 42

4.0 Introduction 42

4.1 Results obtained using the Free-Space Model 42

4.2 Results obtained using the Hata Model 43

4.3 Results obtained using the Walfisch/Ikegami Model 45

4.4 Analysis and Comparison of Measurement and Prediction Results 45

4.4.1 Scenario 1 45

4.4.2 Scenario 2 58

4.5 Differences between Measurement and Prediction Results for Scenario 1 and 2 61

4.6 Proposed Modification of Free-Space, Hata and the Modified Two-Ray Model 61

4.7 Discussion and Interpretation of Results 67

CHAPTER FIVE – CONCLUSIONS AND RECOMMENDATIONS 71

5.1 Introduction 71

5.2 Summary of Results 71

5.3 Significance of Results and Applications 72

5.4 Limitations, Problems Encountered and Solutions Proffered 73

5.5 Conclusions 74

5.6 Recommendations for Further Work 75

REFERENCES 76

APPENDIX A 78

APPENDIX B 85

APPENDIX C 86

APPENDIX D 93

LIST OF FIGURES

Figure **Page**

2-1: General Architecture of a Global System for Mobile Communication (GSM) Network 12

2-2: Call routing for a mobile terminating call 14

2-3: Incident and diffracted ray on a single wedge 17

2-4: Various channels in a communication system 18

2.5: A simple model for Path Loss in Free Space 21

2-6: Propagation mechanisms in urban environment in Non-line-of-Sight (NLOS) 27

2-7: Propagation mechanisms in urban environment in Line-of-Sight (LOS) 28

3-1: A Portion of Zaria Map showing Areas included in the First Scenario 30

3-2: A Portion of ABU Cadastral Map showing Areas included in the Second Scenario 32

3.3: Measurement Area in Scenario 2 34

3.4: Tree structure of the visibility relations 38

4-1a: Received Signal Power from Predictions and Measurements on Kaduna Road (MTN Network) 48

4-1b: Path loss on Kaduna Road (MTN Network) 48

4-2a: Received Signal Power from Predictions and Measurements on Kano Road (MTN Network) 49

4-2b: Path loss on Kano Road (MTN Network) 49

4-3a (i): Received Signal Power from Predictions and Measurements

on Samaru Road (MTN Network) Eastward of Base Station (BS) 50

4-3a (ii): Path loss on Samaru Road (MTN Network) Eastward of BS 50

4-3b (i): Received Signal Power from Predictions and Measurements
on Samaru Road (MTN Network) Southward of BS 51

4-3b (ii): Path loss on Samaru Road (MTN Network) Southward of BS 51

4-4a: Received Signal Power from Predictions and Measurements
on Kaduna Road (GLO Network) 54

4-4b: Path loss on Kaduna Road (GLO Network) 54

4-5a: Received Signal Power from Predictions and Measurements on
Kano Road (GLO Network) 55

4-5b: Path loss on Kano Road (GLO Network) 55

4-6a (i): Received Signal Power from Predictions and Measurements on
Samaru Road (GLO Network) Eastward of BS 56

4-6a (ii): Path loss on Samaru Road (GLO Network) Eastward of BS 56

4-6b (i): Received Signal Power from Predictions and Measurements on
Samaru Road (GLO Network) Southward of BS 57

4-6b (ii): Path loss on Samaru Road (GLO Network) Southward of BS 57

4-7: Received Signal Power from Prediction and Measurement within 60
the Engineering Complex 57

4-8: New Proposed Model of Received Signal Power for Scenario 1 66

4-9: New Proposed Model of Path loss for Scenario 1 66

4-10: New Proposed Model of Received Signal Power for Scenario 2 67

LIST OF TABLES

Table	Page
1-1: Frequency spectrum and their Typical Uses	78
1-2: Allocated Frequencies to the Cellular Operators in Nigeria	5
3-1: Ray parameters for paths 1 and paths 2	40
4-1: Averaged Received Signal Power and Computed Path loss for Kaduna Road [MTN Network]	46
4-2: Averaged Received Signal Power and Computed Path loss for Kano Road [MTN Network]	46
4-3a: Averaged Received Signal Power and Computed Path loss for Samaru Road [MTN Network] – Eastward of BS	47
4 -3b: Averaged Received Signal Power and Computed Path loss for Samaru Road [MTN Network] – Southward of BS	47
4-4: Averaged Received Signal Power and Computed Path loss for Kaduna Road [GLO Network]	52
4-5: Averaged Received Signal Power and Computed Path loss for Kano Road [GLO Network]	52
4-6a: Averaged Received Signal Power and Computed Path loss for Samaru Road [GLO Network] - Eastward of BS	53
4-6b: Averaged Received Signal Power and Computed Path loss for Samaru Road [GLO Network] – Southward of BS	53
4-7: Averaged received signal power along the trajectory within the Engineering Complex (measurements)	58
4-8: Received signal power along ray paths 1 (prediction)	59
4-9: Received signal power along ray paths 2 (prediction)	59
4-10: Sum of Received signal powers along the two ray paths (prediction)	60

4-11: P_R and L_P for Scenario 1 64

4-12: P_R s along the Trajectory in Scenario 2 64

4-13: Input Parameters to the C Program Code for Scenario 2 65

3.2.1.1: Received Signal Power taken on day 1 on MTN BS 79

3.2.1.2: Received Signal Power taken on day 2 on MTN BS 80

3.2.1.3: Received Signal Power taken on day 3 on MTN BS 81

3.2.1.4: Received Signal Power taken on day 1 on GLO BS 82

3.2.1.5: Received Signal Power taken on day 2 on GLO BS 83

3.2.1.6: Received Signal Power taken on day 3 on GLO BS 84

3.2.2.1: Readings taken on day 1 within the Engineering Complex 85

3.2.2.2: Readings taken on day 2 within the Engineering Complex 85

3.2.2.3: Readings taken on day 3 within the Engineering Complex 85

4.1.1(a) Computed Signal Power and Path loss for Free-Space Model (MTN BS) 86

4.1.1 (b): Computed Signal Power and Path loss for Free-Space Model (Glo BS) 87

4.2.1 (a): Computed Signal Power and Path loss for Hata Model (Open/Rural) – MTN BS 88

4.2.1 (b): Computed Signal Power and Path loss for Hata Model (Open/Rural) – Glo BS, Kaduna/Kano Road 89

4.2.1 (c): Computed Signal Power and Path loss for Hata Model (Open/Rural) – Glo BS, Samaru Road 90

4.3.1 (a): Computed Signal Power and Path loss for Walfisch/Ikegami Model (Open/Rural) (MTN BS) 91

4.3.1 (b): Computed Signal Power and Path loss for Walfisch/Ikegami Model (Open/Rural) (Glo BS) 92

4.5.1: Comparison of Measurements and Prediction using Free-Space Model – Kaduna Road (MTN Network) 93

4.5.2: Comparison of Measurements and Prediction using Hata Model – Kaduna Road (MTN Network) 93

4.5.3: Comparison of Measurements and Prediction using Free-Space Model – Kano Road (MTN Network) 93

4.5.4: Comparison of Measurements and Prediction using Hata Model - Kano Road (MTN Network) 94

4.5.5: Comparison of Measurements and Prediction using Free-Space Model – Samaru Road– Eastward of BS (MTN Network) 94

4.5.6: Comparison of Measurements and Prediction using Hata Model – Samaru Road– Eastward of BS (MTN Network) 94

4.5.7: Comparison of Measurements and Prediction using Free-Space Model – Samaru Road– Southward of BS (MTN Network) 95

4.5.8: Comparison of Measurements and Prediction using Hata Model – Samaru Road– Southward of BS (MTN Network) 95

4.5.9: Comparison of Measurements and Prediction using Free-Space Model – Kaduna Road (GLO Network) 95

4.5.10: Comparison of Measurements and Prediction using Hata Model – Kaduna Road (GLO Network) 96

4.5.11: Comparison of Measurements and Prediction using Free-Space Model – Kano Road (GLO Network) 96

4.5.12: Comparison of Measurements and Prediction using Hata Model – Kano Road (GLO Network) 96

4.5.13: Comparison of Measurements and Prediction using Free-Space Model – Samaru Road – Eastward of BS (GLO Network) 97

4.5.14: Comparison of Measurements and Prediction using Hata Model – Samaru Road – Eastward of BS (GLO Network) 97

4.5.15: Comparison of Measurements and Prediction using Free-Space Model – Samaru Road – Southward of BS (GLO Network) 97

4.5.16: Comparison of Measurements and Prediction using Hata Model – Samaru Road – Southward of BS (GLO Network) 98

4.5.17: Comparison of Measurements and Prediction using Modified Two-Ray Model within the Engineering Complex 98

LIST OF ABBREVIATIONS/SYMBOLS

ABU: Ahmadu Bello University

AuC: Authentication Centre

BS: Base Station

BSS: Base Station Subsystem

BSC: Base Station Controller

BTS: Base Transceiver Station

CSPDN: Circuit-Switched Public Data Network

DCMR: Digital Cellular Mobile Radio

DCS: Digital Cellular System

EIR: Equipment Identity Register

EIRP: Effective Isotropic Radiated Power

EM: Electromagnetic

Glo: Globacom

Globacom: Global Communications

GMSC: Gateway Mobile Services Switching Centre

GSM: Global System of Mobile Communications

HLR: Home Location Register

IMEI: International Mobile Equipment Identity

IMSI: International Mobile Subscriber Identity

ISDN: Integrated Services Digital Network

KIL: Kashim Ibrahim Library

LoS: Line-of-Sight

LTV: Linear Time Invariant

ME: Mobile Equipment

MS: Mobile Station

MSC: Mobile Services Switching Centre

MSRN: Mobile Station Roaming Number

MTN: Mobile Telecommunications Network

NCC: National Communication Commission

NLoS: Non-Line-of-Sight

PLMN: Public Land Mobile Network

PSPDN: Packet-Switched Public Data Network

PSTN: Public Switched Telephone Network

UHF: Ultra High Frequency

VHF: Very High Frequency

η: Wave impedance

S: Power density

s: Distance measured from the reference point

k: Wave number

ρ: Principal radius of curvature of the phase front

j: complex operator

Θ: incident angle

ε: relative dielectric constant of the material of the reflecting plane

ε_r: dielectric constant of the reflecting plane

ε_0: permittivity of vacuum

σ: conductivity

ω: angular frequency

R, Γ: reflection coefficient

E(0): electric field at the reference point

E(S): electromagnetic field with respect to the reference point

E_r: received free-space field

$E_{i:}$ incident electric field

f_c: carrier frequency

c: speed of propagation of electromagnetic waves

λ: wavelength

d: distance

P_R: received power

P_T: transmitter power

G_T: transmitter gain

G_R: receiver gain

H_t: transmitter antenna height

A_R: aperture area of receiver antenna

Lp: path loss

L_{50}: mean path loss

h_b: base station antenna height

h_m: mobile station antenna height

a(hm): correction factor for mobile antenna height

L_f: Free-space loss

L_{rts}: rooftop-to-street diffraction

L_{ms}: multi-screen loss

RX: receiver

TX: transmitter

τ: time interval

N: total number of time intervals

$\overline{RxPOW}$: averaged measured received power

F_C: correction factor

T-R: transmitter-receiver

CHAPTER ONE

GENERAL INTRODUCTION

1.1 Introduction

In the past few decades, cellular radio communication systems have been witnessing extensive development, and cellular phones that were initially means of communications in defense quarters and services of dispatch nature are now being used for commercial purposes and are fast becoming more of status symbols. Thus, the demands that a radio system must fulfill are greater by the day. The wind of development in the cellular communications systems blew across Nigeria about half a decade ago. Since then the sector has been witnessing phenomenal changes and statements like “customers’ satisfaction”, “customers’ parliament”, and “unsatisfactory performance of cellular operators”, among others, are rife amidst subscribers of the cellular systems.

Knowing quite well that the satisfactory performance of the radio system depends, among others, on good radio link design, which is also affected by the propagation environments, interest is developed in studying the propagation characteristics of the cellular systems’ signal in some selected locations in Zaria.

Broadly speaking, properties of the mobile radio channel can be categorized into two; namely: narrowband and wideband properties. While the former comprises mainly of the received power of the propagated signals and the path loss, the latter concerns delay spread, angles of arrival and impulse response. Since the second generation of the Cellular Mobile Radio System otherwise known as GSM can adequately be described by the narrowband properties, and this system is what is currently being deployed in the country, the focus in this work is on narrowband properties. Investigation of wideband properties which involve

future systems (3rd and 4th generations) is beyond the scope of this thesis. Although a variety of models based on experimental and empirical works have been developed to predict radio propagation losses, unfortunately, none of them are universally applicable [1].

For the purpose of this work, two different scenarios were selected for the investigation. The first scenario comprised open areas where Base Station transmitters are placed at the center of the cells to provide Cellular services along the selected roads. These roads include Kaduna road, Kano road, and Samaru road. Here, the surroundings of the BSs are mainly low bushes with scattered low buildings that are few and far apart. The second scenario comprised a selected area on the Ahmadu Bello University main campus, Zaria. Here, the focus was to investigate the shadowing and multipath effects of some tall buildings on the signal propagation in this selected area of the campus.

Measurements of received signal powers were taken, along these roads, with a test receiver moving outwards from the serving Base Station transmitters.

Variations of these signals in relation to distance away from the Base Stations, as well as other factors, were closely studied and analyzed. Care was taken not to enter into the field of influence of a next base station. These measurements were carried out on two of the existing cellular mobile network systems in Nigeria – Mobile Telecommunication Network (MTN) and Global Communications Limited (Globacom). The reason for limiting the measurements to two out of the four existing networks was simply because only these two networks had reliable and stable services in the selected scenarios during the period the measurements were being taken.

Also, in the second scenario, measurements of received signal powers were taken within the Faculty of Engineering Complex where the Mechanical Engineering block constitutes a

blockage to the direct line-of-sight (LOS) from the reference MTN base station antennas situated close to the North gate of the University.

The measurements data from both scenarios were then analysed and results obtained were compared with some existing propagation models. The differences from this comparison constituted correction factors to these existing models. Consequently, prediction equations (new models) that are representative of the scenarios studied are proposed.

1.2 Problem Definition

The performance of wireless communication systems depends in a fundamental way on the mobile radio channel. As a consequence, predicting the propagation characteristics between two antennas (Base station antenna and Mobile Station antenna) is one of the most important tasks for the design and installation of wireless communication systems [2].

The problem of predicting the narrowband properties, namely; the received signal powers, P_R s, and the propagation path losses, L_P s, from an understanding of the signal's propagation characteristics, is the basis of this research work.

1.3 Thesis Objectives

The objectives of the thesis are two-fold: first to determine the present performance levels of the mobile systems from an understanding of the mobile radio propagation characteristics, and, secondly, to predict the narrowband properties of the mobile radio signals.

1.4 Motivation

In any profit-oriented outfit there is a popular belief that customers are always right and, as such, they are supposed to be given values for their hard-earned money. However recent events in the country have shown the contrary. There have been many complaints by users of GSM phones with regard to unsatisfactory performance of the Digital Cellular Mobile Radio

(DCMR) Systems. These complaints range from dropped calls, signal fluctuations, to complete signal outages. Consequently, the desire to study the propagation characteristics of the cellular signals with a view to determine their relationship with the performance levels of the DCMR systems motivated this research work.

1.5 Scope of Work

It is quite understood that the DCMR system comprises many subsystems and that optimum operation of each of these subsystems contributes to make the whole systems function satisfactorily. This work only concentrates on the ***air interface*** of the Base Station subsystem that connects subscribers to the GSM 900/1800 networks.

1.6 Frequency Spectrum and their typical Uses

Table 1-1 in Appendix A shows the frequency spectrum of the electromagnetic (e.m.) waves and their typical uses [3].

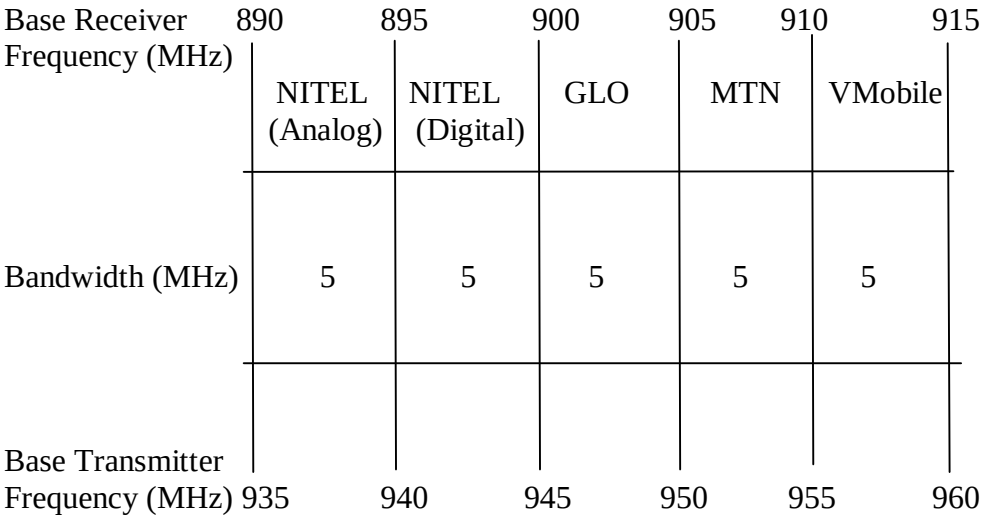
1.7 Frequency Bands of the DCMR System

The DCMR systems, otherwise known as the Global System of Mobile Communications (GSM) and the Digital Cellular System (DCS) systems are frequency- and time-division systems. Each physical channel is characterized by a carrier frequency and a time slot number. GSM frequencies include two bands at 900 MHz and 1800 MHz commonly referred to as GSM-900 and DCS-1800 systems. For the primary band in the GSM-900 system, 124 carriers have been defined and assigned in two sub-bands of 25 MHz each in the 890-915 MHz and 935-960 MHz ranges, with channel widths of 200 KHz. Each carrier is divided into frames of 8 time slots (for full rate), with a frame duration of about 4.6 ms. For DCS -1800 there are two sub-bands of 75 MHz in the 1710-1785 and 1805-1880 MHz ranges [4].

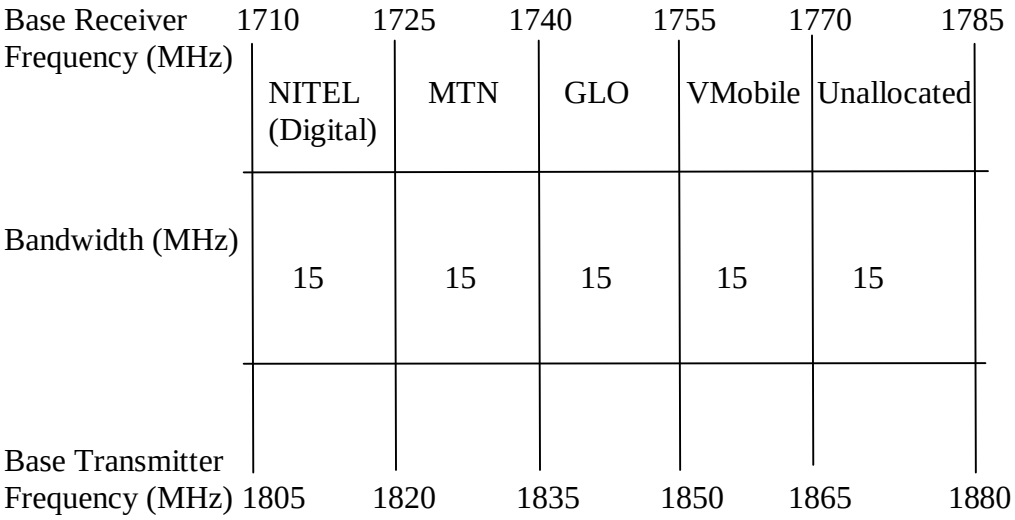
DCMR systems in the country operate in these two frequency bands and table 1-2 shows the frequency sub-bands allocated to the operators by the National Communications Commission (NCC) [5].

Table 1-2: Allocated Frequencies to the Cellular Operators in Nigeria

(a) 900MHz Band



(b) 1800 MHz Band



1.8 Literature Review

Extensive studies, from empirical models to analytical/numerical formulations, have been carried out on predicting the received radio signal strengths in wireless communication systems. Among others, a popular one is introduced by Okumura [6], who has published an empirical technique for predicting the field strength and service area for a given terrain of the land mobile radio system (over the frequency range of 150-2000 MHz, in ranges from 1 km to 100 km, and for base station effective antenna heights between 30 m to 1000 m). Okumura's empirical technique depends on the extensive series of measurements in and around Tokyo, Japan.

Based on Okumura's results, Hata [7] has developed an empirical formula, where propagation loss is easily computable. In the same content, Bullington [8] has introduced a series of nomograms derived from theoretical expressions for radio wave propagation loss calculations. Walfisch and Bertoni [9] have published a theoretical model that considers the effects of buildings on radio propagation, where buildings are assumed as absorbing and diffracting cylinders lying on the earth, and propagation process is reduced to multiple forward diffraction over a series of screens (or knife edges).

Many obstructions in urban environments are not adequately described using the knife edge concept. The tops of buildings can hardly be conceptualized as a knife-edge and the physical characteristics of signal propagating over rooftops are very different from signal propagating over knife-edges (Zhang, et al, 1999).

Furthermore, many urban environments are microcellular. In microcellular environments, the distance covered is not always significantly larger than the height of the obstacles, a requirement in some knife-edge approximation techniques (Deygout 1966). Signal propagation in these environments is often more accurately characterized using the concept of ray tracing. Ray tracing models are considered superior to knife-edge models because they use a more detailed description of the environment.

Ray-tracing-based propagation prediction models are becoming widely accepted as suitable tools for the planning of mobile radio networks in urban environments. Two-dimensional (2D) ray-tracing models have been applied successfully for field prediction when transmitting and receiving heights are quite below the roof top of surrounding buildings. Hence, the modified Two-Ray model used in the prediction of the received signal power in the second scenario in this study is a basic ray tracing approach which assumed only lateral propagation. The transmitting and receiving antennas are assumed to be below the roof top and, therefore, over- roof- top propagations are neglected.

1.9 Thesis Outline

This thesis report begins with a general introduction of the cellular system in chapter one. This chapter also contains the basis for this research work. In chapter two, theoretical backgrounds related to the Digital Cellular System are discussed, and, in chapter three, the methodology used in this work is presented. Chapter Four contains the results obtained and the analysis. Interpretation of the results is also discussed in this chapter. Finally, chapter five rounds off with limitations, problems encountered and the solutions proffered. It also contains conclusions and recommendations for further work.

CHAPTER TWO

THEORETICAL BACKGROUNDS

2.0 Introduction

This chapter provides relevant insights into some theoretical backgrounds in connection with mobile radio propagation studies. It begins by giving a description of the digital cellular system as well as call routing procedure and the choice of VHF/UHF bands for this system. Other issues such as radio link properties, radio and propagation channels, signal impairments, propagation models and their uses are also discussed in this chapter.

2.1 Description of the DCMR System

The DCMR systems are systems that seek to make an efficient use of available channels by using low-power transmitters to allow frequency re-use at much smaller distances. Maximising the number of times each channel may be used in a given geographical area is the key to an efficient cellular system design.

Cellular systems are designed to operate with groups of low-power radios spread out over the geographical service area. Each group of radios serve Mobile Stations (MSs) presently located near them. The area served by each group of radios is called a **cell**. Each cell has an appropriate number of low-power radios for communications within itself. The power transmitted is chosen to be large enough to communicate with the MSs located near the edges of its cell. The radius of each cell may be chosen to be perhaps 28 Km in a start-up system with relatively few subscribers, down to less than 2 Km for a mature system requiring considerable frequency re-use [4]. The GSM network is divided into three main systems: the Mobile Station, the Base Station Subsystem (BSS), and the Network Subsystems [10].

2.1.1 Mobile Station

The mobile station (MS) consists of the mobile equipment (the terminal) and a smart card called the Subscriber Identity Module (SIM). The SIM provides personal mobility, so that the user can have access to subscribed services irrespective of a specific terminal. By inserting the SIM card into another GSM terminal, the user is able to receive calls at that terminal, make calls from that terminal, and receive other subscribed services. The mobile equipment is uniquely identified by the International Mobile Equipment Identity (IMEI). The SIM card contains the International Mobile Subscriber Identity (IMSI) used to identify the subscriber to the system, a secret key for authentication, and other information. The IMEI and the IMSI are independent, thereby allowing personal mobility. The SIM card may be protected against unauthorized use by a password or personal identity number.

2.1.2 Base Station Subsystem (BSS)

The Base Station Subsystem is composed of two parts, the Base Transceiver Station (BTS) and the Base Station Controller (BSC). These communicate across the standardized *Abis* interface, allowing (as in the rest of the system) operation between components made by different suppliers.

The BTS houses the radio transceivers that define a cell and handles the radio-link protocols with the Mobile Station. In a large urban area, there will potentially be a large number of BTSs deployed, thus the requirements for a BTS are ruggedness, reliability, portability, and minimum cost.

The BSC manages the radio resources for one or more BTSs. It handles radio-channel setup, frequency hopping, and handovers. The BSC is the connection between the mobile station and the Mobile services Switching Center (MSC).

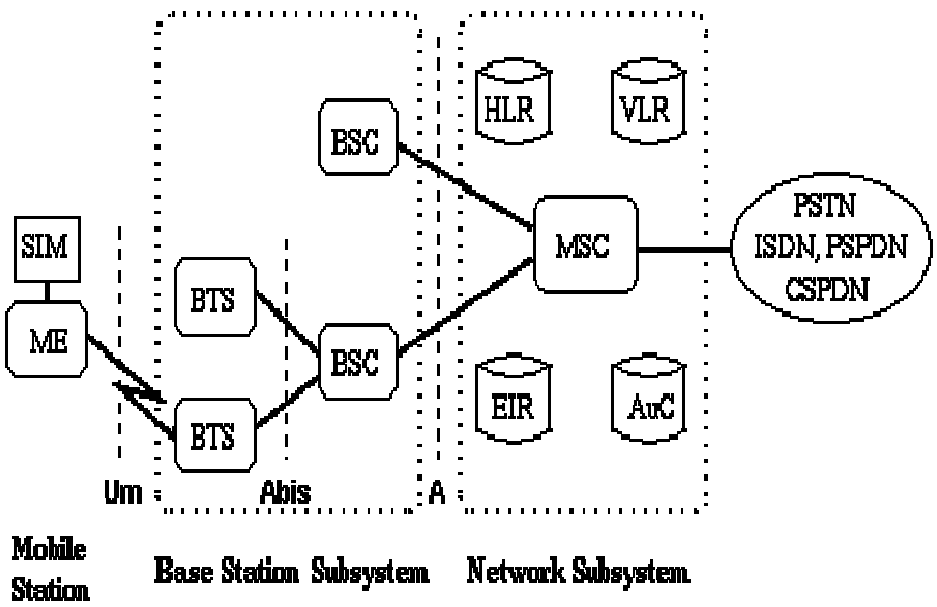
2.1.3 Network Subsystem

The central component of the Network Subsystem is the Mobile services Switching Center (MSC). It acts like a normal switching node of the Public Switched Telephone Network (PSTN) or the Integrated Services Digital Network (ISDN), and additionally provides all the functionalities needed to handle a mobile subscriber, such as registration, authentication, location updating, handovers, and call routing to a roaming subscriber. These services are provided in conjunction with several functional entities, which together form the Network Subsystem. The MSC provides the connection to the fixed networks such as the (PSTN) or the (ISDN), the Packet Switched Public Data Network (PSPDN) or the Circuit Switched Public Data Network (CSPDN). Signalling between functional entities in the Network Subsystem uses Signalling System Number 7 (SS7), used for trunk signalling in ISDN and widely used in current public networks.

The Home Location Register (HLR) and Visitor Location Register (VLR), together with the MSC, provide the call-routing and roaming capabilities of GSM. The HLR contains all the administrative information of each subscriber registered in the corresponding GSM network, along with the current location of the mobile. The location of the mobile is typically in the form of the signalling address of the VLR associated with the mobile station. The actual routing procedure is described in the next section. There is logically one HLR per GSM network, although it may be implemented as a distributed database.

The Visitor Location Register (VLR) contains selected administrative information from the HLR, necessary for call control and provision of the subscribed services, for each mobile currently located in the geographical area controlled by the VLR. Although each functional entity can be implemented as an independent unit, all manufacturers of switching equipment to date implement the VLR together with the MSC, so that the geographical area controlled by the MSC corresponds to that controlled by the VLR, thus simplifying the signalling required. It should be noted that the MSC contains no information about particular mobile stations --- this information is stored in the location registers.

The other two registers are used for authentication and security purposes. The Equipment Identity Register (EIR) is a database that contains a list of all valid mobile equipment on the network, where each mobile station is identified by its International Mobile Equipment Identity (IMEI). An IMEI is marked as invalid if it has been reported stolen or is not type approved. The Authentication Center (AuC) is a protected database that stores a copy of the secret key stored in each subscriber's SIM card, which is used for authentication and encryption over the radio channel. Figure 2-1 shows the general architecture of a GSM network.



SIM Subscriber Identity Module BSC Base Station Controller MSC Mobile services Switching Center
ME Mobile Equipment HLR Home Location Register EIR Equipment Identity Register
BTS Base Transceiver Station VLR Visitor Location Register AuC Authentication Center

Figure 2-1: General Architecture of a GSM network

2.2 Call routing

Unlike routing in the fixed network, where a terminal is semi-permanently wired to a central office, a GSM user can roam nationally and even internationally. The directory number dialed to reach a mobile subscriber is called the Mobile Subscriber ISDN (MSISDN), which is defined by the E.164 numbering plan. This number includes a country code and a National Destination Code which identifies the subscriber's operator. The first few digits of the remaining subscriber number may identify the subscriber's HLR within the home Public Land Mobile Network (PLMN).

An incoming mobile terminating call is directed to the Gateway MSC (GMSC) function. The GMSC is basically a switch which is able to interrogate the subscriber's HLR to obtain routing information, and thus contains a table linking MSISDNs to their corresponding HLR. A simplification is to have a GMSC handle one specific PLMN. It should be noted that the GMSC function is distinct from the MSC function, but is usually implemented in an MSC.

The routing information that is returned to the GMSC is the Mobile Station Roaming Number (MSRN), which is also defined by the E.164 numbering plan. MSRNs are related to the geographical numbering plan, and not assigned to subscribers, nor are they visible to subscribers.

The most general routing procedure begins with the GMSC querying the called subscriber's HLR for an MSRN. The HLR typically stores only the SS7 address of the subscriber's current VLR, and does not have the MSRN. The HLR must therefore query the subscriber's current VLR, which will temporarily allocate an MSRN from its pool for the call. This MSRN is returned to the HLR and back to the GMSC, which can then route the call to the new MSC. At the new MSC, the IMSI corresponding to the MSRN is looked up, and the mobile is paged in its current location area. This is depicted in figure 2-2.

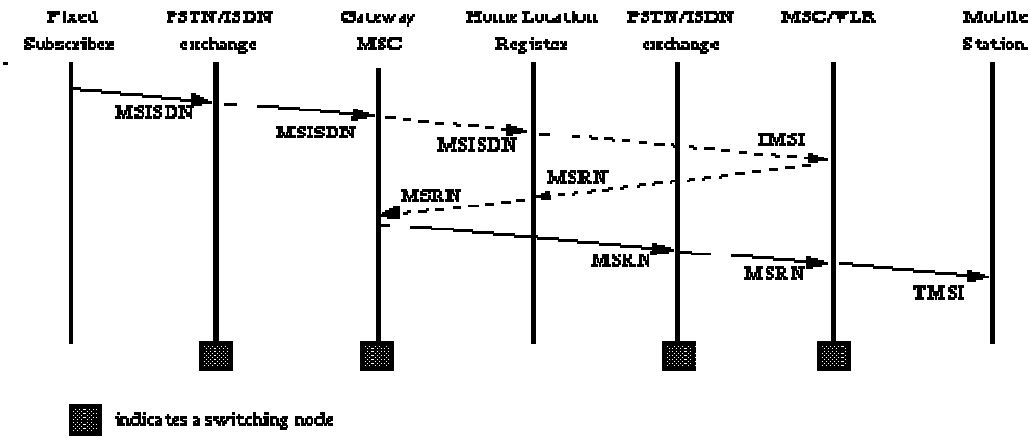


Figure 2-2: Call routing for a mobile terminating call

2.3 Choice of VHF and UHF Bands for DCMR System

The VHF and UHF bands represent an optimum choice for mobile radio because of their relatively short-range propagation characteristics and because radio equipment designed for these bands is reasonably compact and inexpensive. Furthermore, because of the attractive propagation characteristics of VHF and UHF, it is possible to allocate the same channel to different users in areas separated by distances of 50-100 Km with a substantial degree of confidence that, except under abnormal propagation conditions, they will not interfere with each other [11].

2.4 Radio Link Properties

The properties of the radio link are determined by the mechanisms affecting the propagation of the radio waves and these depend on the frequencies used for transmission [12].

The simplest form of radio propagation is direct propagation from a transmitting antenna to a receiving antenna through space. In practice, however, perfect direct propagation is not obtained because of the presence of the earth and imperfections of its atmosphere. Thus,

propagation of waves between a transmitting and receiving antenna can take place over a number of different paths. This situation is referred to as *multipath propagation*. The propagation path changes with the movement of the mobile unit, the base unit and/or the movement of the surroundings and environment [13].

In the case of mobile telecommunications where the used frequency is around 2 GHz and both the transmitter and receiver are close to the ground, the effective propagation mechanisms are typically: free space propagation, reflections, diffractions and wall penetration [14]. Wall penetration is mostly prominent in indoor situations and, for this reasonit is neglected in this investigation. Diffraction phenomenon is also neglected for the purpose of simplicity.

2.4.1 Free Space Propagation (in Line-of-Sight, LOS)

The amplitude of the received free space field can be expressed using [15]:

$$|E_r| = \sqrt{2\eta S} = \sqrt{\frac{P_0 G(\theta,\varphi)\eta}{4\pi d^2}} \qquad (2\text{-}1)$$

where P_0 is the transmitted power, $G(\theta,\varphi)$ is the antenna gain at the angle of the spherical coordinate (θ,φ), η is the wave impedance ($\eta \approx 377\Omega$), S is the power density and d is the distance between transmitter and the observation point.

The electromagnetic field in the case of spherical waves propagates in the free space along its ray as:

$$E(s) = E(0)\frac{\rho}{(s+\rho)}e^{-jks} \qquad (2\text{-}2)$$

where ρ is the principal radii of curvature of the phase front of the field, k is the wave number and s is the distance measured from the reference point. *E(0)* is the strength of the electric field at that reference point calculated by using equation (2-1).

It should be noted that in urban propagation environments different obstacles such as houses, streets, trees, vehicles and pedestrians contribute to the propagating wave. Thus, the free space formula is only valid for certain situations in these environments. The direct field component is present if the transmitter is visible at the receiver point.

However, if the Fresnel zone of the connection path is not clear of obstacles the free space formulas are not valid. In these situations the reflections and diffractions have to be included when calculating the total field at the receiver [15].

2.4.2 Reflection

This occurs when the radio wave impinges the obstacle whose dimensions are considerably larger than the wavelength of the incident wave. A reflected wave can either decrease or increase the signal level at the reception point. In cases where many reflected waves exist, the received signal level tends to be very unstable. This phenomenon is commonly referred to as multipath fading [14]. The reflected wave can be represented by [15]:

$$E_r = E_i \bullet R \tag{2-3}$$

where E_i and E_r are the incident and reflected field strength (vectors) respectively, at the reflection point, R is the reflection coefficient. Assuming specular reflection, the Fresnel reflection coefficient attributed to wall-reflected rays can be computed for vertical polarization as usual for mobile communications using the expression:

$$R(\varepsilon, \theta) = \frac{\sin(\theta) - \sqrt{\varepsilon_r - \cos^2(\theta)}}{\sin(\theta) + \sqrt{\varepsilon_r - \cos^2(\theta)}} \tag{2-4}$$

where ε_r is the complex dielectric constant of the reflecting plane and θ is the angle of incidence ε_r is given by:

$$\varepsilon_r = \varepsilon - j \frac{\sigma}{\omega \varepsilon_0} \qquad (2\text{-}5)$$

where ε is the relative dielectric constant of the material, σ is the conductivity expressed in S/m, ω is $2\pi f$ where f is the carrier frequency and ε_0 is the permittivity of vacuum (8.85 x 10^{-12} F/m).

2.4.3 Diffraction:

This occurs when the direct line of sight (LoS) propagation between the transmitter and the receiver is obstructed by an opaque obstacle whose dimensions are considerably larger than the signal wavelength. The diffraction mechanism allows the reception of radio signals when the LoS conditions are not satisfied, i.e. in Non-Line of Sight (NLoS) case, whether in urban or rural environments [15]. This is illustrated in figure 2-3.

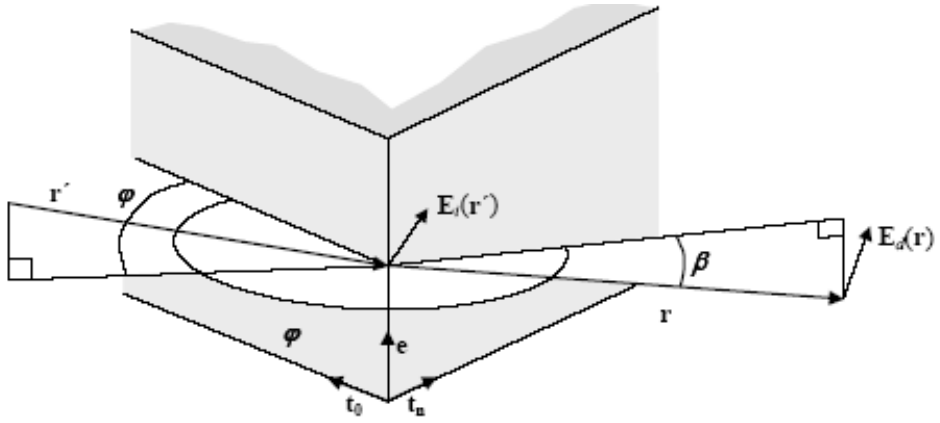


Figure 2-3: Incident and diffracted ray on a single wedge

Of all the foregoing propagation mechanisms only direct and wall- reflected rays are considered in the second scenario of this study.

2.5 Radio and Propagation Channel

Propagation channel is the physical medium between antennas where electromagnetic waves are propagated. Obstacles influencing the propagation of EM waves, whether they are static (man-made and natural obstacles such as buildings, hills and mountains) or time-varying (moving vehicles, and atmospheric variation) are considered to be part of the propagation channel. The propagation channel is assumed to be bi-directional and linear. Furthermore, for mobile and portable applications, it is assumed that the channel varies with time, making it a linear time-variant (LTV) system.

In certain applications, the channel variation is quite slow compared to the transmission rate. Such channels are called quasi-static. The propagation channel together with the transmit and receive antennas, constitute the radio channel [16]. This is illustrated in figure 2-4.

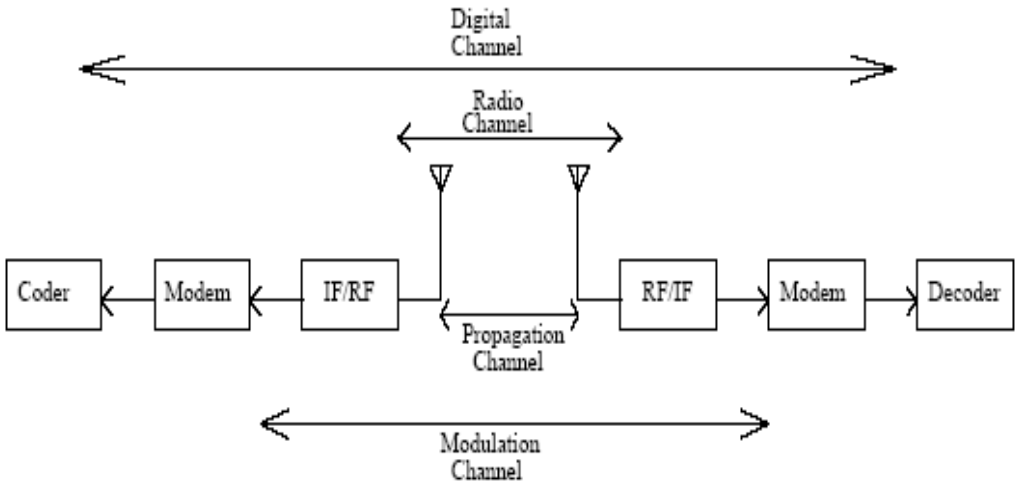


Figure 2-4: Various channels in a communication system

2.6 Signal Impairments

Communication quality between a base station and mobile or portable transceiver depends, among other factors, on the type and degree of impairments the signal undergoes in the radio channel. Some of the more important impairments that need to be included as essential parts of a realistic radio channel model are path loss, shadowing and multipath propagation.

2.6.1 Path loss

Path loss is when the transmitted signal suffers a loss proportional to $1/d^n$, where d is the distance between transmit and receive antennas and n is a positive number typically between 2 and 6. For free space transmission, n = 2 and the free space path loss is given (in dB) by [16]:

$$L_{FS} = +20\log_{10} f_c + 20\log_{10} d + 32.4 \qquad (2\text{-}6)$$

where d is the distance between transmit and receive antennas (in km) and f_c is the carrier frequency in MHz. Although free-space assumption is quite optimistic, it provides a useful figure of reference for path loss.

2.6.2 Shadowing

This is the loss of signal strength, which is typically contributed to a diffracted wave emanating from an obstacle between transmitter and receiver. Shadowing is sometimes called "slow fading," since, from a mobile viewpoint, passing through a shadow region takes considerable time.

2.6.3 Multipath Propagation

This occurs as radio waves reflect off hills, buildings, vehicles, and other obstacles; they establish different transmission paths from transmit to receiver antennas. A path is likely to include many reflections in an urban environment, whereas in rural areas, one reflection per path may be more common. The multipath creates one of the most difficult problems in the mobile radio environment: fading. Fading can be categorized as either frequency-selective or flat fading.

Frequency-selective fading is when the transmitted signal follows several paths, each arriving at the receiver antenna at different times. The result is the dispersion of the received signal in time. The signal dispersion in time is typically identified by associating a delay spread with the signal. Different environments produce different delay profiles.

Flat fading is when the transmitted wave scatters off many obstacles, particularly close to the mobile. The result is that the phase and amplitude of each ray arriving at the receive antenna are different. Now, assuming that several rays arrive from all directions at the receive antenna at the same time (i.e. with the same delay), the combined sum of these rays may add up constructively or destructively, from reinforcement to total cancellation or fading.

2.7 Propagation Models

A propagation model is a set of mathematical expressions, diagrams, and algorithms used to represent the radio characteristics of a given environment. Propagation models are used either for radio system design or for radio network planning purposes. These two application

areas present different requirements for the model. For radio system design purposes the mean electric field, the signal variance and the precise estimation of the short term fading are usually required whereas in network planning only the mean value of the electric field is needed. On the other hand, in network planning the model has to be computationally efficient in order to estimate the received field strength values for a large geographical area.

Although many varieties of propagation models can be found in the literature, the main ones are: Free -space Path loss model, Empirical Models and Deterministic Models.

2.7.1 Free-space Path loss Model (Analytical) [4]

Consider an idealized system shown in figure 2-5 where a base station transmitter is transmitting at an average power level of P_T , and d is the transmitter – receiver (T-R) separation distance.

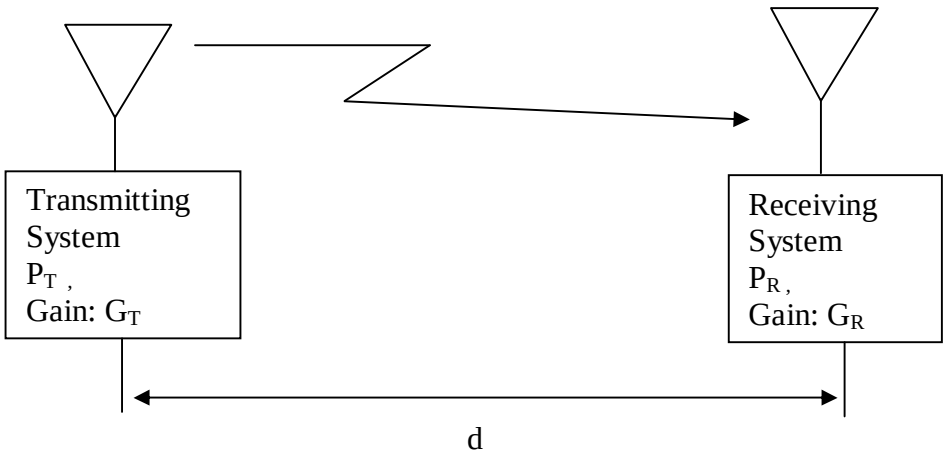


Figure 2.5: A simple model for Path Loss in Free Space

The received power level, P_R, at the receiving antenna, MS can be calculated analytically as follows:

For an isotropic antenna in free space:

$$p_R = \frac{P_T}{4\pi d^2} \qquad (2\text{-}7)$$

For an isotropic antenna radiating uniformly in all directions (spherical pattern), the power density, P_R is given by equation (2-7).

When a directional transmitting antenna with a power gain factor G_T, is used, the power density at the receiver site is G_T times equation (2-7), i.e.

$$p_{R,(direc.)} = p_R G_T = \frac{P_T G_T}{4\pi d^2} \qquad (2\text{-}8)$$

If the receiving antenna has an aperture area A_R, then the power captured by the receiver is $P_{R,(direc.)}$ times A_R.

i.e.

$$\overline{p}_{R,(direc.)} = \frac{P_T G_T A_R}{4\pi d^2} \qquad (2\text{-}9)$$

The aperture area is related to the gain of the receiving antenna and the wavelength by [4]:

$$G_R = \frac{4\pi A_R}{\lambda^2} \qquad (2\text{-}10)$$

where

$\lambda = \frac{c}{f}$, and f = the transmission frequency in Hz

$c = 3\times10^8 m/s$ is the free-space speed of propagation for electromagnetic waves, and λ is the wavelength in m.

Now the total received power P_R is:

$$P_R = A_R \, p_R \qquad (2\text{-}11)$$

Substituting for A_R and p_R from above, we have:

$$P_R = \left[\frac{\lambda}{4 \pi d} \right]^2 P_T G_T G_R \qquad (2\text{-}12)$$

The path propagation loss, L_P which denotes the loss associated with propagation of e.m. waves from the transmitter to the receiver, is given by:

$$L_P = \left[\frac{4 \pi d}{\lambda} \right]^2 \qquad (2\text{-}13)$$

It can be seen that this loss depends on the carrier frequency and the T-R separation distance. The product $P_T G_T$ is called the Equivalent Isotropic Radiated Power (EIRP). If P_T and P_R are expressed in same unit of dBm in equation (2-12), then P_R and L_P can be expressed in dBm and dB [14] as follows:

$$P_R = 20 \log \left[\frac{\lambda}{4 \pi d} \right] + P_T + G_T + G_R \text{ (dBm)} \qquad (2\text{-}14)$$

$$L_P = 20 \log \left[\frac{4 \pi d}{\lambda} \right] \text{ (dB)} \qquad (2\text{-}15)$$

2.7.2 Empirical Models [17]

The analytical model of the propagation of radio waves (e.g. GSM signal) in real-world environment is complicated. Consequently, several empirical models have been suggested for calculating propagation path losses. The two widely used models are the Hata-Okumura model and the Walfisch-Ikegami model.

2.7.2.1 The Hata-Okumura model

The Hata-Okumura computation model was first described by Yoshihisa Okumura [6]. Masaharu Hata simplified the considerations from Okumura [7]. The empirical model of Hata-Okumura was especially designed for the prediction of the path loss in urban areas. Neither obstacles between transmitter and receiver nor buildings in the local environment of the transmitter/receiver are considered for the prediction of the path loss. Local effects (shadowing/reflections) close to the transmitter or receiver are not considered either. The model is calibrated for a receiver height of 1.5 m, i.e. indoor coverage in general and especially in multifloor buildings cannot be predicted with this model with an acceptable accuracy.

Hata's model is applicable to urban, suburban, and open environment. The Hata's model for urban and open area is given by:

Urban Area:

$$L_{50} = 69.55 + 26.16 \log f_c - 13.82 \log h_b - a(h_m) + (44.9 - 6.55 \log h_b) \log d \text{ (dB)} \quad (2\text{-}16)$$

where f_c = frequency in MHz,

L_{50} = mean path loss in dB,

h_b = BS antenna height in m,

$a(h_m)$ = correction factor for mobile antenna height in dB,

d = distance from base station in Km.

The range of the parameters for which the Hata model is valid is:

$$150 \le f_c \le 1{,}500 \text{ MHz},$$
$$30 \le h_b \le 200 \text{ m}, \qquad (2\text{-}17)$$
$$1 \le h_m \le 10 \text{ m and } 1 \le d \le 20 \text{ Km}.$$

The correction factor for urban environment is given as:

$$a(h_m) = 8.29(\log 1.54 h_m)^2 - 1.1 \text{ dB, for } f_c \le 200 \text{ (MHz)} \qquad (2\text{-}18)$$

or

$$a(h_m) = 3.2(\log 11.75 h_m)^2 - 4.97 \text{ dB, for } f_c \ge 400 \text{ (MHz)} \qquad (2\text{-}19)$$

Open Area:

$$L_{50} = L_{50}(urban) - 4.78(\log f_c)^2 + 18.33 \log f_c - 40.94 \text{ (dB)} \qquad (2\text{-}20)$$

2.7.2.2 Walfisch-Ikegami Model [4, 17]

The Walfisch-Ikegami model also known as the European Committee of Science and Technology, COST 231 model, is used to estimate path loss in an urban environment for cellular communication. This model is a combination of the empirical and deterministic models for estimating the path loss in urban environment over the frequency range of 800-2000 MHz.

The model contains three elements: free-space loss, roof-to-street diffraction and scatter loss, and multiscreen (i.e., diffraction and scatter loss from other structures) loss. The expressions used in this model are:

$$L_{50} = L_f + L_{rts} + L_{ms} \qquad (2\text{-}21)$$

$$\text{or } L_{50} = L_f \text{ when } L_{rts} + L_{ms} \le 0 \qquad (2\text{-}22)$$

where:

L_{50} = Mean path loss, (dB)

L_f = Free space loss, (dB)

L_{rts} = Rooftop-to-street diffraction and scatter loss, (dB)

and L_{ms} = Multiscreen loss, (dB)

Applying this model to scenario 1, which is an open area where signal characteristics due to locations of MS from BS is of interest, the model can be reduced to equation (2-22).

i.e. $$L_{50} = L_f = 32.4 + 20\log d + 20\log f_c \qquad (2\text{-}23)$$

Substituting the applying respective base station frequencies, in this case 900 and/or 1800 MHz, we have:

$$L_{50} = L_f = 91.48 + 20\log d \qquad (2\text{-}24)$$

or

$$L_{50} = L_f = 97.51 + 20\log d\ , \qquad (2\text{-}25)$$

As evident from equations (2-24) and (2-25), the path loss only depends on distance d between MS and BS. The range of parameters for which the model is valid is:

$$\begin{aligned} &800 \le f_c \le 2000 && \text{(MHz)},\\ &4 \le h_b \le 50 && \text{(m)},\\ &1 \le h_m \le 3 && \text{(m)},\\ &0.02 \le d \le 5 && \text{(Km)}. \end{aligned} \qquad (2\text{-}26)$$

2.7.3 Deterministic models

There are several weaknesses in the empirical or Free-Space models for propagation studies in microcellular environments. If the base station antenna height is below the rooftops of the surrounding buildings, the nature of the propagation phenomena changes. This situation can not be analyzed with statistical methods anymore because the size of the individual buildings is large compared to the cell size and the exact geometrical properties of the building cannot be ignored. Furthermore, the near environment of the base station antenna also has a strong

effect on propagation. The effect of the nearest buildings on the radio wave propagation can be taken into account by using ray-tracing models [16].

Deterministic propagation models are generally based on ray optical techniques. Here, the common idea is to describe the wave propagation with rays launched from the transmitting antenna. These rays are reflected and diffracted at walls and similar obstacles.

A basic form of ray tracing techniques which considers direct rays and wall-reflected rays is used in the prediction of received signal power in the second scenario studied in this investigation.

Figures 2-6 and 2-7 illustrate various propagation mechanisms from transmitter to receiver in NLOS and LOS situations respectively.

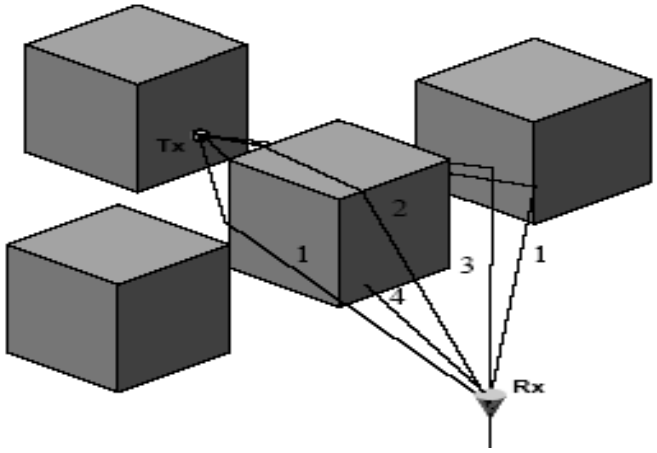


Figure 2-6: Propagation mechanisms in urban environment (NLOS): 1) diffracted wave, 2) over -rooftop diffracted wave, 3) reflected wave and 4) building penetrated wave.

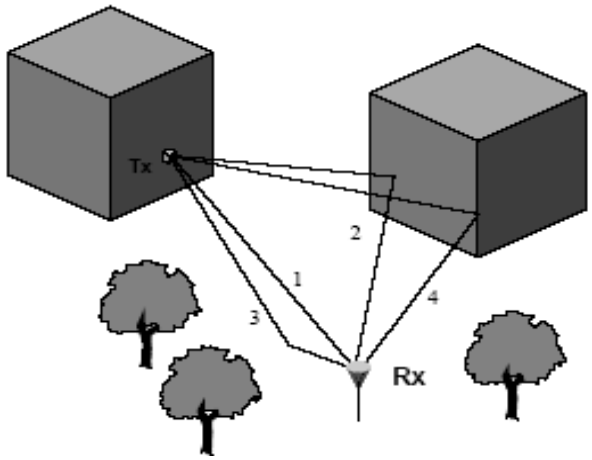


Figure 2-7: Propagation mechanisms in urban environment (LOS): 1) direct wave, 2) wall-, and 3) ground-reflected waves and 4) diffracted wave.

It should be noted that the total received signal power at the receiver can be estimated as a sum of the ray components arriving from various paths.

2.8 Uses of Propagation Models

Propagation models are used for the following [17], among others:

- To determine how many base stations are required to provide the coverage requirements needed for the network.
- To predict interference levels as the performance of the network is affected by the chosen propagation model during the network design stage.
- To determine other aspects of the system including hand off optimization, power level adjustments, and antenna placements.

It is important to state that no propagation model can account for all perturbations experienced in the real world. Therefore using one or more models for determining the path losses in the network is essential.

CHAPTER THREE

METHODOLOGY

3.0 Introduction

In order to study the propagation characteristics of Cellular Mobile Radio signals, two distinct set of scenarios were chosen. The first set of scenario consisted open areas (along some selected high ways) in and around Zaria metropolis. The objective here was to study attenuation of received signal strength as the receiver was moved away from the Base station transmitter sites.

The second set of scenario comprised a selected number of high buildings in a campus environment. Specifically, the buildings are Electrical, Mechanical, Civil, Faculty Lecture Theatres that mainly constitute the Engineering Complex; the Alexandra and Ribadu blocks, the Kashim Ibrahim Library (KIL) and the Senate Building on the Ahmadu Bello University (ABU) main campus, Zaria. The objective here was to study the multipath propagation and shadowing effects of these buildings on the transmitted signal from the BS. Also, attempt was made to predict the received signal powers at these two scenarios.

3.1 Description of the Measurement Environment

3.1.1 First Scenario

This comprised open/rural areas along highways where a BS transmitter was located close to the road side and served the surrounding areas that were mainly farmland and scattered low houses. These roads are: Kaduna road, Kano road, and Samaru road. Figure 3-1 shows these roads on a portion of Zaria map obtained from the Urban and Regional Planning Department, ABU, Zaria.

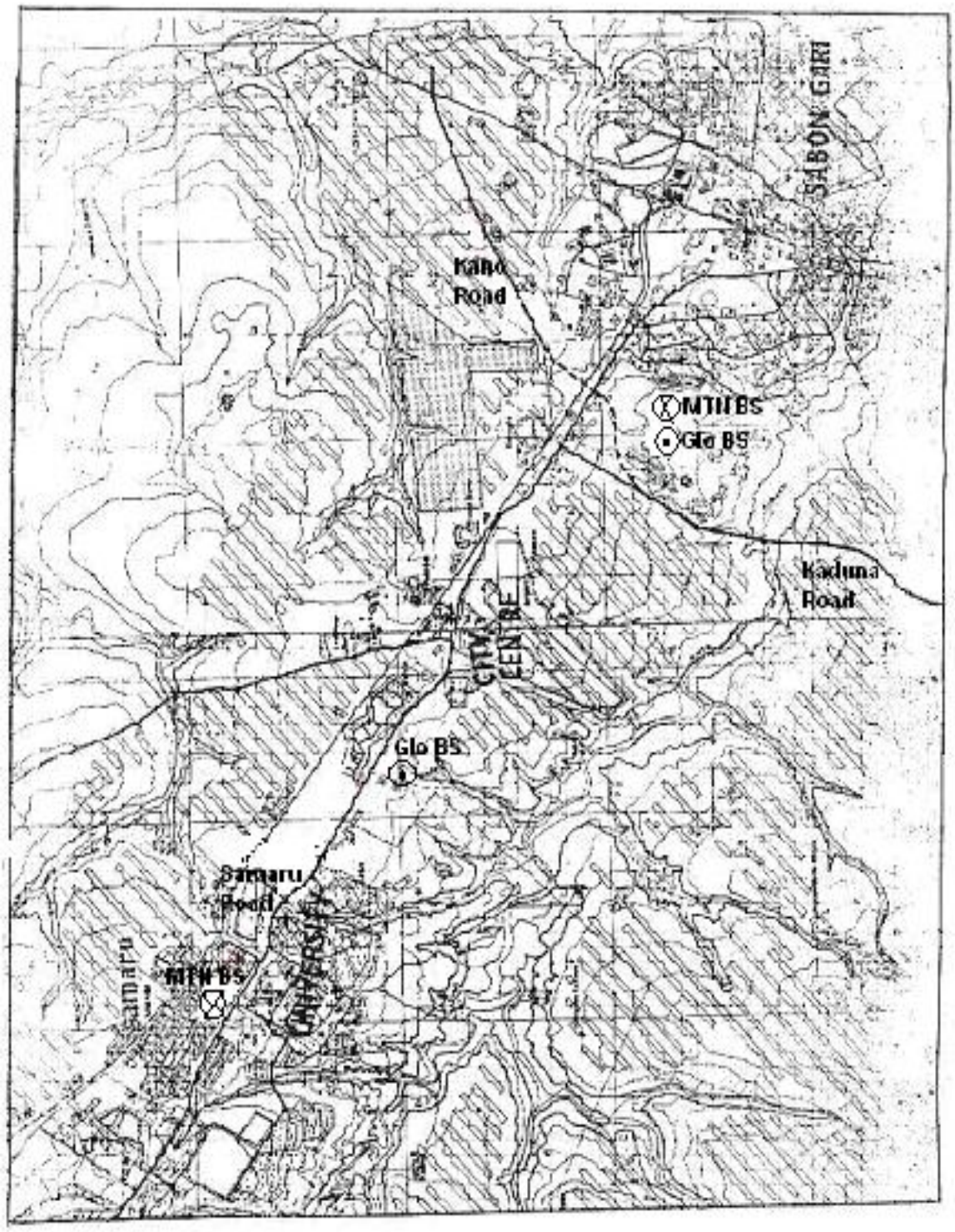


Figure 3.1: A Portion of Zaria Map showing Areas included in the First Scenario

3.1.2 Second Scenario

In this scenario, the buildings of Electrical Engineering, Mechanical Engineering, Civil Engineering and Faculty Lecture Theatres form a somewhat partial enclosure. The serving BS was located along Samaru road just after the North gate of the campus. However, some buildings located along the propagation paths from the BS to the MS whose heights were below that of the BS antenna height were excluded in the modeling. Only buildings whose heights are above or close to that of the BS antennas were included.

Figure 3-2 shows this area as curled from the ABU Master Plan cadastral map obtained from the Urban and Regional Planning Department, ABU, Zaria. .

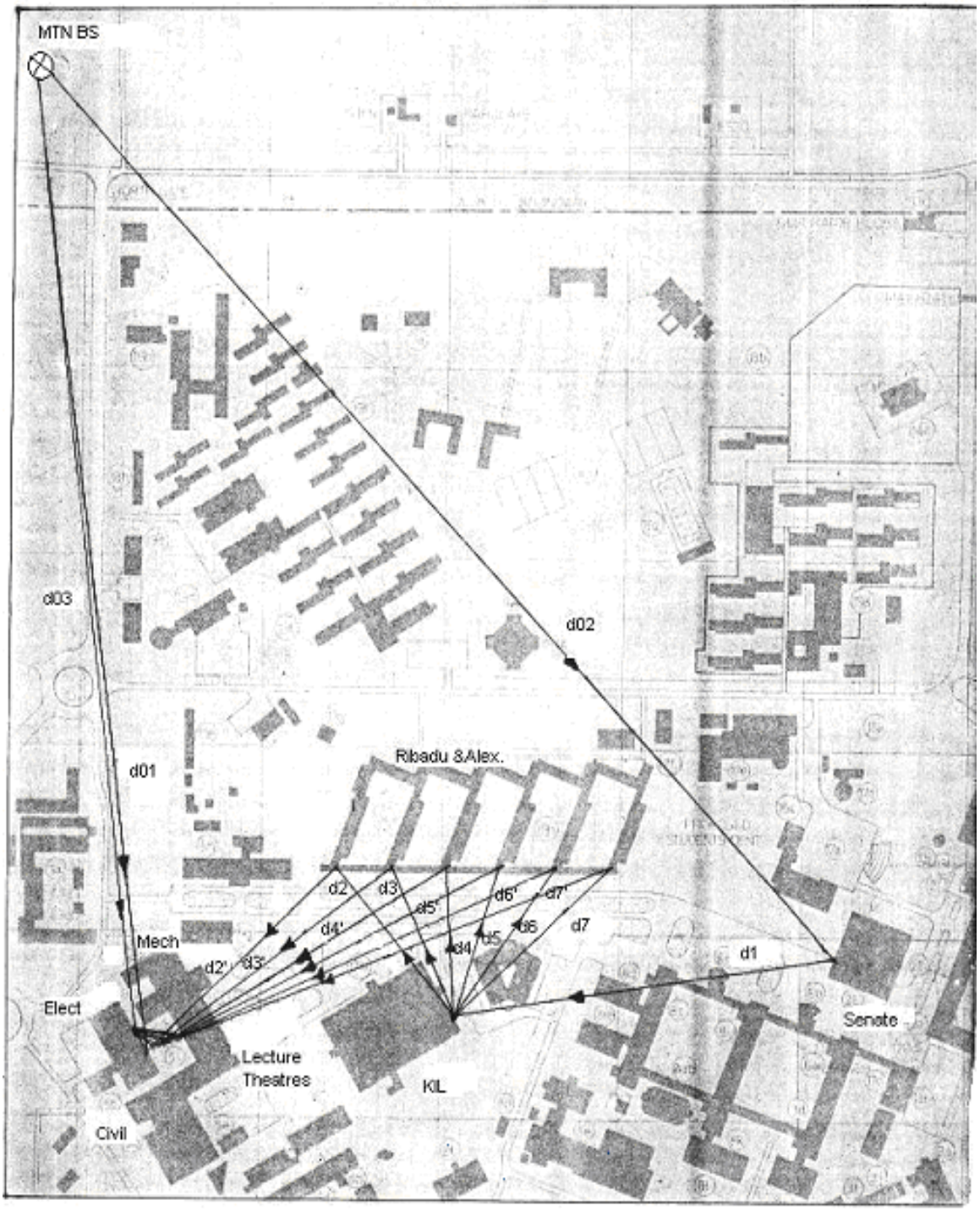


Figure 3.2: A Portion of Zaria Map showing Areas included in the Second Scenario

3.2 Experimental Setup

3.2.1 First Scenario

Experimental measurements were collected in the first scenario with the use of a Cellular Mobile Network Analyser (Model Sagem OT160) capable of measuring received signal power in decibel milliwatts (dBm). (See Appendix D for a note on accuracy and reliability of this analyser).The transmitting antenna (owned by MTN) was a vertical dipole located at a height, H_t of 32.00 m and transmitting at frequencies 900/1800 MHz, with a radiated power, P_t = 46 dBm, transmitting antenna gain, G_t = 18 dBi, and Effective Isotropic Radiated Power, EIRP = 64 dBm and expected minimum received power for good link R_M = 102 dBm. Similarly the parameters of the Glo BS antenna used were: height, H_t =33.00 m (for the BS on Kaduna/Kano roads), H_t =28.00 m (for the BS on Samaru road). Other parameters were frequency f_c = 900/1800 MHz, P_t = 47 dBm, G_t = 17.5 dBi, EIRP = 64.5 dBm, R_M = 104 dBm. All these other parameters, except the transmitting antenna heights, were the same for the two Glo BSs. For Kaduna and Kano roads, the antenna was located at the Hanwa New Extension Area, off Samaru road, Kwangila area, Zaria, for both MTN and Glo BSs; and for Samaru road the antenna was located along Samaru road near the North Gate of ABU, Zaria for MTN while that of Glo was located at Zango area near the Conoil filling station (see map in Fig. 3-1). The receiving antenna, which was a short antenna with gain G_R = 1.5 [18] (≈ 1.76 dB), was carried on a moving motorcycle at a height of 1.1 m, and a steady velocity of 40 $Kmhr^{-1}$ (approx. 11.1 ms^{-1}). During measurements, readings of received signal powers were taken as the motorcycle moved away from the serving base stations. Care was taking not to enter into the serving regions of a next base station transmitting antennas.

It is important to state that the Cellular Mobile Network Analyser was used to take readings of received signal powers on all the Glo BSs considered and only the MTN BS on Samaru road. Due to the fact that this device was not available for use throughout the period readings were being taken, it was used to calibrate a Sony Ericsson mobile phone (model T200) which was then used to take readings on MTN BS on Kaduna/Kano road.

The readings obtained are shown in Appendix A.

3.2.2 Second Scenario

In this scenario, measurements of received signal power were taken at various receiving points within the Engineering Complex along a trajectory that was 20 m from the Mechanical Engineering block. The receiving points were spaced 5m apart. The readings were taken over a period of two hours at 20 minutes intervals, and repeated for three days. These readings are shown in Appendix B. Furthermore, prediction of the received signal power was also carried out using modified two-ray model, which is a basic ray-optical approach. Figure 3.3 shows a sketch of the measurement area in this scenario.

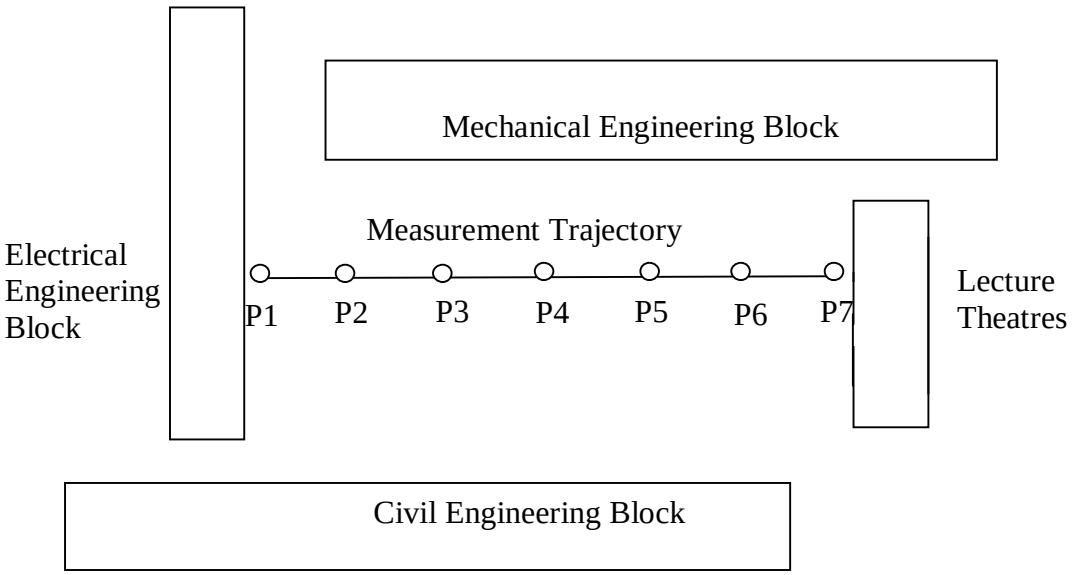


Figure 3.3: Measurement Area in Scenario 2

3.3 Prediction of Received Signal Power using modified Two-Ray Model

The received signal power, P_R for isotropic antenna, using the two-ray model can be expressed as [15]:

$$P_R = P_T \left(\frac{\lambda}{4\pi} \right)^2 \left| \frac{1}{d_1} \exp\left(-jkd_1\right) + \Gamma(\theta) \frac{1}{d_2} \exp\left(-jkd_2\right) \right|^2 \quad (3\text{-}1)$$

where P_T is the transmitter power, d_1 is the direct distance from the transmitter to the receiver, d_2 is the distance through reflection on the ground, θ is the angle of incidence of the reflected ray and $\Gamma(\theta)$ is the reflection coefficient from the ground. In our own case, the rays arriving at the receiving points are of two classes; direct rays and wall-reflected rays up to a maximum order of three. Therefore, received power at each point was computed using the class of ray(s) illuminating it. From equation (3-1), the first term in the modulus sign represents a direct ray while the second term represents a ground-reflected ray. For our purpose, this equation was adapted and modified as follows:

$$P_R = P_T \left(\frac{\lambda}{4\pi} \right)^2 \left| \frac{1}{d_l} \exp\left(-jkd_l\right) + \prod_q \Gamma_{qi} \frac{1}{\sum d_i} \exp\left(-jk \sum d_i\right) \right|^2 \quad (3\text{-}2)$$

where d_l is the path length of the direct rays, $\sum d_i$ is the total path length of rays illuminating receiver location i along the reflection paths, and Γ_{qi} is the reflection coefficient of the qth ray. Consequently, received power at locations illuminated only by direct ray was computed using:

$$P_R = P_T \left(\frac{\lambda}{4\pi} \right)^2 \left| \frac{1}{d_l} \exp\left(-jkd_l\right) \right|^2 \quad (3\text{-}3)$$

and that at locations illuminated only by wall-reflected ray(s) that has/have undergone up to a maximum order of three reflections (i.e. q=3) was computed using:

$$P_R = P_T \left(\frac{\lambda}{4\pi} \right)^2 \left| \prod_q \Gamma_{qi} \frac{1}{\sum d_i} \exp\left(- jk \sum d_i \right) \right|^2 \qquad (3\text{-}4)$$

For a directional transmitting antenna with a gain G_T and a receiver antenna with a gain G_R, equations (3-3) and (3-4) respectively become

$$P_R = P_T G_T G_R \left(\frac{\lambda}{4\pi} \right)^2 \left| \frac{1}{d_l} \exp\left(- jk d_l \right) \right|^2 \qquad (3\text{-}5)$$

and

$$P_R = P_T G_T G_R \left(\frac{\lambda}{4\pi} \right)^2 \left| \prod_q \Gamma_{qi} \frac{1}{\sum d_i} \exp\left(- jk \sum d_i \right) \right|^2 \qquad (3\text{-}6)$$

The magnitude of the exponential term is approximately unity. Therefore expressing equations (3-5) and (3-6) in dBm, we have

$$P_R = P_T + G_T + G_R + 20 \log \left(\frac{\lambda}{4\pi} \right) \frac{1}{d_l} \qquad (3\text{-}7)$$

and

$$P_R = P_T + G_T + G_R + 20 \log \left(\frac{\lambda}{4\pi} \right) \frac{1}{\sum d_i} \prod_q \Gamma_{qi} \qquad (3\text{-}8)$$

Substituting the parameters of the MTN BS and using f_c = 900 MHz, we have:

$$P_{R(D)} = 46 + 18 + 1.76 + 20 \log \left(\frac{1}{12\pi} \right) \frac{1}{d_l}$$

$$= 65.76 - 31.53 \frac{1}{d_l} \qquad (3\text{-}9)$$

and $$P_{R(R)} = 46 + 18 + 1.76 + 20\log\left(\frac{1}{12\pi}\right)\frac{1}{\sum d_i}\prod_q \Gamma_{qi}$$

$$= 65.76 - 31.53\frac{1}{\sum d_i}\prod_q \Gamma_{qi} \qquad (3\text{-}10)$$

Values of d_l, d_i and Γ_{qi} used in the prediction are shown in table 3.1.

3.4 Data bases used in the second scenario

Data bases used with ray-optical models contain information on the kind of obstacles between the transmitter (BS) and the receiver (MS). These data bases also contain information on the location of buildings and are generally vector-oriented. In the vector format, the shape of every building is defined by its corners and its height. Consequently, all buildings are represented by cylinders with a polygonal plan view (see figure 3-2).

The buildings considered in the region of interest were constructed of concrete. Therefore, electrical parameters for dry concrete were used. These are relative permittivity, ε_r = 4 to 6 and conductivity, σ = 10^{-4} S/m [19]. The value ε_r = 6 was found to give prediction values of P_R closest to the corresponding measurement values. These values are used in equation (2-4) in the computation of the Fresnel reflection coefficient.

3.5 Visibility Relations

In the second scenario, there were two types of sources providing electromagnetic energy to the receiver locations; the primary source and the secondary sources. The former comprised the BS transmitter while the latter resulted from reflections from the walls of the senate

building, the Kashim Ibrahim Library (KIL) and Alexander and Ribadu blocks. The visibility relationships between the transmitter, the various ray paths and the receiver locations are illustrated in a tree structure shown in figure 3-4.

Preprocessed data base:

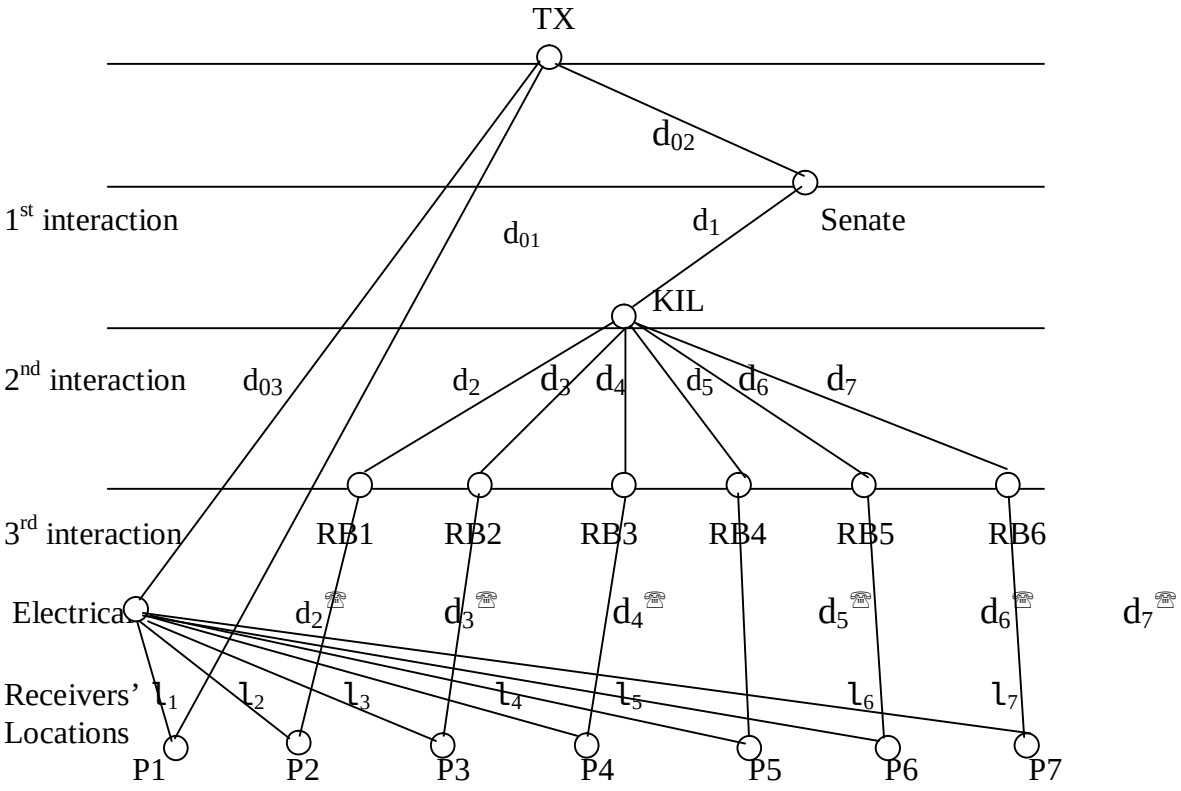


Figure 3.4: Tree structure of the visibility relations

Although many other rays might still possibly reached each of the receiver locations from the Ribadu blocks other than the ones shown for points P2 through P7, the dominant rays for each of the locations were considered. This was because these other possible rays' contribution to total received power could be negligible.

3.6 Determination of the Ray Parameters

For the classes of rays considered, parameters such as path lengths and incident angles were estimated from the cadastral map of the campus. These were then used to compute the reflection coefficients of each of the reflected rays. The various ray paths, and the values obtained for the path lengths and angles of incidence are shown in table 3.1.

Table 3.1: Ray parameters for paths 1 and paths 2

Ray paths	**Path lengths (in m)**	**Incident angles, Θ (in degrees),**	**Reflection coefficients**, Γ
d_{01}(direct)	708.0	_	_
d_{02}(direct)	861.6	_	_
d_{03}(direct)	688.0	_	-
d_1	290.4	26.5	-0.6727
d_2	124.8	63.0	-0.4597
d_2☏	192.0	43.0	-0.5483
d_3	105.6	54.0	-0.4923
d_3☏	211.2	38.0	-0.5804
d_4	96.0	42.5	-0.5513
d_4☏	223.2	29.5	-0.6460
d_5	98.4	31.0	-0.6334
d_5☏	240.0	20.0	-0.7373
d_6	127.2	21.5	-0.7215
d_6☏	307.2	12.5	-0.8242
d_7	153.6	16.0	-0.7820
d_7☏	336.0	8.5	-0.8763
$d_{03}+l_1$	707.2	76.0	-0.4305
$d_{03}+l_2$	708.8	72.0	-0.4374
$d_{03}+l_3$	710.4	68.0	-0.4461
$d_{03}+l_4$	712.0	64.3	-0.4558
$d_{03}+l_5$	715.2	60.0	-0.4693
$d_{03}+l_6$	718.4	56.3	-0.4829
$d_{03}+l_7$	723.2	53.8	-0.4931

The received power at location P1 was predicted from

$$P_{R1} = \left[65.76 - 31.53 \left(\frac{1}{d_{01}} + \frac{1}{d_{03} + l_1} \Gamma(\theta) \right) \right] \quad (3\text{-}11)$$

and that at locations P2 to P7 was predicted from

$$P_{Ri} \Big|_{i = 2 \text{ to } 7} = \left[65.76 - 31.53 \left(\frac{1}{d_i} \Gamma(\theta_i) + \frac{1}{\sum d} \prod_q \Gamma qi \right) \right] \quad (3\text{-}12)$$

where q = 3.

The results obtained are shown in table 4.10 in Chapter Four.

CHAPTER FOUR

ANALYSIS AND RESULTS

4.0 Introduction

In this chapter, analysis of data obtained through measurements is carried out. Comparison is then made with computed values using the Free-Space, Hata and the modified Two-Ray models. These models are then modified with appropriate correction factors to obtain models proposed for the specific outdoor environments under investigation.

4.1 Results obtained using the Free Space Loss Model

Considering equation (2-14), received power is:

$$P_R = 20\log\left[\frac{\lambda}{4\pi d}\right] + P_T + G_T + G_R \qquad (4\text{-}1)$$

Substituting BS parameters and receiving antenna gain;

(a) For MTN BS:

P_T = 46 dBm, G_T = 18 dBi, G_R =1.76 dB;

$$\lambda = \frac{c}{f_1} = \frac{3\times10^8}{900\times10^6} = \frac{1}{3}m \text{, or } \lambda = \frac{c}{f_2} = \frac{3\times10^8}{1800\times10^6} = \frac{1}{6}m \text{ .}$$

$$P_R = 20\log\left[\frac{\lambda}{4\pi d}\right] + 46 + 18 + 1.76$$

$$P_R = 20\log\left[\frac{1}{3\times4\times\pi\times d}\right] + 65.76 = -20\log\left[12\pi d\right] + 65.76$$

$$= 34.23 - 20\log d \text{ dBm, for } f_c = 900 \text{ MHz} \qquad (4\text{-}2)$$

Or

$$P_R = 28.21 - 20\log d \text{ dBm, for } f_c = 1800 \text{ MHz.} \qquad (4\text{-}3)$$

(b) For Glo BS:

P_T = 47 dBm, G_T = 17.5 dBi, G_R = 1.76 dB;

$$P_R = 20\log\left[\frac{\lambda}{4\pi d}\right] + 47 + 17.5 + 1.76$$

$$P_R = 20\log\left[\frac{1}{3\times 4\times \pi \times d}\right] + 66.26 = -20\log\left[12\pi d\right] + 66.26$$

$$= 34.73 - 20\log d \quad \text{dBm, for } f_c = 900 \text{ MHz} \qquad (4\text{-}4)$$

Or,

$$P_R = 28.71 - 20\log d \quad \text{dBm, for } f_c = 1800 \text{ MHz.} \qquad (4\text{-}5)$$

The path loss for both networks and frequencies can be obtained using the expression:

$$L_P = EIRP - P_R \qquad (4\text{-}6)$$

From equations (4-2), (4-3), (4-4) and (4-5) it can be observed that the received power on Glo network, for corresponding distances and frequencies, is more than that on MTN network only by 0.5 dBm, the value by which the EIRP of the former BS transmitter exceeds that of the latter. This was because MTN used a lower BS transmitter power and a higher BS transmitter gain while Globacom used the converse of this.

4.2 Results obtained using the Hata Model

(a) MTN BS - Urban

From equation (2-16), mean path loss L_{50}, for urban area is given as:

$$L_{50} = 69.55 + 26.16\log f_c - 13.82\log h_b - a(h_m) + (44.9 - 6.55\log h_b)\log d \qquad (4\text{-}7)$$

Substituting for f_c, h_b and ah_m we have:

$$L_{50} = 69.55 + 26.16\log 900 - 13.82\log 32 + 1.0171 + (44.9 - 6.55\log 32)\log d$$

$$= 127.05 + 35.04\log d\,, \quad f_c = 900 \text{ MHz} \tag{4-8}$$

Or

$$L_{50} = 134.92 + 35.04\log d\,, \text{ for } f_c = 1800 \text{ MHz} \tag{4-9}$$

For the first scenario in this study (i.e. Open/Rural areas),

$$L_{50} = L_{50}(urban) - 4.78(\log f_c)^2 + 18.33\log f_c - 40.94 \tag{4-10}$$

$$= 98.54 + 35.04 \log d \text{ dB, for } f_c = 900 \text{ MHz} \tag{4-11}$$

Or

$$L_{50} = 103.00 + 35.04 \log d\,, \text{dB for } f_c = 1800 \text{ MHz} \tag{4-12}$$

(b) Glo BS:

Using equation (4-10) and inputting appropriate values of transmitting antenna heights, we have:

For Kaduna/Kano road,

$$L_{50} = 98.35 + 34.95 \log d\,, \text{dB for } f_c = 900 \text{ MHz} \tag{4-13}$$

and $L_{50} = 102.82 + 34.95 \log d$, dB for $f_c = 1800$ MHz (4-14)

Similarly, for Samaru road,

$$L_{50} = 99.34 + 35.42 \log d \text{ ,dB for } f_c = 900 \text{ MHz} \tag{4-15}$$

and $L_{50} = 103.81 + 35.42 \log d$, dB for $f_c = 1800$ MHz (4-16)

The received signal power is computed using:

$$P_R = EIRP - L_{50} \tag{4-17}$$

4.3 Results obtained using the Walfisch/Ikegami Model

The expression for path loss for this Model is that of free space and is given as:

$$L_{50} = L_f = 32.4 + 20 \log d + 20 \log f_c \text{ dB} \quad (4\text{-}18)$$

Applying it to scenario 1, and inputting the BS frequencies, we have:

$$L_{50} = 91.48 + 20 \log d \text{ dB for } f_c = 900 \text{ MHz}, \quad (4\text{-}19)$$

Or $$L_{50} = 97.51 + 20 \log d \text{ dB, for } f_c = 1800 \text{ MHz} \quad (4\text{-}20)$$

It should be noted that these expressions give the same values of path loss for corresponding distances from the BS as that of Free-Space in section 4.1. For this reason, this model is not examined any further.

Values obtained for P_R s and L_{50} s, for all the foregoing three cases are shown in Appendix C.

4.4 Analysis and Comparison of Measurements and Prediction Results

4.4.1 Scenario 1

For each of the considered networks, in the first scenario, measured received signal power over a period of three days were averaged and results obtained were tabulated. This was then used to determine the path loss over the radio path. The results obtained are shown in tables 4-1 through

4-6. Also, received signal power and computed path loss from measurements, Free-Space and Hata models are plotted in figures 4-1 through 4-6.

Table 4-1: Averaged Measured Received Signal Power and Computed Path loss for Kaduna Road [MTN Network]; $P_T = 46$ dBm, $G_T = 18$dBi, $G_R = 1.76$ dB, $f_c = 900$ MHz

Distance (m)	Received Signal Power, P_R (dBm)	Computed Path loss, L_P (dB)	$EIRP$ (dBm)
200.00	-67.67	131.67	64.00
1166.55	-73.89	137.89	64.00
1536.88	-87.00	151.00	64.00
2240.53	-87.00	133.00	64.00
2559.00	-91.00	151.00	64.00
2777.50	-99.00	163.00	64.00
2944.15	-104.92	168.92	64.00

Table 4-2: Averaged Measured Received Signal Power and Computed Path loss for Kano Road,[MTN Network]; $P_T = 46$ dBm, $G_T = 18$dBi, $G_R = 1.76$ dB, $f_c = 900$ MHz

Distance (m)	Received Signal Power, P_R (dBm)	Computed Path loss, L_P (dB)	$EIRP$ (dBm)
200.00	-67.67	131.67	64.00
1481.33	-73.89	137.89	64.00
1666.50	-83.89	147.89	64.00
2070.16	-87.00	151.00	64.00
2255.33	-91.00	155.00	64.00
2510.86	-91.45	155.45	64.00
2807.13	-90.78	154.78	64.00
2962.67	-96.56	160.56	64.00
3099.69	-103.67	169.67	64.00

Table 4-3(a): Averaged Measured Received Signal Power and Computed Path loss for Samaru Road [MTN Network] -Eastward of BS; P_T = 46 dBm, G_T = 18dBi, G_R = 1.76 dB, f_c = 900 MHz

Distance (m)	Received Signal Power (dBm)	Computed Path loss , L_P (dB)	$EIRP$ (dBm)
200	-66.00	130.00	64.00
550.00	-67.67	131.67	64.00
825.00	-72.34	136.34	64.00
1375.00	-77.00	141.00	64.00
1925.00	-78.00	142.00	64.00
2475.00	-87.00	151.00	64.00
3025.00	-103.50	167.50	64.00
3575.00	-106.33	170.33	64.00

Table 4-3(b): Averaged Measured Received Signal Power and Computed Path loss for Samaru Road[MTN Network] - Southward of BS; P_T = 46 dBm, G_T = 18dBi, G_R = 1.76 dB, f_c = 900 MHz

Distance (m)	Received Signal Power (dBm)	Computed Path loss, L_P (dB)	$EIRP$ (dBm)
200.00	-64.00	128.00	64.00
550.00	-67.67	131.67	64.00
825.00	-77.00	141.00	64.00
1375.00	-83.33	147.33	64.00
1925.00	-89.33	153.33	64.00
2475.00	-99.00	163.00	64.00
3025.00	-101.67	165.67	64.00
3575.00	-104.37	168.37	64.00

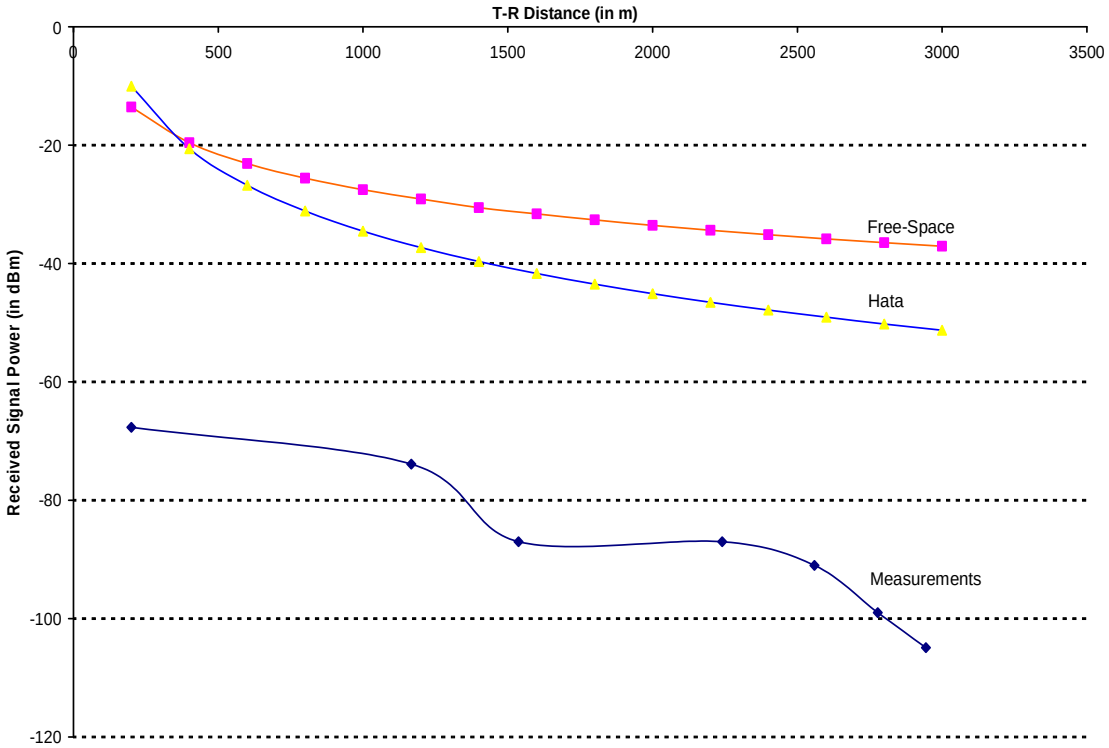


Figure 4-1 (a): Received Signal Power from Prediction and Measurement on Kaduna Road (MTN) Network

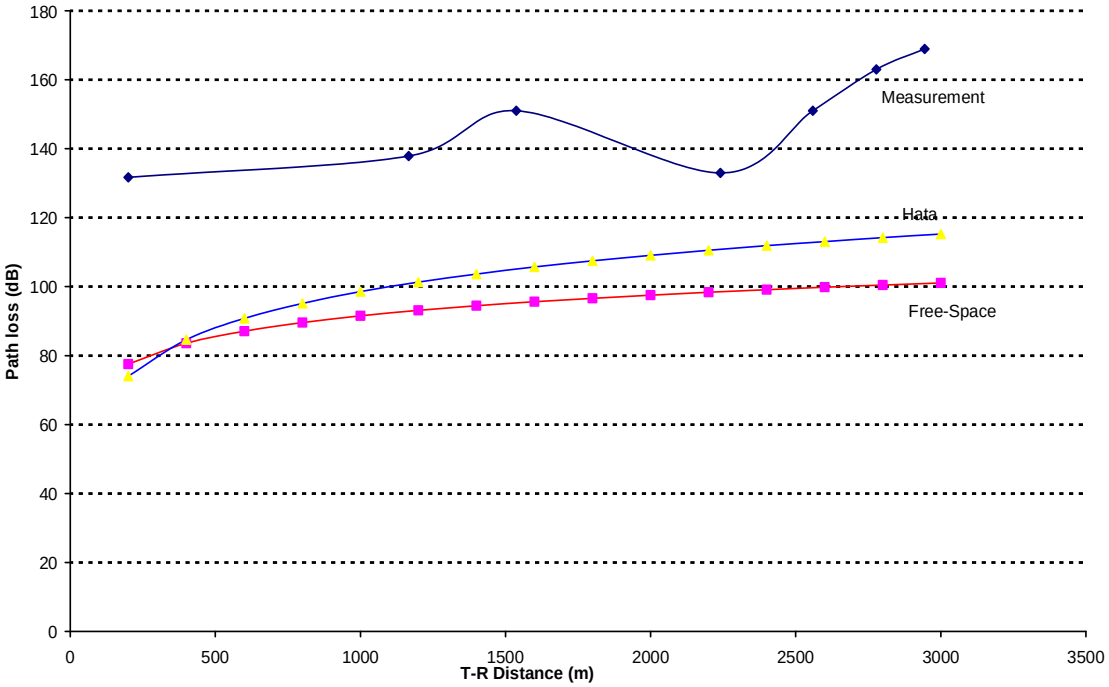


Figure 4-1 (b): Path loss on Kaduna Road (MTN Network)

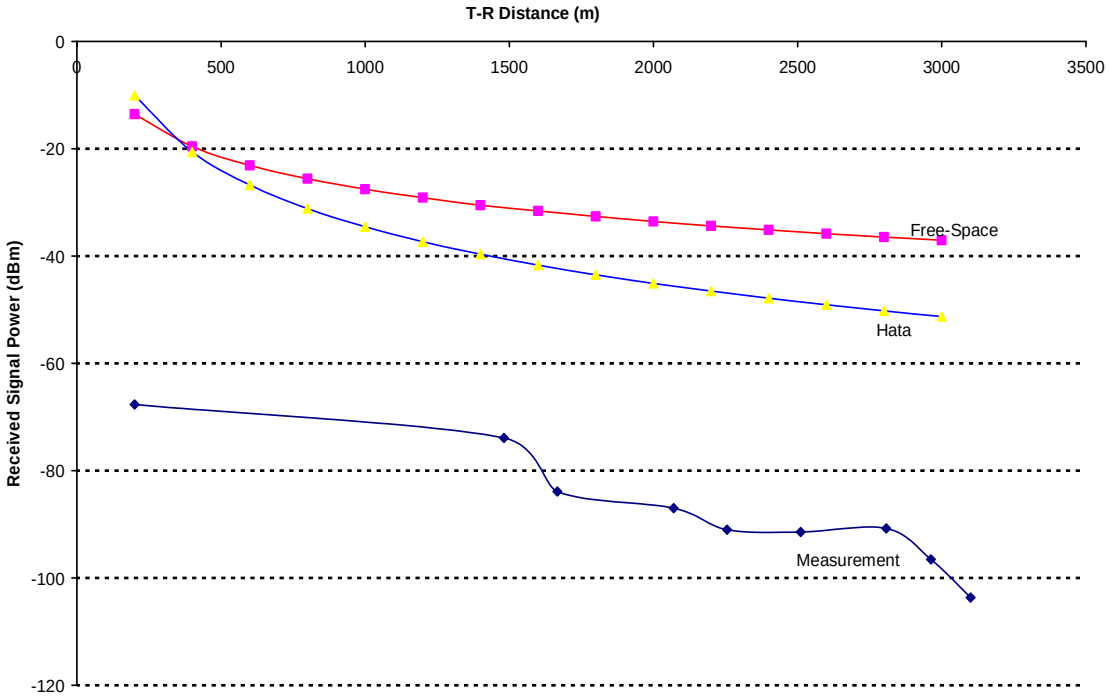


Figure 4-2 (a): Received Signal Power on Kano Road (MTN Network)

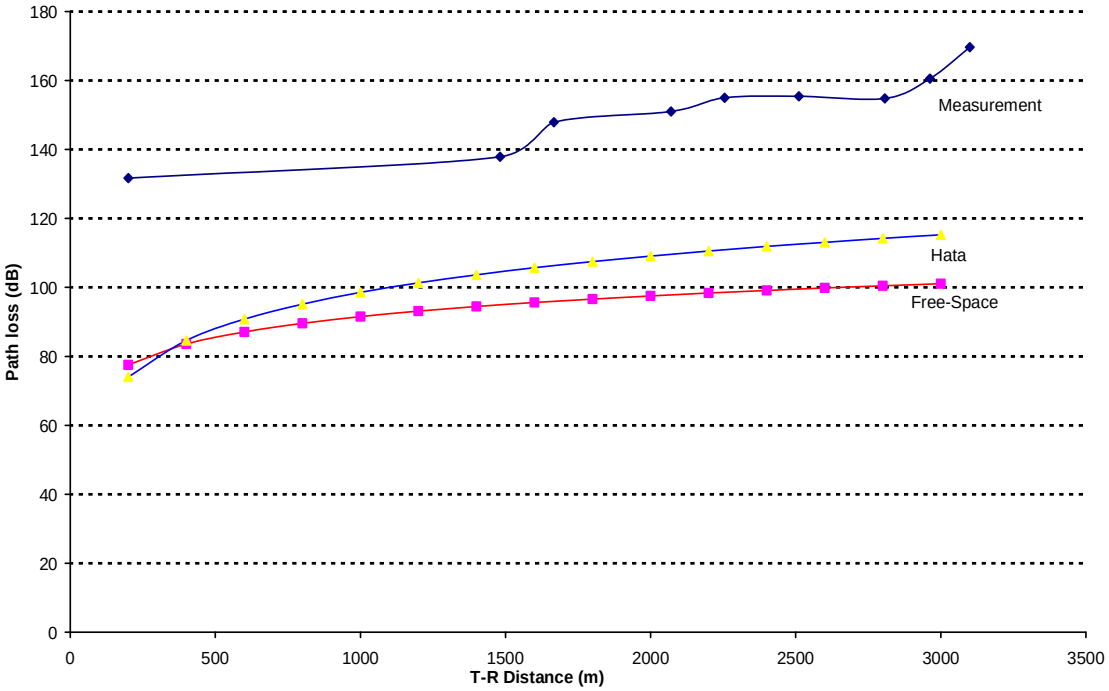


Figure 4-2 (b): Path loss on Kano Road (MTN Network)

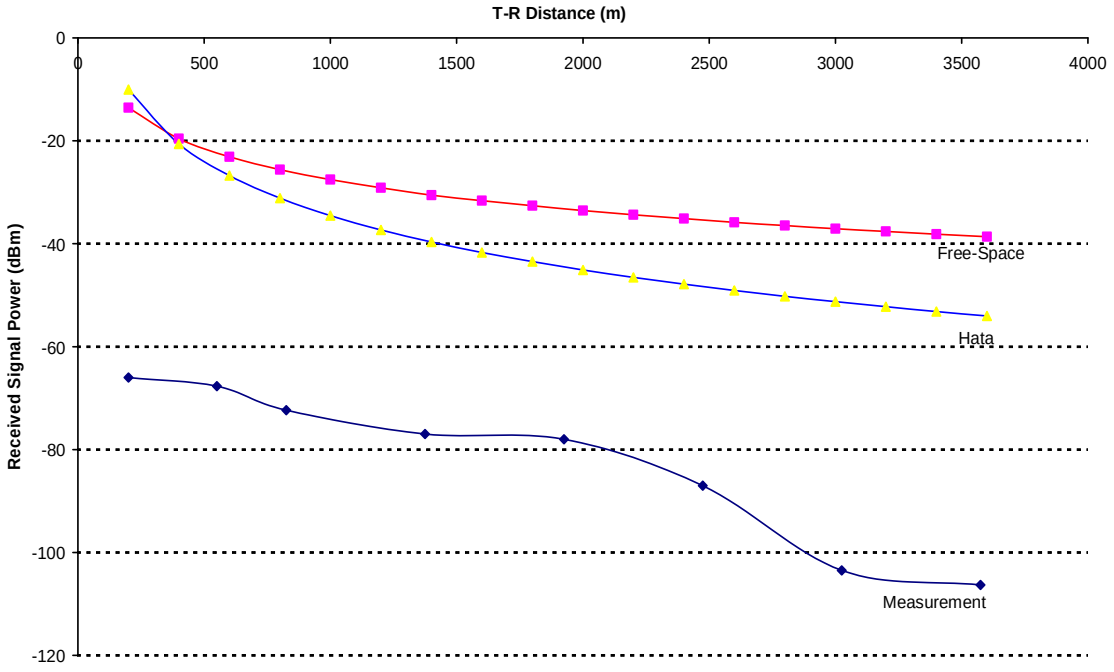


Figure 4-3a (i): Received Signal Power on Samaru Road (MTN Network) Eastward of BS

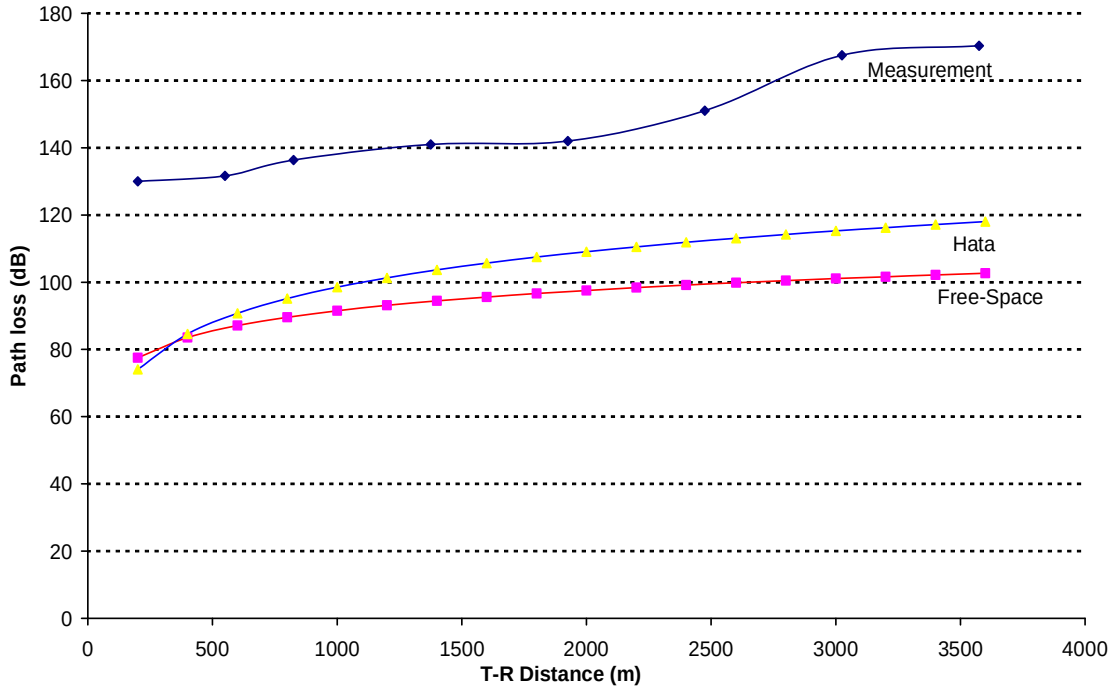


Figure 4-3a (ii): Path loss on Samaru Road (MTN Network) Eastward of BS

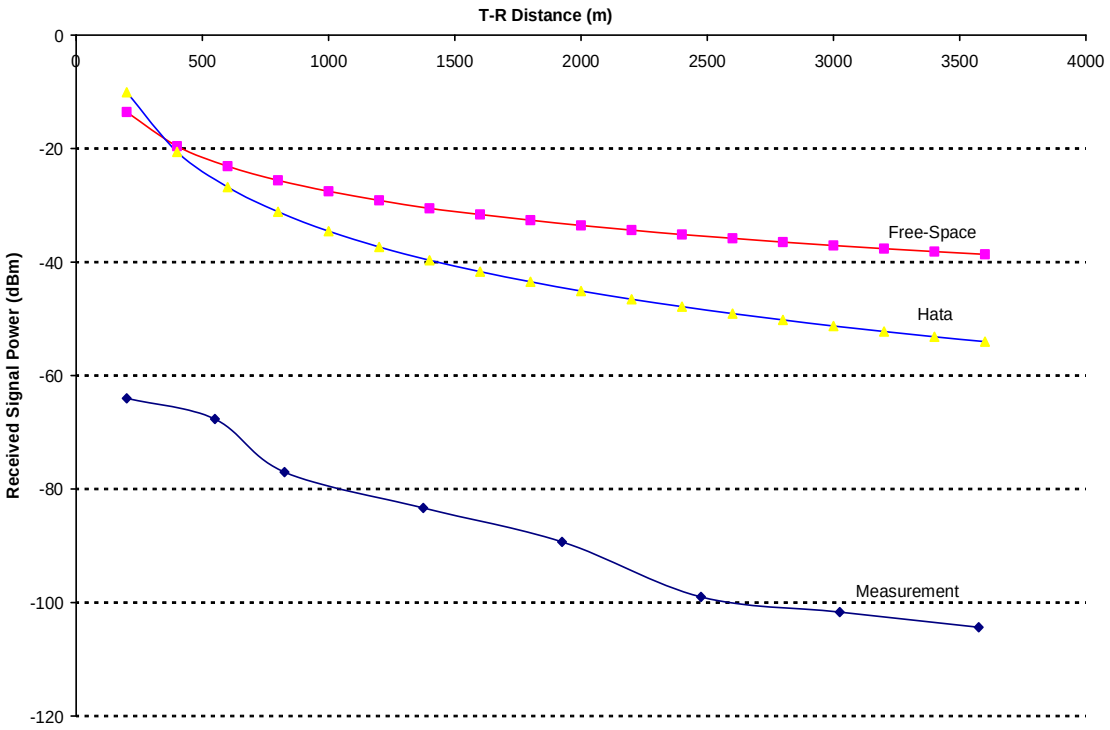


Figure 4-3b (i): Received Signal Power on Samaru Road (MTN Network) Southward of BS

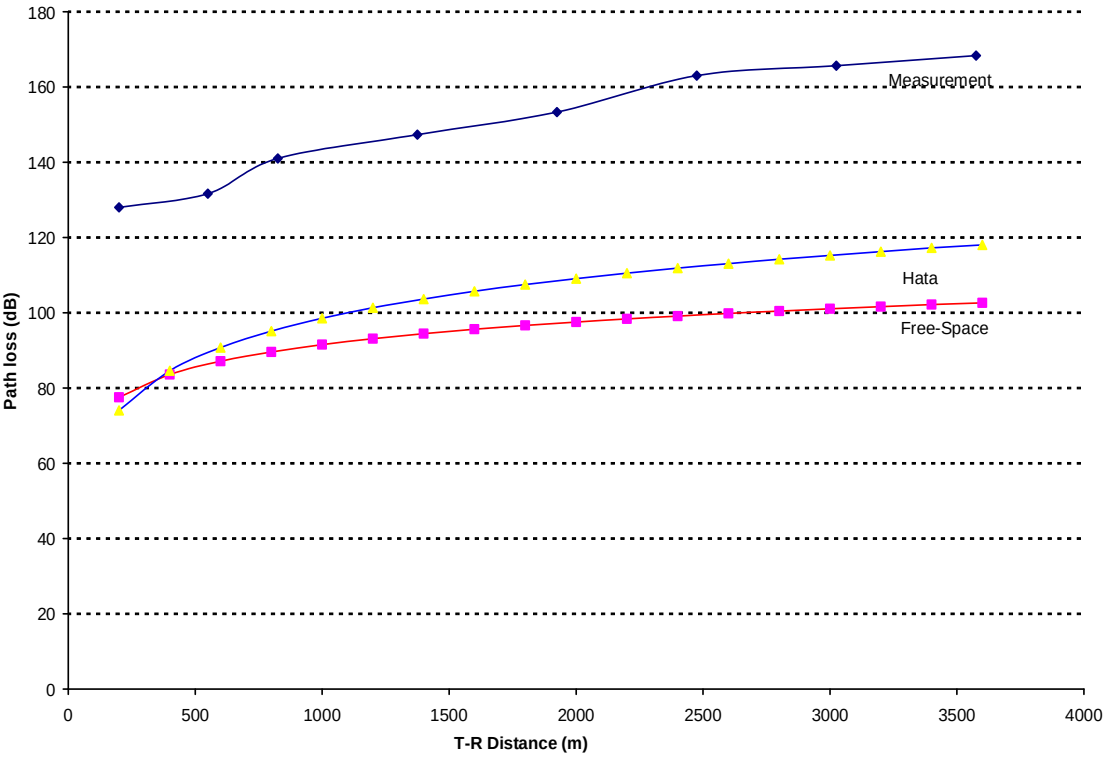


Figure 4-3b (ii): Path loss on Samaru Road (MTN Network) Southward of BS

Table 4-4: Averaged Measured Received Signal Power and Computed Path loss for Kaduna Road, [Glo Network]; P_T = 47 dBm, G_T = 17.5 dBi, G_R = 1.76 dB, f_c = 900 MHz

Distance (m)	Received Signal Power, P_R (dBm)	Computed Path loss, L_P (dB)	$EIRP$ (dBm)
200.00	-67.67	132.17	64.50
550.00	-74.12	138.62	64.50
825.00	-75.45	139.95	64.50
1375.00	-87.00	151.50	64.50
1925.00	-84.33	148.83	64.50
2475.00	-99.67	164.17	64.50

Table 4-5: Averaged Measured Received Signal Power and Computed Path loss for Kano Road, [Glo Network]; P_T = 47 dBm, G_T = 17.5 dBi, G_R = 1.76 dB, f_c = 900 MHz

Distance (m)	Received Signal Power (dBm)	Computed Path loss, L_P (dB)	$EIRP$ (dBm)
200.00	-67.67	132.17	64.50
550.00	-69.23	133.73	64.50
825.00	-78.78	143.28	64.50
1375.00	-83.67	148.17	64.50
1925.00	-77.00	141.50	64.50
2475.00	-98.33	162.83	64.50
2750.00	-101.89	166.39	64.50

Table 4-6 (a): Averaged Measured Received Signal Power and Computed Path loss for Samaru Road. Glo Network] - Eastward of BS; P_T = 47 dBm, G_T = 17.5 dBi, G_R = 1.76 dB, f_c = 900 MHz

Distance (m)	Received Signal Power (dBm)	Computed Path loss, L_P (dB)	$EIRP$ (dBm)
50.00	-67.00	131.50	64.50
550.00	-70.78	135.28	64.50
825.00	-77.67	142.17	64.50
1375.00	-80.23	144.73	64.50
1925.00	-85.45	149.95	64.50
2475.00	-92.22	156.72	64.50

Table 4-6 (b): Averaged Measured Received Signal Power and Computed Path loss for Samaru Road. [Glo Network] - Southward of BS; P_T = 47 dBm, G_T = 17.5 dBi, G_R = 1.76 dB, f_c = 900 MHz

Distance (m)	Received Signal Power (dBm)	Computed Path loss, L_P (dB)	$EIRP$ (dBm)
50.00	-63.67	128.17	64.50
550.00	-75.45	139.95	64.50
825.00	-69.22	133.72	64.50
1375.00	-74.12	138.62	64.50
1925.00	-77.00	141.50	64.50
2475.00	-98.33	162.83	64.50

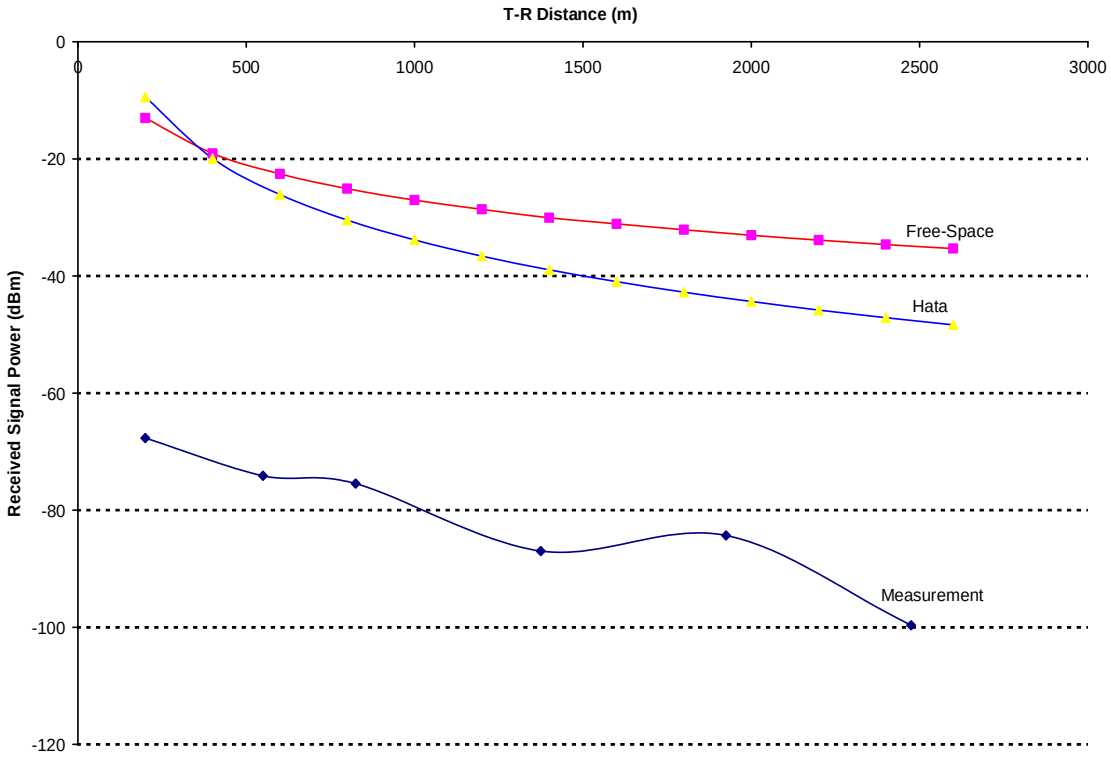


Figure 4-4a: Received Signal Power on Kaduna Road (GLO BS)

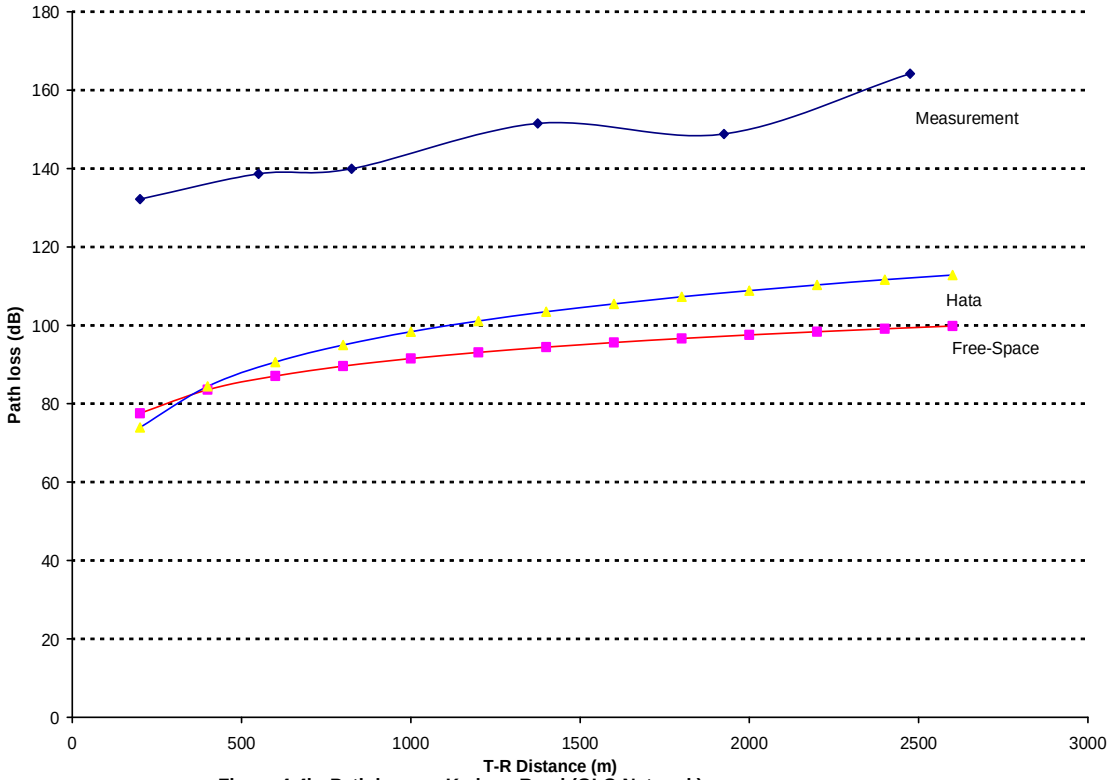


Figure 4-4b: Path loss on Kaduna Road (GLO Network)

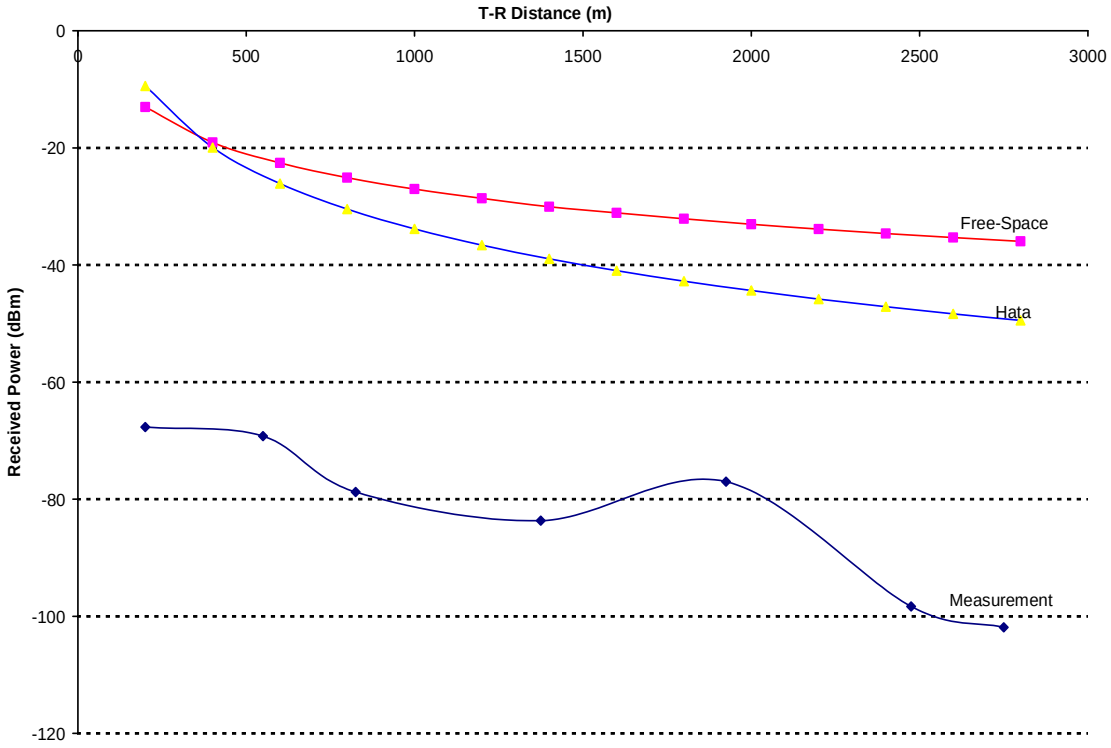


Figure 4-5a: Received Signal Power on Kano Road (GLO BS)

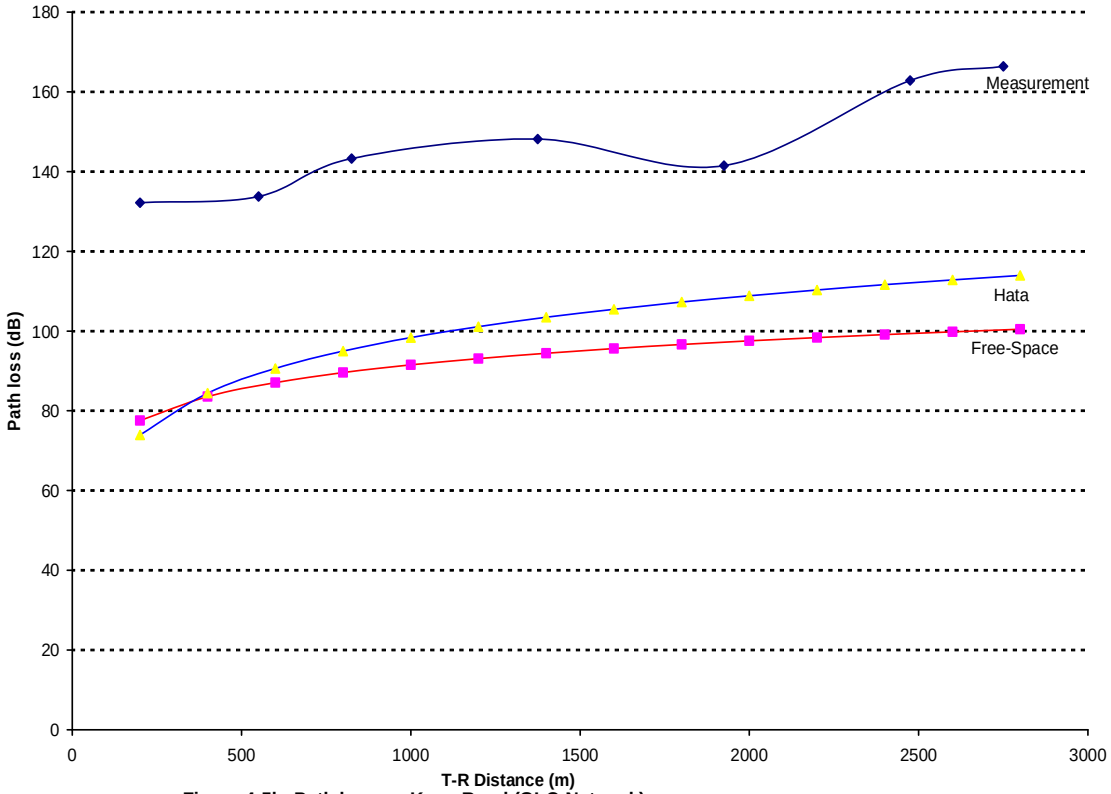


Figure 4-5b: Path loss on Kano Road (GLO Network)

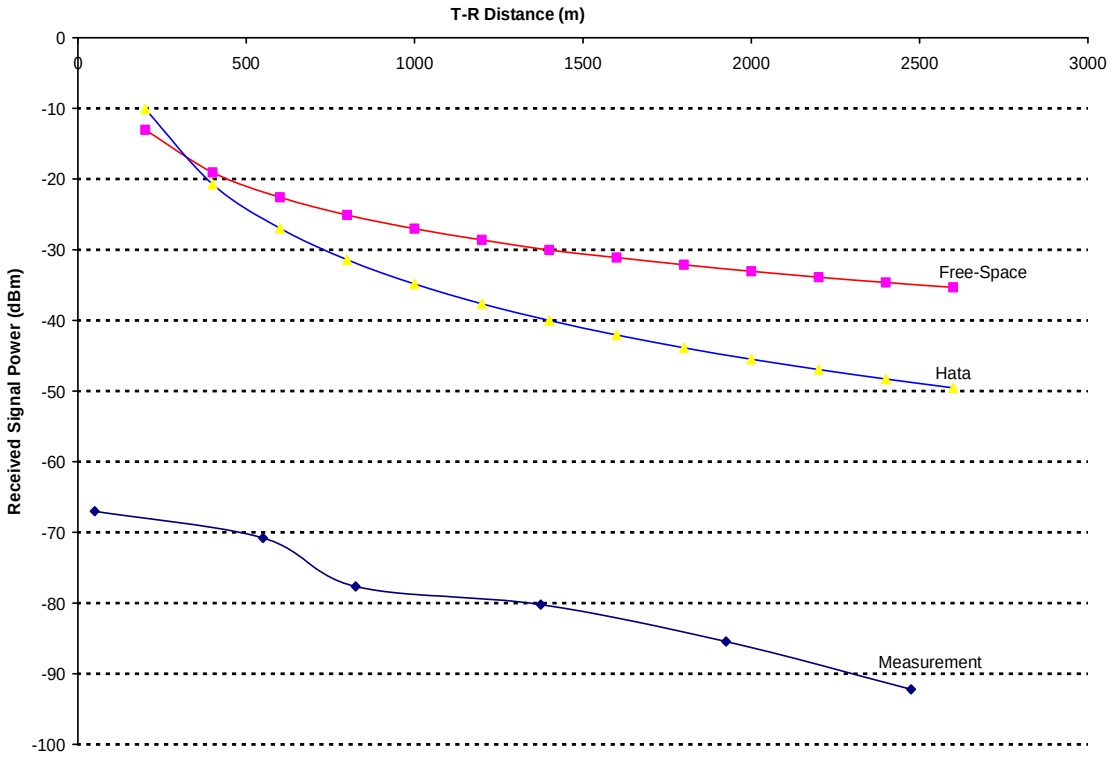


Figure 4-6a (i): Received Signal Power on Samaru Road (GLO Network) - Eastward of BS

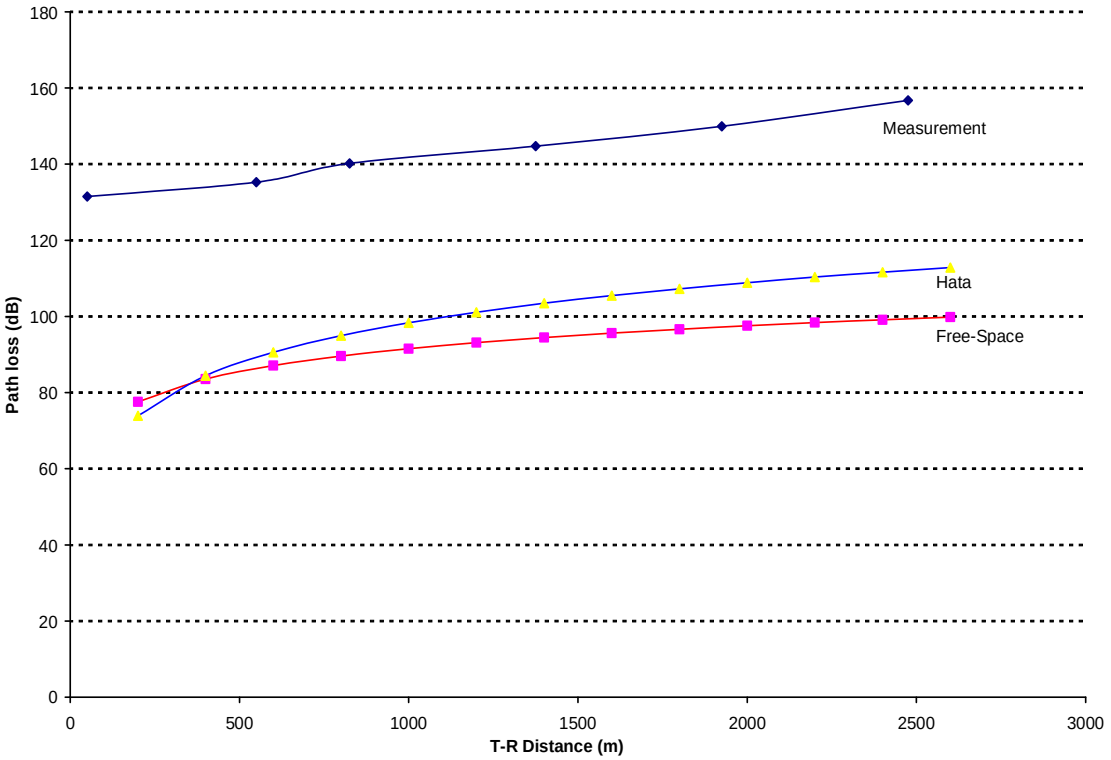


Figure 4-6a (ii): Path loss on Samaru Road (GLO Network) Eastward of BS

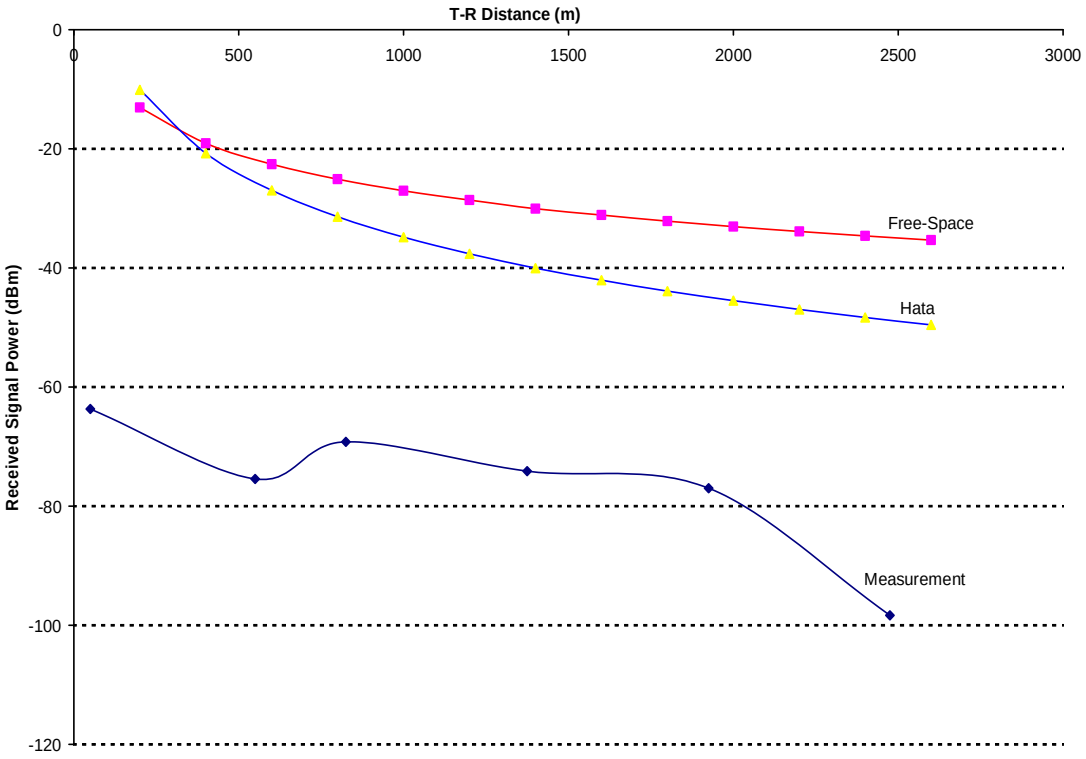


Figure 4-6b (i): Received Signal Power on Samaru Road (GLO Network) Southward of BS

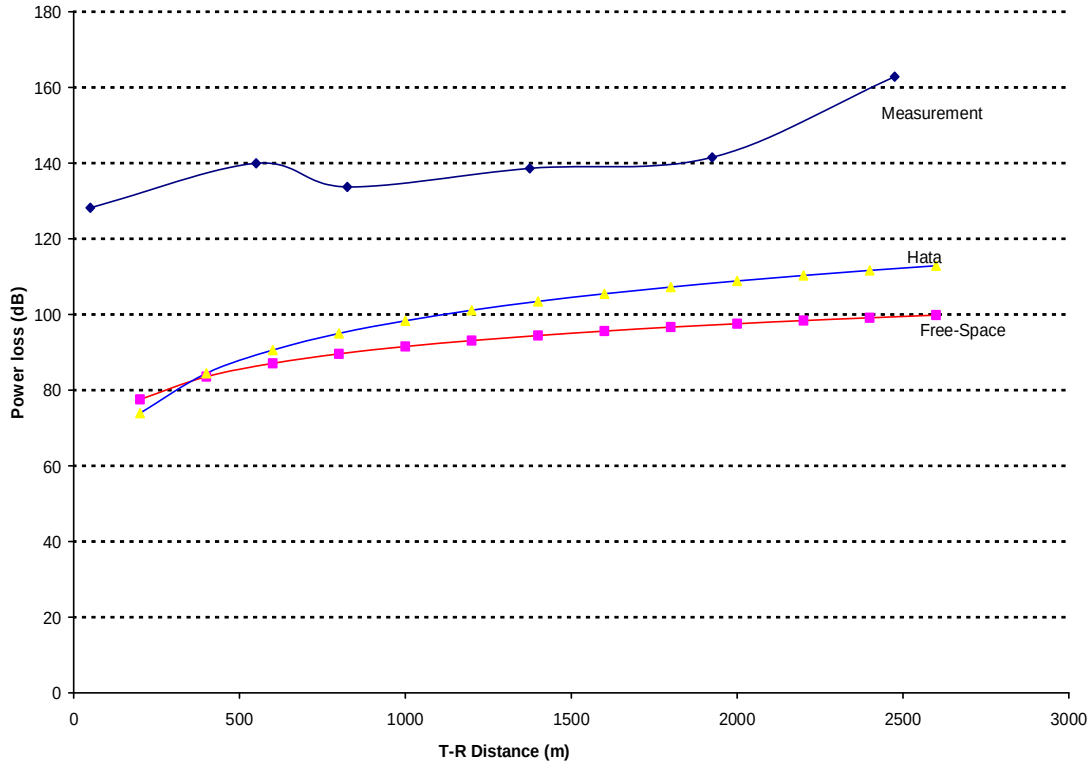


Figure 4-6b (ii): Path loss on Samaru Road (GLO Network) Southward of BS

4.4.2 Scenario 2

In this scenario, data obtained from measurements of received signal power at various receiving locations in the measurement area discussed in section 3.2.2 were averaged using the expression:

$$\overline{\text{RxPOW}} \quad \text{at } P_{R\,m}\Big|_{\text{m = 1 to k}} = \frac{\sum_{\tau=1}^{N} \left(RxPOW\right)_{\tau}}{N} \qquad (4\text{-}21)$$

where $P_{R\,m}$ is the averaged received signal power at each of the measurement locations, m, k = 7, is the number of the measurement locations along the trajectory. $\left(RxPOW\right)_{\tau}$ is the received signal power at each of the time interval τ, and N = 21, is the total number of time intervals measurements were taken.

The values obtained are given in table 4-7.

Table 4-7: Averaged received signal power along the trajectory within the Complex; f_c = 900 MHz

Receiver Point	P1	P2	P3	P4	P5	P6	P7
RxPOW (dBm)	-69.00	-75.35	-78.02	-82.27	-85.13	-82.46	-89.25
Distance (m) along the trajectory	0	5	10	15	20	25	30

Similarly, predicted received signal powers at each of the receiver locations along the trajectory were computed using equations (3-9) and (3-10) in section 3.3 and the ray parameters in table 3-1. This computation is in two parts; part one consists of the received signal power at each of the locations as a result of ray paths through the senate building, the Kashim Ibrahim Library, the Ribadu Halls and finally the locations on the trajectory. Part two consists of the ray path that is singly reflected by the Electrical Engineering block before finally reaching the receiver locations along the trajectory. The resultant received power at each of the locations was then taken as the summation of the received power along these two paths. Values obtained are shown in tables 4-8 to 4-10. Received signal power for both measurements and prediction is also shown in figure 4-7. The sum of the received powers along these two parts is given in table 4-10.

Table 4-8: Received signal power at each of the receiver locations along ray paths 1 (prediction); f_c = 900 MHz

Receiver Point	P1	P2	P3	P4	P5	P6	P7
RxPOW (dBm)	-22.77	-44.52	-43.43	-41.53	-39.29	-37.73	-36.80
Distance (m) along the trajectory	0	5	10	15	20	25	30

Table 4-9: Received signal power at each of the receiver locations along ray paths 2 (prediction); f_c = 900 MHz

Receiver Point	P1	P2	P3	P4	P5	P6	P7
RxPOW (dBm)	-30.08	-29.96	-29.81	-29.64	-29.43	-29.22	-29.09

Distance (m) along the trajectory	0	5	10	15	20	25	30

Table 4-10: Sum of Received signal powers along the two ray paths (prediction); f_c = 900 MHz

Receiver Point	P1	P2	P3	P4	P5	P6	P7
RxPOW (dBm)	-52.85	-74.48	-73.24	-71.17	-68.72	-66.95	-65.89
Distance (m) along the trajectory	0	5	10	15	20	25	30

The plot of prediction and measurement results is shown in figure 4.7

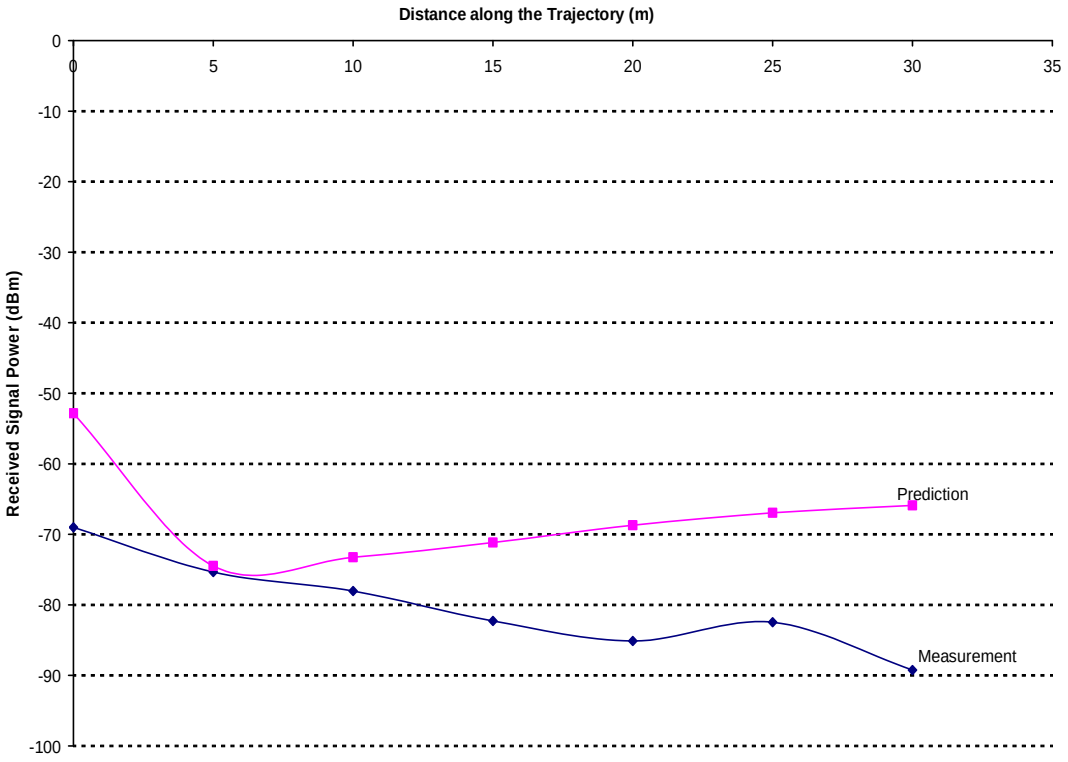


Figure 4.7: Received Signal Power within the Engineering Complex

It should be noted that the distance (m) in tables 4-7 to 4-10 and figure 4.7 is that between the receiving locations along the trajectory and not the one used for the computation. The distances used in the computation are shown in table 3-1.

4.5 Differences between Measurements and Prediction Results for Scenario 1 and 2

From the plotted graphs of figures 4-1 to 4-7, a comparison was made between the values of received signal power and path loss obtained from both measurements and predictions at regular distance of 500 m for scenario 1 (see Appendix D). Similarly, for scenario 2, using figure 4-7, a comparison was also made between these values along the trajectory within the Engineering complex. For both scenarios, the differences were determined using the expression:

$$\textit{Difference} = \textit{(Prediction values)} - \textit{(Measurement values)} \qquad (4\text{-}22)$$

The mean difference was then computed using:

$$\textit{Mean difference} = \left(\frac{\sum differences}{N} \right) \qquad (4\text{-}23)$$

The differences are given in tables 4.5.1 to 4.5.17 in appendix D.

For the Free-Space and the Hata models applied to scenario 1, the total mean difference was found to be +55.45 dBm and -42.58 dB respectively for MTN network. For the GLO network, these values are respectively +54.01 dBm and -42.92 dB. Similarly, the total mean difference for the modified Two-Ray model used for the Engineering complex was found to be +12.60 dBm.

4.6 Proposed Modification of the Free-Space, Hata and the Modified Two-Ray Model

From figures 4-1 to 4-7, it is obvious that the considered models are not suitable for the scenarios studied in this investigation going by the differences between the measured and the predicted received signal powers and the computed path losses. Therefore, a modification is

necessary to these models. Using the respective computed differences obtained in the last section, which are termed the correction factors, F_c , the following modified models are proposed for the scenarios studied in this investigation.

$$P_R \text{ (Modified)} = [34.23 - 20\log d] - F_{C1,MTN}$$

i.e. $$P_R \text{ (Modified)} = [34.23 - 20\log d] - 55.45 \text{ dBm} \quad (4\text{-}24)$$

for MTN Network,

and $$P_R \text{ (Modified)} = [34.73 - 20\log d] - F_{C1,Glo}$$

$$= [34.73 - 20\log d] - 54.01 \text{ dBm} \quad (4\text{-}25)$$

for GLO Network.

Averaging the P_R (Modified) over the two networks, we have:

$$P_R \textbf{ (Modified)} = [34.48 - 20\log d] - 54.73 \textbf{ dBm} \quad \textbf{(4-26)}$$

In the same manner the modified model of Hata is given as:

$$L_{50} \text{ (Modified)} = [98.54 + 35.04\log d] + F_{C2,MTN}$$

$$= [98.54 + 35.04\log d] + 42.58 \text{ dB} \quad (4\text{-}27)$$

for MTN Network. For GLO network on Kaduna/Kano roads,

$$L_{50} \text{ (Modified)} = [98.35 + 34.95\log d] + F_{C2,GLO}$$

$$= [98.35 + 34.95\log d] + 42.92 \text{ dB} \quad (4\text{-}28)$$

Similarly, for GLO Networks on Samaru road;

$$L_{50} \text{ (Modified)} = [99.34 + 35.42\log d] + F_{C2,GLO}$$

$$= [99.34 + 35.42\log d] + 42.92 \text{ dB} \quad (4\text{-}29)$$

Averaging the L_{50} (Modified) over the two networks, we have:

$$L_{50}\ \textbf{\textit{(Modified)}} = [98.74 + 35.14\log d] + 42.81\ \textbf{\textit{dB}} \qquad \textbf{\textit{(4-30)}}$$

It should be noted that the foregoing modified expressions for the received signal power and path loss are for 900 MHz BS transmitter frequency. To obtain equivalent expressions at 1800 MHz, the observed difference of -6.02 dBm and 4.47 dB should be added respectively.

For the modified Two-Ray model, the modified expression for received signal power along the trajectory for the purpose of the second scenario in this study is given as:

$$P_{R1} = \left[P_T + G_T + G_R + 20\log\left(\frac{\lambda}{4\pi}\right)\left(\frac{1}{d_1} + \frac{1}{d_2}\Gamma(\theta)\right)\right] - F_C$$

$$= \left[65.67 - 31.53\left(\frac{1}{d_{01}} + \frac{1}{d_{03} + l_1}\Gamma(\theta)\right)\right] \textbf{\textit{-12.60 dBm}} \qquad (4\text{-}31)$$

for the receiver location 1.

For the receiver locations 2-7, the modified expression is:

$$P_{R2-7} = \left[P_T + G_T + G_R + 20\log\left(\frac{\lambda}{4\pi}\right)\left(\frac{1}{d_i}\Gamma(\theta_i) + \frac{1}{\sum d}\prod_q \Gamma qi\right)\right] - F_C$$

$$= \left[65.76 - 31.53\left(\frac{1}{d_i}\Gamma(\theta_i) + \frac{1}{\sum d}\prod_q \Gamma qi\right)\right] - 12.60\ dBm \qquad \textbf{\textit{(4-32)}}$$

Values of P_R and L_P obtained from the new models are given in table 4-11 and 4-12 for scenario 1 and 2 respectively while the plots are shown in figures 4.8 to 4.10.

Table 4-11 showing P_R and L_P (f_c = 900 MHz) for Scenario 1

Distance (in m)	P_R (in dBm)	L_P (in dB)
200	-66.22	116.99
400	-72.24	127.57
600	-75.76	133.75
800	-78.26	138.14
1000	-80.20	141.55
1200	-81.78	144.33
1400	-83.12	146.68
1600	-84.28	148.72
1800	-85.31	150.52
2000	-86.22	152.13
2200	-87.05	153.58
2400	-87.80	154.91
2600	-88.50	156.13
2800	-89.14	157.26
3000	-89.74	158.32
3200	-90.30	159.30
3400	-90.83	160.23
3600	-91.33	161.10

Table 4-12 showing P_R s along the trajectory in Scenario 2; f_c = 900 MHz

Receiver Point	P1	P2	P3	P4	P5	P6	P7
P_R (in dBm)	-65.45	-87.08	-85.84	-83.77	-81.32	-79.55	-78.49
Distance along the Trajectory	0	5	10	15	20	25	30

The new proposed models are coded in C Programming Language (see Appendix D for the C Program Code). Tables 4-11 and 4-13 show a summary of the parameters that are inputs to the codes and the results obtained.

Table 4-13: Input Parameters to the C Program Code for Scenario 2; f_c = 900 MHz

Receiver Location	Angle of Incidence for location 1/Path 1 (degrees)	Total Path length for Location 1/Path 1 (m)	Direct/Total Path Length for Location1/ Path 2 (m)	1st Angle of Incidence (in degrees)	2nd Angle of incidence (in degrees)	3rd Angle of incidence (in degrees)	P_R (dBm)
P1	76.0	707.2	708.0	-	-	-	-65.45
P2	72.0	708.8	1468.8	26.5	63.0	43.0	-87.08
P3	68.0	710.4	1468.8	26.5	54.0	38.0	-85.84
P4	64.3	712.0	1471.2	26.5	42.5	29.5	-83.77
P5	60.0	715.2	1490.4	26.5	31.0	20.0	-81.32
P6	56.3	718.4	1586.4	26.5	21.5	12.5	-79.55
P7	53.8	723.2	1641.6	26.5	16.0	8.5	-78.49

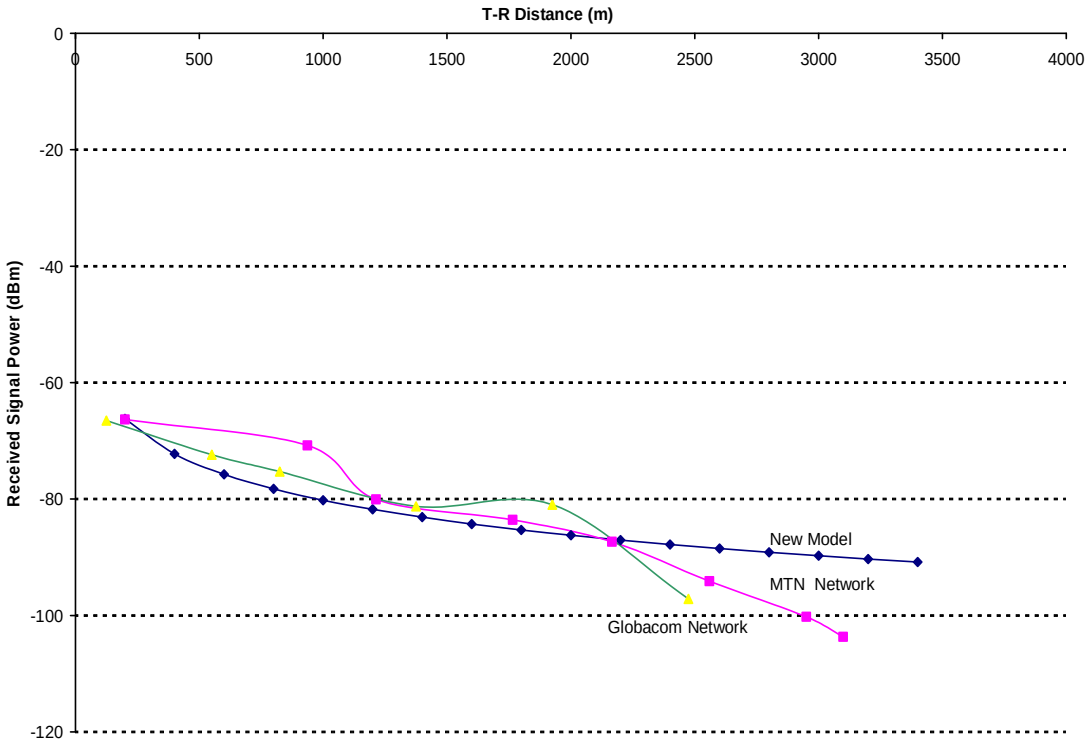


Figure 4.8: New Proposed Prediction Model Versus Averaged Measured Received Signal Power for Scenario 1

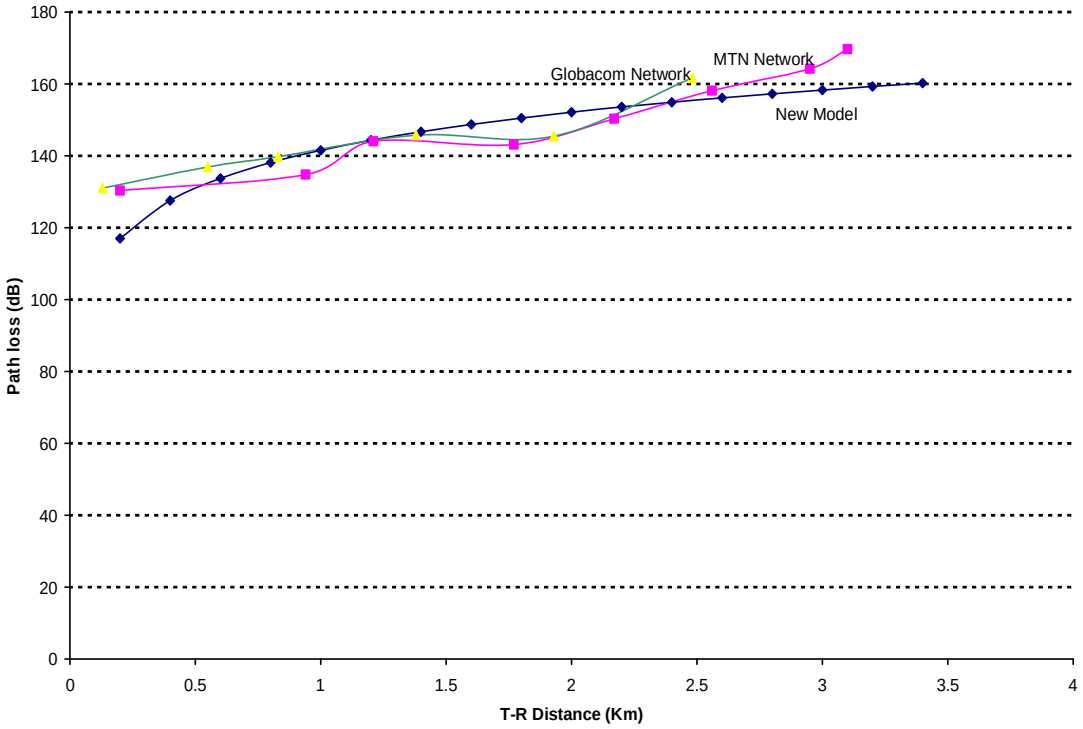


Figure 4.9: New Proposed Prediction Model Versus Computed Path Loss for Scenario 1

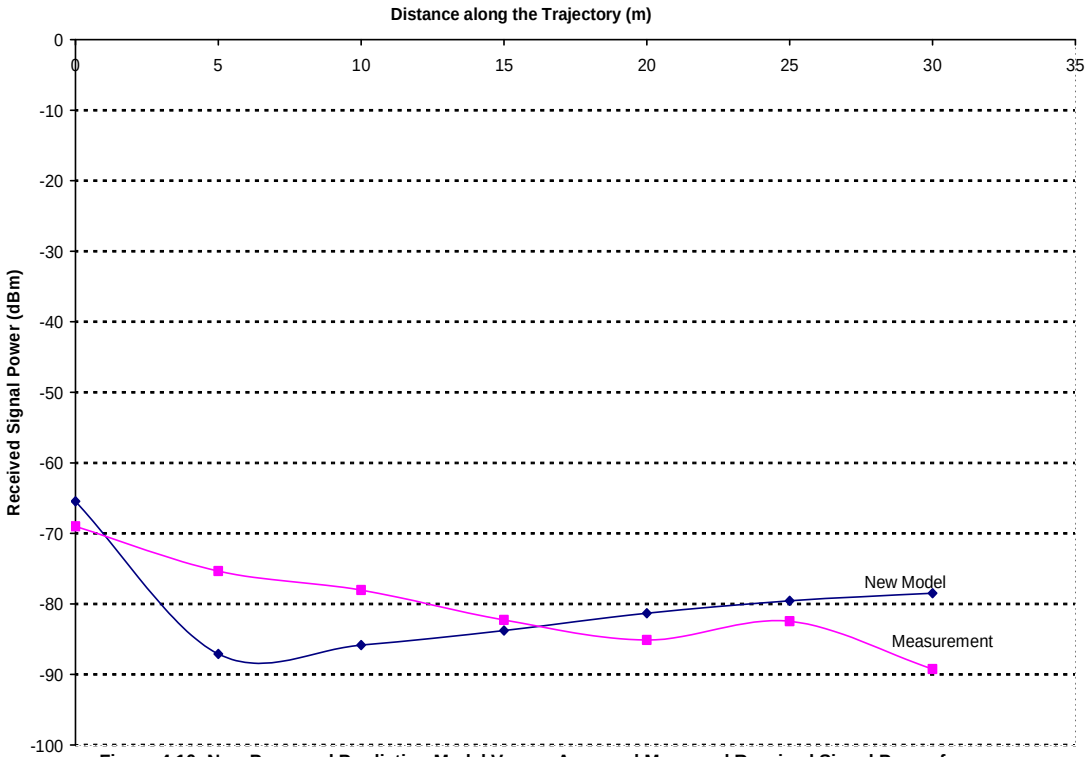


Figure 4.10: New Proposed Prediction Model Versus Averaged Measured Received Signal Power for Scenario 2

4.7 Discussion and Interpretation of Results

In this study, existing propagation models of Free-Space, Hata, and Walfisch/Ikegami were closely examined. Similarly, measurements were carried out on the selected base stations in order to obtain the nature of the variations of some narrowband properties of the channel, mainly the received signal power and path loss along the radio path. The values obtained were plotted and the results compared.

First and foremost, the Walfisch/Ikegami model for open/rural areas was found to give, approximately, same values of path loss, and consequently, same values of received signal power as that of Free-Space model. For this reason, it was not considered any further.

A closer look at figures 4-1 to 4-7 shows that the variations of the received signal power and path loss with distance, on the plotted curves of Free-Space and Hata, are exponential in a

somewhat linear manner. However, the measurement curves reveal, a non-linear exponential variation as ‘rises’ and ‘falls’ are noticed along the length of the curves. This possibly is due to other parameters of the channels that were not taken into consideration in the models.

Therefore, from the preceding analyses, it could be stated that given the complexity of the cellular radio channels and the somewhat simple phenomena considered by the models, the difference between prediction and measurement results are reasonable. For received signal power and path loss, the averaged differences are 54.73 dBm and 42.81 dB respectively, for scenario 1 (see tables 4.5.1 through 4.5.16 in Appendix D). This is because the Free-Space model applied to scenario 1 is a free-space propagation loss equation, and is mainly a function of transmitter frequency and BS-MS separation distance at the exclusion of other factors. As a matter of fact, the radio channel in scenario 1 in this study is far removed from free space. Although the receiver experienced direct line -of-sight (LOS) with the BS antenna especially within the first few hundred meters from the BS, thereafter it experienced a combination of other phenomena such as obstructed LOS due to curvatures of the roads, reflections and scattering by the road surface, variations of the terrains topography, etc. These explain why the values of averaged received signal powers from measurements are lower than those obtained through predictions. Because these other phenomena are difficult to model, the total mean difference of 54.73 dBm for both MTN and GLO networks by which these phenomena can be approximated, provide an appropriate correction factor to the Free-Space model.

For the Hata model, the predicted path loss values are observed to be higher than those of Free-Space for the same BS-MS separation distance (see figures 4-1 to 4-6). This is because the Hata model considered transmitter and receiver height in addition to the transmitter

frequency and BS-MS separation distance. However, these values of path loss are still lower than those obtained from measurements owing to the sundry other phenomena in the radio channel mentioned above, and the fact that the Hata model was developed for some propagation scenarios in Japan. Consequently, the total mean difference of 42.81 dB for both MTN and GLO networks, account for this observed difference and serve as correction factor to the model of Hata for scenario 1 in this investigation. Furthermore, from equations (4-2) and (4-3), (4-4) and (4-5), it was noted that the received signal powers decrease by 6.02 dBm for every doubling of the radio frequency and also for every doubling of the distance. Similarly, from equations (4-11) and (4-12), (4-13) and (4-14), (4-15) and (4-16), it was noted that the path loss values also increase by 4.47 dB for every doubling of the frequency. Therefore, when the values of the received signal power and path loss are computed at 900 MHz, corresponding values at 1800 MHz can be obtained by using these constants.

In addition, from tables 4-1, 4-2, and 4-3, it can be seen that the measured signal power near the circumference of the cells of MTN BSs on Kaduna/Kano and Samaru roads exceed the minimum values of 102 dBm necessary for BS-MS good link. The implication of this is that any communication link between the BS and a mobile would be terminated when the mobile comes within this distance ($\approx\geq$ 3.00 Km) from the BS. This, however, is not the case on these roads on Glo BSs.

In the second scenario, shadowing and multipath propagation characteristics of the radio signal were studied. Values of the averaged received signal power from measurements are seen to be lower than those from prediction at all the receiver locations. This is because the modified Two-Ray model used in the prediction considered only direct rays and wall-reflected rays that are simple propagation phenomena. Complex phenomena like diffraction

by wall corners, building transmissions and scattering by trees are not included in the model, and these explain the observed difference. This difference is made up for by the total mean difference of 12.60 dBm (see table 4.5.17 in Appendix D). This value serves as the correction factor with which the model is corrected to approximate measurement values. The averaged measurement values of received signal power revealed the shadowing effects of the Mechanical building, which obstructed the LOS from the BS. The value was highest at P1 which was a direct LOS from the BS and decreased along the trajectory as the receiver moved from the lit region to the shadow region.

CHAPTER FIVE

CONCLUSIONS AND RECOMMENDATIONS

5.0 Introduction

This chapter provides a summary of the results obtained as well as their significance and applications. This is followed with limitations, problems encountered and the solutions proffered to solve these problems. It rounds off with conclusions and recommendations for further work.

5.1 Summary of Results

In this investigation, it was discovered that the MTN BSs in the first scenario performed below optimum as the measured signal power near the circumference of the cells fell below the minimum values of -102 dBm necessary for good BS-MS link. This was not the case for Glo BSs as the measured signal power did not fall below the minimum required value of -104 dBm anywhere along the propagation path. Also multipath and shadowing effects appeared to have contributed to the received signal power degradation in the second scenario. Finally, new models were developed by modifying some existing ones; and could be used for the prediction of the received signal power and the propagation path losses along the radio paths, in the Nigerian environments. These new models are:

$$P_R \text{ (Modified)} = [34.48 - 20\log d] - 54.73 \quad \textbf{dBm}$$

$$L_{50} \text{ (Modified)} = [98.74 + 35.14\log d] + 42.81 \quad \textbf{dB}$$

for the received signal power and propagation path loss respectively, for scenario 1; and for scenario 2, the expressions for the received signal power are:

$$P_{R1} = \left[P_T + G_T + G_R + 20\log\left(\frac{\lambda}{4\pi}\right)\left(\frac{1}{d_1} + \frac{1}{d_2}\Gamma(\theta)\right)\right] - F_C$$

$$= \left[65.67 - 31.53\left(\frac{1}{d_{01}} + \frac{1}{d_{03} + l_1}\Gamma(\theta)\right)\right] \textbf{\textit{-12.60 dBm}}$$

for the receiver location 1, and

$$P_{R2-7} = \left[P_T + G_T + G_R + 20\log\left(\frac{\lambda}{4\pi}\right)\left(\frac{1}{d_i}\Gamma(\theta_i) + \frac{1}{\sum d}\prod_q \Gamma qi\right)\right] - F_C$$

$$= \left[65.76 - 31.53\left(\frac{1}{d_i}\Gamma(\theta_i) + \frac{1}{\sum d}\prod_q \Gamma qi\right)\right] - 12.60\ dBm \qquad \textbf{\textit{(4-32)}}$$

for the receiver locations 2-7

5.2 Significance of Results and Applications

The results obtained in this research are significant in that novel formulae for obtaining received signal powers and propagation path losses in some selected Nigerian environments have been obtained. The significance of the results also lies in the mean differences between results obtained using the new proposed models and the existing Free-Space Loss Model and the Hata Model, for the prediction of received signal powers, P_Rs and propagation path losses, L_ps. For scenario 1 studied in this investigation, the averaged differences of 54.73 dBm and 42.81 dB for P_Rs and L_ps between the new model and the existing Free-Space Loss Model and the Hata Model, respectively, are too significant to be neglected. Similarly, for scenario 2, the averaged difference of 12.60 dBm between the new proposed model and the existing modified Two-Ray Model is also too significant to be neglected.

The results of this investigation have relevant applications in the Cellular Mobile Telephone Industry in Nigeria as the new proposed models can be used in network planning

- for prediction of P_Rs over a given propagation path (rural and urban) prior to actual system deployment.
- for prediction of L_ps over a given propagation path (rural) prior to actual system deployment.
- as a mean of determining performance (in terms of signal strength levels) of a given Cellular Mobile Telephone System's network by using the new models to determine P_Rs and L_ps and comparing these value with minimum required values for good BS-MS link.

5.3 Limitations, Problems Encountered and Solutions Proffered

Main limitations confronted in the course of this work were:

- Unavailability of sophisticated communication equipment that could be used for the measurement data collection. This necessitated the method adopted in this work. Consequently, this limited the number of samples and the accuracy of the measurement data used.
- The prediction in scenario 2 was largely dependent on the database of the area as contained in the cadastral map. Therefore, the accuracy of the prediction would depend on the accuracy of this map.

Some main problems encountered and the solutions proffered were:

- Unavailability of official data on the parameters of the Base Stations studied posed a serious problem. Use had to be made of the data obtained from staff in the establishments. This was greatly time-wasting as these data could not be obtained in good time, and was also responsible for the delay in completing the investigation.

- Lack of a device that could be used to ascertain the BSs' transmitter power over the period of days the measurements were being taken. Therefore, the transmitter power for both MTN and Glo BSs were assumed to be constant.

5.4 Conclusions

The subject of this thesis has been the study of Cellular Mobile Radio Propagation Characteristics taking the MTN and GLO networks as the case study. The Phenomena that characterize propagation of Cellular Mobile Radio signals such as path loss, shadowing and multipath, were examined. Furthermore, the impacts of these propagation characteristics on the narrowband properties of the signals; namely the received signal power and path loss along the radio paths, have been studied. From the results obtained, it can be stated that the objectives for which this investigation was embarked upon have been achieved. For example, it was discovered in scenario 1 that the performance of MTN networks in the areas studied would be below optimum as subscribers would experience lost of signals toward the circumference of the cells. This is because values of received signal power at these locations were below the minimum required level for good link. Obviously, this is quite undesirable. In addition, a solution has been proffered to the problem of prediction of the narrowband properties as the proposed models for these quantities can be used for their prediction prior to system deployment.

In scenario 2, shadowing and multipath phenomena were seen to contribute to reduction of the received signal power within the Engineering Complex. Although it was noted that the overall received signal power decreases along the trajectory, none of the values was below the minimum required level, probably because the complex is just about 700 to 800 m from the BS. Furthermore, the developed modified Two-Ray model can be used for the prediction

of the received signal power in this scenario. Finally, it is important to state that, due to the limitations highlighted above, the results obtained in this investigation are preliminary. More investigations that take care of these limitations should be conducted in order to improve on these results.

5.5 Recommendations for Further Work

Going by the findings in this research, it is recommended that the management of MTN should deploy more BSs on the outskirts of the current serving cells on the roads considered in the first scenario. This becomes necessary in order to improve the level of received signal powers at these locations. They should also carry out periodic measurements of received signal powers and path loss on their BS's across the country in order to ensure that these values do not fall below the minimum levels required for good link. This is because system performance has been linked to the levels of the received signal powers along the radio paths. Although the same was not observed on Glo BSs studied in this investigation, the management of Glo should also perform regular measurements of received powers and path loss on their networks across the country in order to ensure that these quantities are within tolerable limits. Besides, for further research on this study, it is recommended that the topography of the terrain that constitutes scenario 1 should be included in the modelling of the radio channel. Also, for built-up areas such as the second scenario in this study, other propagation phenomena like diffraction by wall corners, scattering by trees and transmission through the buildings should be included. These will serve to improve the accuracy of the new models.

REFERENCES

[1] Mike Golio (editor): "The RF & Microwave Handbook", CRC Press, London, 2001.

[2] T.S Rappaport: "Wireless Communications: Principles and Practice", Prentice Hall, New Jersey, 1996.

[3] Ray Horak with Mark A. Miller: "Communication Systems and Networks (Voice, Data, and Broadband Technologies)", Wiley Publishing Inc., Indianapolis, 2002.

[4] Vijay K. Garg and Joseph E. Wilkes: "Principles and Applications of GSM", Prentice Hall, New Jersey, 1999.

[5] Nigerian Communications Commission: "*Guidelines on Interconnection of Telecommunications Networks*", Retrieved from www.ncc.gov.ng on February 6, 2004

[6] Okumura, Y., Ohmori, E. and Kawano, T.: "*Field Strength and Its Variability in VHF and UHF Land Mobile Radio Services*", Review Electrical Communications Lab., No. 9-10, pp. 825-873, 1968.

[7] Hata, M: "*Empirical Formula for Propagation Loss in Land Mobile Radio Services*", IEEE Transaction on Vehicular Technology, Vol. VT-29, No. 3, pp 317-325, 1980.

[8] Bullington, K.: "*Radio Propagation for Vehicular Communications*", IEEE Transaction on Vehicular Technology, Vol. VT-26, No 4, 1977.

[9] Walfisch, J. and Bertoni, H.L: "*A Theoretical Model of UHF Propagation in Urban Environments*", IEEE Transaction on Antenna and Propagation, Vol. 36, No. 12, pp 1788-1796, 1988

[10] John Scourias: "*Overview of the Global System for Mobile Communications*", Retrieved from www.shoshin.uwaterloo.ca on February 8, 2004.

[11] Parsons, J.D.: "The Mobile Radio Propagation Channel", Pentech Press, London, 1994.

[12] Flood, J.E: "Telecommunications Networks", Peter Peregrinus, Stevenage, 1975.

[13] Feher, K.: "Wireless Digital Communication: Modulation and Spread Spectrum Applications", Prentice Hall, New Jersey, 1995.

[14] Neskovic, A., Neskovic, N. and Paunovic, G.: "*Modern Approaches in Modeling of Mobile Radio Propagation Environments*", University of Belgrade IEEE Publication, 2000.

[15] Heiska, K.: "*On the Modeling of WCDMA System Performance with Propagation Data*", Electromagnetic Laboratory Report Series, Espoo April, 2004 Retrieved from www.libhut.fi on 12th March, 2005.

[16] Kalbasi, K.: "*Simulation of Interference and Diversity Scenarios Using Propagation Models*", Hewlett-Packard, Retrieved from www.eesof.tm.agilent.co on 1st February, 2005.

[17] Vijay K. Garg, Kenneth F. Smolik and Joseph E. Wilkes: "Applications of CDMA in Wireless/Personal Communications", Prentice Hall Inc, New Jersey, 1997.

[18] Fraser, W.: "Telecommunications: An Introductory Textbook for Engineering Students", Macdonald & Co., London, 1970.

[19] Bertoni, H.L "Radio Propagation for Modern Wireless Systems", Prentice Hall Inc, New Jersey, 2000.

APPENDIX A

Table 1-1: Frequency spectrum and their Typical Uses

Band Designation	**Frequency Range**	**Wavelength**	**Usage**
Audible	20 Hz – 20 KHz	> 100 Km	Acoustics
Extremely/Very Low Frequency (ELF/VLF) Radio	3 KHz – 30 KHz	100 Km – 10 Km	Navigation, Weather, Submarine Communications
Low Frequency (LF) Radio	30 KHz – 300 KHz	10 Km – 1 Km	Navigation, Maritime Communications
Medium Frequency (MF) Radio	300 KHz – 3 MHz	1 Km – 100 m	Navigation, AM Radio
High Frequency (HF) Radio	3 MHz – 30 MHz	100 m – 10 m	Citizens Band (CB) Radio
Very High Frequency (VHF) Radio	30 MHz – 300 MHz	10 m – 1 m	Amateur (HAM) Radio, VHF TV, FM Radio
Ultra High Frequency (UHF) Radio	300 MHz – 3 GHz	1 m – 10 cm	Microwave, Satellite, UHF TV
Super High Frequency (SHF) Radio	3 GHz – 30 GHz	10 cm – 1 cm	Microwave, Satellite
Extremely High Frequency (EHF) Radio	30 GHz – 300 GHz	1 cm – 1 mm	Microwave, Satellite
Infrared	10^3 – 10^5 GHz	300 μm – 3 μm	Infrared
Visible Light	10^{13} – 10^{15} GHz	1 μm – 0.3 μm	Fiber Optics
X – Rays	10^{15} – 10^{18} GHz	10^3 μm – 10^7 μm	X – Rays Examinations
Gamma and Cosmic Rays	$>10^8$ GHz	$<10^7$ μm	Cancer Therapy, Astronomy and Physics

Table 3.2.1.1: Received Signal Power taken on day 1 on MTN BS

KADUNA ROAD f_c = 900MHz		KANO ROAD f_c = 900MHz		SAMARU ROAD f_c = 900MHz		
Distance (m)	Signal Power (dBm)	Distance (m)	Signal Power (dBm)	Distance (m)	Signal Power (dBm)	
					EWBS	SWBS
200.00	- 67.67	200.00	-67.67	50.00	-64.00	-63.50
722.15	- 72.34	1555.40	-72.34	550.00	-66.34	-67.00
1222.10	-72.34	1666.50	-82.34	825.00	-71.01	-73.43
1944.25	-87.00	2133.12	-97.00	1375.00	-74.45	-79.00
2177.56	-77.00	2222.00	-77.00	1925.00	-75.50	-85.00
2499.75	-99.00	2333.10	-72.34	2475.00	-85.00	-94.67
2833.05	-103.50	2444.20	-72.34	3025.00	-101.34	-101.01
		2555.30	-82.34	3575.00	-106.25	-104.70
		2666.40	-101.00			
		2888.60	-106.33			

Table 3.2.1.2 Received Signal Power taken on day 2 on MTN BS

KADUNA ROAD f_c = 900MHz		KANO ROAD f_c = 900MHz		SAMARU ROAD f_c = 900MHz		
Distance (m)	Signal Power (dBm)	Distance (m)	Signal Power (dBm)	Distance (m)	Signal Power (dBm)	
					EWBS	SWBS
200.00	- 67.67	200.00	-67.67	50.00	-68.00	-65.65
1444.30	- 77.00	1388.75	-72.34	550.00	-69.67	-67.34
1777.60	-72.34	1610.95	-82.34	825.00	-74.34	-78.79
2555.35	-77.00	2055.35	-97.00	1375.00	-78.17	-87.66
2777.50	-97.00	2288.66	-77.00	1925.00	-79.10	-92.18
2999.70	-101.00	2644.18	-72.34	2475.00	-86.46	-101.85
		3221.90	-72.34	3025.00	-104.99	-103.00
		3388.55	-82.34	3575.00	-106.50	-103.71
		3532.98	-101.00			

Table 3.2.1.3: Received Signal Power taken on day 3 on MTN BS

KADUNA ROAD f_c = 900MHz		KANO ROAD f_c = 900MHz		SAMARU ROAD f_c = 900MHz		
Distance (m)	Signal Power (dBm)	Distance (m)	Signal Power (dBm)	Distance (m)	Signal Power (dBm)	
					EWBS	SWBS
200	- 67.67	200	-67.67	50.00	-66.00	-62.85
1333.2	- 72.34	1499.85	-77.00	550.00	-67.00	-68.67
1610.95	-77.00	1722.05	-87.00	825.00	-71.67	-78.79
2222.0	-97.00	2022.02	-87.00	1375.00	-78.38	-83.33
2721.95	-99.00	2255.33	-99.00	1925.00	-79.40	-90.81
2833.05	-97.00	2555.3	-101.00	2475.00	-89.54	-100.48
3055.25	-106.33	2755.28	-101.00	3025.00	-103.67	-101.00
		2944.15	-106.33	3575.00	-106.25	-104.70

Table 3.2.1.4: Received Signal Power taken on day 1 on GLO BS

KADUNA ROAD f_c = 900MHz		KANO ROAD f_c = 900MHz		SAMARU ROAD f_c = 900MHz		
Distance (m)	Signal Power (dBm)	Distance (m)	Signal Power (dBm)	Distance (m)	Signal Power (dBm)	
					EWBS	SWBS
200.00	- 67.67	200.00	-67.67	50.00	-97.00	-97.00
550.00	- 72.34	550.00	-72.34	550.00	-67.67	-77.00
825.00	-77.00	825.00	-77.00	825.00	-67.67	-67.67
1375.00	-87.00	1375.00	-87.00	1375.00	-72.34	-82.34
1925.00	-77.00	1925.00	-77.00	1925.00	-77.00	-77.00
2475.00	-97.00	2475.00	-99.00	2475.00	-101.67	-99.00
		2750.00	-101.00			

Table 3.2.1.5: Received Signal Power taken on day 2 on GLO BS

KADUNA ROAD f_c = 900MHz		KANO ROAD f_c = 900MHz		SAMARU ROAD f_c = 900MHz		
Distance (m)	Signal Power (dBm)	Distance (m)	Signal Power (dBm)	Distance (m)	Signal Power (dBm)	
					EWBS	SWBS
200.00	- 67.67	200.00	-67.67	50.00	-77.00	-87.00
550.00	- 67.67	550.00	-67.67	550.00	-72.34	-72.34
825.00	-77.00	825.00	-72.34	825.00	-67.67	-72.34
1375.00	-97.00	1375.00	-87.00	1375.00	-67.67	-67.67
1925.00	-77.00	1925.00	-77.00	1925.00	-77.00	-77.00
2475.00	-101.00	2475.00	-97.00	2475.00	-97.00	-99.00
		2750.00	-103.67			

Table 3.2.1.6 Received Signal Power taken on day 3 on GLO BS

KADUNA ROAD f_c = 900MHz		KANO ROAD f_c = 900MHz		SAMARU ROAD f_c = 900MHz		
Distance (m)	Signal Power (dBm)	Distance (m)	Signal Power (dBm)	Distance (m)	Signal Power (dBm)	
					EWBS	SWBS
200.00	- 67.67	200.00	-67.67	50.00	-87.00	-97.00
550.00	- 82.34	550.00	-67.67	550.00	-72.34	-77.00
825.00	-72.34	825.00	-87.00	825.00	-67.67	-67.67
1375.00	-77.00	1375.00	-77.00	1375.00	-67.67	-72.34
1925.00	-99.00	1925.00	-77.00	1925.00	-72.34	-77.00
2475.00	-101.00	2475.00	-99.00	2475.00	-99.00	-97.00
		2750.00	-101.00			

APPENDIX B

Table 3.2.2.1: Readings taken on day 1 along the trajectory within the Engineering Complex; f_c = 900 MHz

Time (in mins)	RxPOW P_1 (dBm)	RxPOW P_2 (dBm)	RxPOW P_3 (dBm)	RxPOW P_4 (dBm)	RxPOW P_5 (dBm)	RxPOW P_6 (dBm)	RxPOW P_7 (dBm)
00	-67.67	-77.00	-77.00	-97.00	-97.00	-101.00	-101.00
20	-77.00	-77.00	-77.00	-97.00	-101.00	-97.00	-97.00
40	-67.67	-67.67	-77.00	-77.00	-97.00	-97.00	-97.00
60	-67.67	-67.67	-67.67	-77.00	-97.00	-97.00	-97.00
80	-67.67	-77.00	-97.00	-77.00	-97.00	-97.00	-101.00
100	-67.67	-67.67	-77.00	-97.00	-97.00	-97.00	-77.00
120	-67.67	77.00	-77.00	-77.00	-97.00	-77.00	-101.00

Table 3.2.2.2: Readings taken on day 2 along the trajectory within the Engineering Complex; f_c = 900 MHz

Time (in mins)	RxPOW P_1 (dBm)	RxPOW P_2 (dBm)	RxPOW P_3 (dBm)	RxPOW P_4 (dBm)	RxPOW P_5 (dBm)	RxPOW P_6 (dBm)	RxPOW P_7 (dBm)
00	-67.67	-67.67	-67.67	-97.00	-77.00	-67.67	-97.00
20	-67.67	-67.67	-67.67	-97.00	-97.00	-77.00	-77.00
40	-67.67	-67.67	-77.00	-101.00	-97.00	-77.00	-97.00
60	-67.67	-67.67	-77.00	-101.00	-97.00	-77.00	-77.00
80	-67.67	-67.67	-77.00	-77.00	-97.00	-97.00	-97.00
100	-67.67	-67.67	-77.00	-97.00	-77.00	-97.00	-77.00
120	-67.67	-67.67	-77.00	-97.00	-77.00	-97.00	-97.00

Table 3.2.2.3: Readings taken on day 3 along the trajectory within the Engineering Complex; f_c = 900 MHz

Time (in mins)	RxPOW P_1 (dBm)	RxPOW P_2 (dBm)	RxPOW P_3 (dBm)	RxPOW P_4 (dBm)	RxPOW P_5 (dBm)	RxPOW P_6 (dBm)	RxPOW P_7 (dBm)
00	-67.67	-67.67	-77.00	-77.00	-67.67	-77.00	-77.00
20	-77.00	-67.67	-77.00	-77.00	-67.67	-97.00	-101.00
40	-77.00	-67.67	-77.00	-97.00	-97.00	-97.00	-97.00
60	-77.00	-67.67	-77.00	-101.00	-97.00	-97.00	-97.00
80	-67.67	-67.67	-97.00	-77.00	-97.00	-97.00	-101.00
100	-67.67	-67.67	-77.00	-77.00	-77.00	-97.00	-97.00
120	-67.67	-67.67	-77.00	-77.00	-97.00	-77.00	-97.00

APPENDIX C

Table 4.1.1(a) Computed Signal Power and Path loss for Free-Space Model (MTN BS)

Distance (Km)	P_R (in dBm) *For* $f_c = 900$	L_P (dB) *For* $f_c = 900$ *MHz*	P_R (dBm) For $f_c = 1800$	L_P (dB) *For* $f_c = 1800$ *MHz*	$EIRP$ (dBm)
0.2	-11.79	75.79	-17.81	81.81	64.00
0.4	-17.81	81.81	-23.83	87.83	64.00
0.6	-21.33	85.33	-27.35	91.35	64.00
0.8	-23.83	87.83	-29.85	93.85	64.00
1.0	-25.77	89.77	-31.79	95.79	64.00
1.2	-27.35	91.35	-33.37	97.37	64.00
1.4	-28.69	92.69	-34.71	98.71	64.00
1.6	-29.85	93.85	-35.87	99.87	64.00
1.8	-30.88	94.87	-36.90	100.89	64.00
2.0	-31.79	95.79	-37.81	101.81	64.00
2.2	-32.62	96.62	-38.64	102.64	64.00
2.4	-33.37	97.37	-39.39	103.39	64.00
2.6	-34.07	98.07	-40.09	104.09	64.00
2.8	-34.71	98.71	-40.73	104.75	64.00
3.0	-35.31	99.31	-41.33	105.33	64.00

Table 4.1.1 (b): Computed Signal Power and Path loss for Free-Space Model (Glo BS)

Distance (Km)	P_R (dBm) for $f_c = 900$	L_P (in dB) For $f_c = 900$ *MHz*	P_R (in dBm) for $f_c = 1800$	L_P (in dB) for $f_c = 1800$ *MHz*	$EIRP$ (dBm)
0.2	-11.29	75.79	-17.31	81.81	64.50

0.4	-17.31	81.81	-23.33	87.83	64.50
0.6	-20.83	85.33	-26.85	91.35	64.50
0.8	-23.33	87.83	-29.35	93.85	64.50
1.0	-25.27	89.77	-31.29	95.79	64.50
1.2	-26.85	91.35	-32.87	97.37	64.50
1.4	-28.29	92.69	-34.21	98.71	64.50
1.6	-29.35	93.85	-35.37	99.87	64.50
1.8	-30.37	94.87	-36.39	100.89	64.50
2.0	-31.29	95.79	-37.31	101.81	64.50
2.2	-32.12	96.62	-38.14	102.64	64.50
2.4	-32.87	97.37	-38.89	103.39	64.50
2.6	-33.57	98.07	-39.59	104.09	64.50
2.8	-34.21	98.71	-40.23	104.73	64.50
3.0	-34.81	99.31	-40.83	105.33	64.50

Table 4.2.1 (a): Computed Signal Power and path loss for Hata Model (Open/Rural) – MTN BS

Distance (Km)	P_R (in dBm) for $f_c = 900$	L_P (idB) for $f_c = 900$ *MHz*	P_R (dBm) for $f_c = 1800$ *MHz*	L_P (dB) for $f_c = 1800$ *MHz*	$EIRP$ (dBm)
0.2	-10.05	74.05	-14.51	78.51	64.00
0.4	-20.60	84.60	-25.06	89.06	64.00
0.6	-26.77	90.77	-31.23	95.23	64.00
0.8	-31.14	95.14	-35.60	99.60	64.00
1.0	-34.54	98.54	-39.00	103.00	64.00
1.2	-37.32	101.32	-41.77	105.77	64.00

1.4	-39.66	103.66	-44.12	108.12	64.00
1.6	-41.69	105.69	-46.15	110.15	64.00
1.8	-43.48	107.48	-47.94	111.94	64.00
2.0	-45.09	109.09	-49.55	113.55	64.00
2.2	-46.54	110.54	-51.00	115.00	64.00
2.4	-47.86	111.86	-52.32	116.32	64.00
2.6	-49.08	113.08	-53.54	117.54	64.00
2.8	-50.21	114.21	-54.67	118.67	64.00
3.0	-51.26	115.26	-55.72	119.72	64.00

Table 4.2.1 (b): Computed Signal Power and path loss for Hata Model (Open/Rural) – Glo BS, Kaduna/Kano Road

Distance (Km)	P_R (dBm), for $f_c = 900$	L_P (dB) for $f_c = 900$ *MHz*	P_R (dBm) for $f_c = 1800$ *MHz*	L_P (dB) for $f_c = 1800$ *MHz*	$EIRP$ (dBm)
0.2	-9.42	73.92	-13.89	78.39	64.50
0.4	-19.94	84.44	-24.41	88.91	64.50
0.6	-26.10	90.60	-30.57	95.07	64.50
0.8	-30.46	94.96	-34.93	99.43	64.50
1.0	-33.85	98.35	-38.32	102.82	64.50
1.2	-36.62	101.12	-41.09	105.59	64.50
1.4	-38.96	103.46	-43.43	107.93	64.50
1.6	-40.98	105.48	-45.45	109.95	64.50
1.8	-42.77	107.27	-47.24	111.74	64.50
2.0	-44.37	108.87	-48.84	113.34	64.50
2.2	-45.82	110.32	-50.29	114.79	64.50

2.4	-47.14	111.64	-51.61	116.11	64.50
2.6	-48.35	112.85	-52.82	117.32	64.50
2.8	-49.48	113.98	-53.95	118.45	64.50
3.0	-50.53	115.03	-55.00	119.50	64.50

Table 4.2.1 (c): Computed Signal Power and path loss for Hata Model (Open/Rural) – Glo BS, Samaru Road

Distance (Km)	P_R (dBm), for $f_c = 900$	L_P (dB) for $f_c = 900$ *MHz*	P_R (dBm) for $f_c = 1800$	L_P (dB) for $f_c = 1800$ *MHz*	*EIRP* (dBm)
0.2	-10.08	74.58	-14.55	79.05	64.50
0.4	-20.74	85.24	-25.21	89.71	64.50
0.6	-26.98	91.48	-31.45	95.95	64.50
0.8	-31.41	95.91	-35.88	100.38	64.50
1.0	-34.84	99.34	-39.31	103.81	64.50
1.2	-37.64	102.14	-42.11	106.61	64.50
1.4	-40.02	104.52	-44.49	108.99	64.50
1.6	-42.07	106.57	-46.54	111.04	64.50
1.8	-43.88	108.38	-48.35	112.85	64.50
2.0	-45.50	110.00	-49.97	114.47	64.50
2.2	-46.97	111.47	-51.44	115.94	64.50
2.4	-48.31	112.81	-52.78	117.28	64.50
2.6	-49.54	114.04	-54.01	118.51	64.50

2.8	-50.68	115.18	-55.15	119.65	64.50
3.0	-51.74	116.24	-56.21	120.71	64.50

Table 4.3.1 (a): Computed Signal Power and path loss of Walfisch/Ikegami Model - Open/Rural (MTN BS)

Distance (Km)	P_R (dBm), for $f_c = 900$ *MHz*	L_P (dB) for $f_c = 900$ *MHz*	P_R (dBm) for $f_c = 1800$	L_P (dB) *for* $f_c = 1800$ *MHz*	$EIRP$ (dBm)
0.2	-13.50	77.50	-19.53	83.53	64.00
0.4	-19.52	83.52	-25.55	89.55	64.00
0.6	-23.04	87.04	-29.07	93.07	64.00
0.8	-25.54	89.54	-31.57	95.57	64.00
1.0	-27.48	91.48	-33.51	97.51	64.00
1.2	-29.06	93.06	-35.09	99.09	64.00
1.4	-30.40	94.40	-36.43	100.43	64.00
1.6	-31.56	95.56	-37.59	101.59	64.00
1.8	-32.59	96.59	-38.62	102.62	64.00
2.0	-33.50	97.50	-39.53	103.53	64.00
2.2	-34.33	98.33	-40.36	104.36	64.00
2.4	-35.08	99.08	-41.11	105.11	64.00
2.6	-35.79	99.79	-41.81	105.81	64.00

2.8	-36.42	100.42	-42.45	106.45	64.00
3.0	-37.02	101.02	-43.05	107.05	64.00

Table 4.3.1 (b): Computed Signal Power and path loss of Walfisch/Ikegami Model (Open/Rural) (Glo BS)

Distance (Km)	P_R (dBm) for $f_c = 900$ *MHz*	L_P (dB) for $f_c = 900$ *MHz*	P_R (dBm) for $f_c = 1800$ *MHz*	L_P (dB) for $f_c = 1800$ *MHz*	$EIRP$ (dBm)
0.2	-13.00	77.50	-19.03	83.53	64.50
0.4	-19.02	83.52	-25.05	89.55	64.50
0.6	-22.54	87.04	-28.57	93.07	64.50
0.8	-25.04	89.54	-31.07	95.57	64.50
1.0	-26.98	91.48	-33.01	97.51	64.50
1.2	-28.56	93.06	-34.59	99.09	64.50
1.4	-29.90	94.40	-35.93	100.43	64.50
1.6	-31.06	95.56	-37.09	101.59	64.50
1.8	-32.09	96.59	-38.12	102.62	64.50
2.0	-33.00	97.50	-39.03	103.53	64.50
2.2	-33.83	98.33	-39.86	104.36	64.50
2.4	-34.58	99.08	-40.61	105.11	64.50
2.6	-35.29	99.79	-41.31	105.81	64.50
2.8	-35.92	100.42	-41.95	106.45	64.50
3.0	-36.52	101.02	-42.55	107.05	64.50

APPENDIX D

Table 4.5.1: Comparison of Measurements and Prediction using Free-Space Model – Kaduna Road (MTN Network); f_c = 900 MHz

T-R Separation (m)	500	1000	1500	2000	2500	3000
Measured P_R (dBm)	-69.33	-72.67	-86.00	-86.00	-88.00	-104.67
Predicted P_R (dBm)	-21.33	-27.33	-30.67	-33.33	-36.00	-37.33
Difference (dBm)	48.00	45.34	55.33	52.67	52.00	67.34

Table 4.5.2: Comparison of Measurements and Prediction using Hata Model – Kaduna Road (MTN Network) ; f_c = 900 MHz

T-R Separation (m)	500	1000	1500	2000	2500	3000
Measured L_{50} (dB)	132.00	135.00	150.00	140.00	144.00	168.00
Predicted L_{50} (dB)	87.00	97.00	106.00	109.00	112.00	115.00
Difference (dB)	-45.00	-38.00	-44.00	-31.00	-32.00	-53.00

Table 4.5.3: Comparison of Measurements and Prediction using Free-Space Model – Kano Road (MTN Network) ; f_c = 900 MHz

T-R Separation (m)	500	1000	1500	2000	2500	3000
Measured P_R (dBm)	-68.39	-70.32	-73.55	-85.16	-90.97	-97.42
Predicted P_R (dBm)	-21.33	-27.33	-30.67	-33.33	-36.00	-37.33
Difference (dBm)	47.06	42.99	42.88	51.83	54.97	60.09

Table 4.5.4: Comparison of Measurements and Prediction using Hata Model – Kano Road (MTN Network); f_c = 900 MHz

T-R Separation (m)	500	1000	1500	2000	2500	3000
Measured L_{50} (dB)	132.00	136.00	138.00	149.00	154.00	161.00
Predicted L_{50} (dB)	87.00	97.00	106.00	109.00	112.00	115.00
Difference (dB)	-45.00	-39.00	-32.00	-40.00	-42.00	-46.00

Table 4.5.5: Comparison of Measurements and Prediction using Free-Space Model – Samaru Road– Eastward of BS (MTN Network) ; f_c = 900 MHz

T-R Separation (m)	500	1000	1500	2000	2500	3000	3500
Measured P_R (dBm)	-68.00	-72.00	-77.33	-80.00	-87.33	-102.67	-106.00
Predicted P_R (dBm)	-21.33	-27.33	-30.67	-33.33	-36.00	-37.33	-38.00
Difference (dBm)	46.67	44.67	46.66	46.67	51.33	65.34	68.00

Table 4.5.6: Comparison of Measurements and Hata Model – Samaru Road– Eastward of BS (MTN Network) ; f_c = 900 MHz

T-R Separation (m)	500	1000	1500	2000	2500	3000	3500
Measured L_{50} (dB)	130.00	137.00	141.00	143.00	150.00	166.00	170.00
Predicted L_{50} (dB)	87.00	97.00	106.00	109.00	112.00	115.00	116.00
Difference (dB)	-43.00	-40.00	-35.00	-34.00	-38.00	-51.00	-54.00

Table 4.5.7: Comparison of Measurements and Prediction using Free-Space Model – Samaru Road– Southward of BS (MTN Network) ; f_c = 900 MHz

T-R Separation (m)	500	1000	1500	2000	2500	3000	3500
Measured P_R (dBm)	-68.00	-78.00	-85.33	-92.00	-98.67	-102.67	-105.33
Predicted P_R (dBm)	-21.33	-27.33	-30.67	-33.33	-36.00	-37.33	-38.00
Difference (dB)	46.67	50.67	54.66	58.67	62.67	65.34	67.33

Table 4.5.8: Comparison of Measurements and Prediction using Hata Model – Samaru Road– Southward of BS (MTN Network) ; f_c = 900 MHz

T-R Separation (m)	500	1000	1500	2000	2500	3000	3500
Measured L_{50} (dB)	130.00	142.00	147.00	153.50	161.50	165.00	168.00
Predicted L_{50} (dB)	87.00	97.00	106.00	109.00	112.00	115.00	116.00
Difference (dB)	-43.00	-45.00	-41.00	-44.50	-49.50	-50.00	-52.00

Table 4.5.9: Comparison of Measurements and Prediction using Free-Space Model – Kaduna Road (GLO Network); f_c = 900 MHz

T-R Separation (m)	500	1000	1500	2000	2500
Measured P_R (dBm)	-73.00	-78.00	-87.33	-84.67	-100.00
Predicted P_R (dBm)	-21.11	-26.67	-30.57	-33.06	-35.56
Difference (dBm)	51.89	51.33	56.76	51.61	64.44

Table 4.5.10: Comparison of Measurements and Prediction using Hata Model – Kaduna Road (GLO Network); f_c = 900 MHz

T-R Separation (m)	500	1000	1500	2000	2500
Measured L_{50} (dB)	137.50	143.00	150.00	148.50	165.00
Predicted L_{50} (dB)	87.50	98.00	104.00	108.00	112.00
Difference (dB)	-50.00	-45.00	-46.00	-40.50	-53.00

Table 4.5.11: Comparison of Measurements and Prediction using Free-Space Model – Kano Road (GLO Network); f_c = 900 MHz

T-R Separation (m)	500	1000	1500	2000	2500
Measured P_R (dBm)	-68.00	-81.00	-82.67	-77.33	-98.67
Predicted P_R (dBm)	-21.11	-26.67	-30.57	-33.06	-35.56
Difference (dBm)	46.89	54.33	52.10	44.27	63.11

Table 4.5.12: Comparison of Measurements and Prediction using Hata Model – Kano Road (GLO Network); f_c = 900 MHz

T-R Separation (m)	500	1000	1500	2000	2500
Measured L_{50} (dB)	132.50	143.33	146.67	142.33	162.00
Predicted L_{50} (dB)	87.50	98.00	104.00	108.00	112.00
Difference (dB)	-45.00	-45.33	-42.67	-34.33	-50.00

Table 4.5.13: Comparison of Measurements and Prediction using Free-Space Model – Samaru Road –Eastward of BS (GLO Network) ; f_c = 900 MHz

T-R Separation (m)	500	1000	1500	2000	2500
Measured P_R (dBm)	-70.00	-78.89	-81.11	-85.56	-92.22
Predicted P_R (dBm)	-21.11	-26.67	-30.57	-33.06	-35.56
Difference (dBm)	48.89	52.22	50.54	52.50	56.66

Table 4.5.14: Comparison of Measurements and Hata Model – Samaru Road – Eastward of BS (GLO Network) ; f_c = 900 MHz

T-R Separation (m)	500	1000	1500	2000	2500
Measured L_{50} (dB)	134.00	144.00	146.00	150.00	156.00
Predicted L_{50} (dB)	89.00	100.00	106.00	110.00	114.00
Difference (dB)	-45.00	-44.00	-40.00	-40.00	-42.00

Table 4.5.15: Comparison of Measurements and Free-Space Model – Samaru Road – Southward of BS (GLO Network); f_c = 900 MHz

T-R Separation (m)	500	1000	1500	2000	2500
Measured P_R (dBm)	-74.67	-68.67	-73.33	-78.67	-99.00
Predicted P_R (dBm)	-21.11	-26.67	-30.57	-33.06	-35.56
Difference (dBm)	53.56	42.00	42.76	45.61	63.44

Table 4.5.16: Comparison of Measurements and Prediction using Hata Model – Samaru Road –Southward of BS (GLO Network); f_c = 900 MHz

T-R Separation (m)	500	1000	1500	2000	2500
Measured L_{50} (dB)	139.00	131.50	138.00	142.50	164.00
Predicted L_{50} (dB)	89.00	100.00	106.00	110.00	114.00
Difference (dB)	-50.00	-31.50	-32.00	-32.50	-50.00

Table 4.5.17: Comparison of Measurements and Prediction using Modified Two-Ray Model within the Engineering Complex; f_c = 900 MHz

Receiver Locations	P1	P2	P3	P4	P5	P6	P7
Measured PR (dBm)	-69.00	-75.35	-78.02	-82.27	-85.13	-82.46	-89.25
Predicted PR (dBm)	-56.37	-78.00	-76.76	-74.69	-72.24	-70.47	-69.41
Difference (dBm)	12.63	-2.65	1.26	7.58	12.89	11.99	19.84

THE C PROGRAM CODE

```
# include<stdio.h>
# include<math.h>
# include<conio.h>
int main(void)
{
        int e, location;
        float PaLenOne, PaLenTwo, DirectPath, PathLength, dist,Rad,RadOne,RadTwo,
        RadThree;
        float Ang,AngOne,AngTwo, AngThree,PI;
        double g, q, r, s,k,x,a,b,c,m;
        char ch;
        e=6,PI=3.141592654;

        /* This segment computes the Received Signal Power OR Path loss in Scenario 1*/
        printf("Do you want to compute the Received Signal Power and Path loss  \n");
        printf("for the First Scenario or the Other scenario?");
        printf("\n Enter the first letter of your choice:");
        ch=getche();
        if(ch=='F')
        {printf("\n Do you want to use the Modified Semi-empirical or the Modified Hata
                        model?");
         printf("\n Enter the First letter of your choice:");
         ch=getche();
         if(ch=='S')
        {printf("\n Enter the T-R separation distance in m:");
         scanf("%f",&dist);
    printf("\nThe Received Signal Power, in dBm, for freq=900 MHz and freq=1800 MHz
    are:\n\n    %.2f,%.2f",34.48-20*log10(dist)-54.73,34.48-20*log10(dist)-54.73-6.02);}
         printf("\n\n");
         if(ch=='H')
        {printf("\n Enter the T-R separation distance in Km:");
         scanf("%f",&dist);
         printf("\n The Path loss,in dB,for freq=900 MHz and freq=1800 MHz are: \n\n
                  %.2f,%.2f", 98.74+35.14*log10(dist)+42.81,98.74+35.14*
                  log10(dist)+42.81+4.47);}
         printf("\n\n");
        }

         /* This segment computes the Received Signal Power in Scenario 2*/
        else if(ch=='O')
         {printf("\n Enter the Receiver location:");
         scanf("%d",&location);
         switch(location)

        {case 1:printf("Enter the angle of incidence for location 1:");
                  scanf("%f",&Ang);
```

```
        printf("Enter the total pathlength along the reflection path:");
        scanf("%f",&PathLength);
        printf("Enter the DirectPath length for location 1:");
        scanf("%f",&DirectPath);

        Rad = Ang*PI/180;
        g = fabs(sqrt(e-cos(Rad)*cos(Rad)));
        k = (sin(Rad)-g)/(sin(Rad)+g);
        x = fabs(k);

        printf("\n");
        printf("The Received Signal Power at location 1,in dBm, is: %.2f",

        65.76+20*log10(0.02653*(1/DirectPath))+65.76+20*log10(0.02653*
        (1/PathLength)*x)-12.60);
        printf("\n\n");
        break;
case 2:printf("Enter the angle of incidence for location 2 along path 1:");
        scanf("%f",&Ang);
        printf("Enter the total PathLength for location 2 along path 1:");
        scanf("%f",&PaLenOne);
        printf("Enter the total PathLength for location 2 along path 2:");
        scanf("%f",&PaLenTwo);

        Rad = Ang*PI/180;
        g = fabs(sqrt(e-cos(Rad)*cos(Rad)));
        k = (sin(Rad)-g)/(sin(Rad)+g);
        x = fabs(k);

        printf("Enter the first angle of incidence for location 2 along path 2:");
        scanf("%f",&AngOne);

        RadOne = AngOne*PI/180;
        q = fabs(sqrt(e-cos(RadOne)*cos(RadOne)));
        a = (sin(RadOne)-q)/(sin(RadOne)+q);

        printf("Enter the second angle of incidence for location 2 along path 2:");
        scanf("%f",&AngTwo);

        RadTwo = AngTwo*PI/180;
        r = fabs(sqrt(e-cos(RadTwo)*cos(RadTwo)));
        b = (sin(RadTwo)-r)/(sin(RadTwo)+r);

        printf("Enter the third angle of incidence for location 2 along path 2:");
        scanf("%f",&AngThree);
```

```
        RadThree = AngThree*PI/180;
        s = fabs(sqrt(e-cos(RadThree)*cos(RadThree)));
        c = (sin(RadThree)-s)/(sin(RadThree)+s);
        m = fabs(a*b*c);

        printf("\n");
        printf("The Received Signal Power at location 2,in dBm, is: %.2f",
                65.76+20*log10(0.02653*x/PaLenOne)+65.76+20*log10(0.02653*
                m/PaLenTwo)-12.60);
        printf("\n\n");
        break;
case 3:printf("Enter the angle of incidence for location 3 along path 1:");
        scanf("%f",&Ang);
        printf("Enter the total PathLength for location 3 along path 1:");
        scanf("%f",&PaLenOne);
        printf("Enter the total PathLength for location 3 along path 2:");
        scanf("%f",&PaLenTwo);

        Rad = Ang*PI/180;
        g = fabs(sqrt(e-cos(Rad)*cos(Rad)));
        k = (sin(Rad)-g)/(sin(Rad)+g);
        x = fabs(k);

        printf("Enter the first angle of incidence for location 3 along path 2:");
        scanf("%f",&AngOne);

        RadOne = AngOne*PI/180;
        q = fabs(sqrt(e-cos(RadOne)*cos(RadOne)));
        a = (sin(RadOne)-q)/(sin(RadOne)+q);

        printf("Enter the second angle of incidence for location 3 along path 2:");
        scanf("%f",&AngTwo);

        RadTwo = AngTwo*PI/180;
        r = fabs(sqrt(e-cos(RadTwo)*cos(RadTwo)));
        b = (sin(RadTwo)-r)/(sin(RadTwo)+r;

        printf("Enter the third angle of incidence for location 3 along path 2:");
        scanf("%f",&AngThree);

        RadThree = AngThree*PI/180;
        s = fabs(sqrt(e-cos(RadThree)*cos(RadThree)));
        c = (sin(RadThree)-s)/(sin(RadThree)+s);
        m = fabs(a*b*c);

        printf("\n");
```

```
        printf("The Received Signal Power at location 3,in dBm, is: %.2f",
                 65.76+20*log10(0.02653*x/PaLenOne)+65.76+20*log10(0.02653*
                m/PaLenTwo)-12.60);
        printf("\n\n");
        break;
case 4:printf("Enter the angle of incidence for location 4 along path 1:");
        scanf("%f",&Ang);
        printf("Enter the total PathLength for location 4 along path 1:");
        scanf("%f",&PaLenOne);
        printf("Enter the total PathLength for location 4 along path 2:");
        scanf("%f",&PaLenTwo);

        Rad = Ang*PI/180;
        g = fabs(sqrt(e-cos(Rad)*cos(Rad)));
        k = (sin(Rad)-g)/(sin(Rad)+g);
        x = fabs(k);

        printf("Enter the first angle of incidence for location 4 along path 2:");
        scanf("%f",&AngOne);

        RadOne = AngOne*PI/180;
        q = fabs(sqrt(e-cos(RadOne)*cos(RadOne)));
        a = (sin(RadOne)-q)/(sin(RadOne)+q);

        printf("Enter the second angle of incidence for location 4 along path 2:");
        scanf("%f",&AngTwo);

        RadTwo = AngTwo*PI/180;
        r = fabs(sqrt(e-cos(RadTwo)*cos(RadTwo)));
        b = (sin(RadTwo)-r)/(sin(RadTwo)+r);

        printf("Enter the third angle of incidence for location 4 along path 2:");
        scanf("%f",&AngThree);

        RadThree = AngThree*PI/180;
        s = fabs(sqrt(e-cos(RadThree)*cos(RadThree)));
        c = (sin(RadThree)-s)/(sin(RadThree)+s);
        m = fabs(a*b*c);

        printf("\n");
        printf("The Received Signal Power at location 4,in dBm, is: %.2f",
                 65.76+20*log10(0.02653*x/PaLenOne)+65.76+20*log10(0.02653*
                 m/PaLenTwo)-12.60);
        printf("\n\n");
        break;
case 5:printf("Enter the angle of incidence for location 5 along path 1:");
```

```
        scanf("%f",&Ang);
        printf("Enter the total PathLength for location 5 along path 1:");
        scanf("%f",&PaLenOne);
        printf("Enter the total PathLength for location 5 along path 2:");
        scanf("%f",&PaLenTwo);

        Rad = Ang*PI/180;
        g = fabs(sqrt(e-cos(Rad)*cos(Rad)));
        k = (sin(Rad)-g)/(sin(Rad)+g);
        x = fabs(k);

        printf("Enter the first angle of incidence for location 5 along path 2:");
        scanf("%f",&AngOne);

        RadOne = AngOne*PI/180;
        q = fabs(sqrt(e-cos(RadOne)*cos(RadOne)));
        a = (sin(RadOne)-q)/(sin(RadOne)+q);

        printf("Enter the second angle of incidence for location 5 along path 2:");
        scanf("%f",&AngTwo);

        RadTwo = AngTwo*PI/180;
        r = fabs(sqrt(e-cos(RadTwo)*cos(RadTwo)));
        b = (sin(RadTwo)-r)/(sin(RadTwo)+r);

        printf("Enter the third angle of incidence for location 5 along path 2:");
        scanf("%f",&AngThree);

        RadThree = AngThree*PI/180;
        s = fabs(sqrt(e-cos(RadThree)*cos(RadThree)));
        c = (sin(RadThree)-s)/(sin(RadThree)+s);
        m = fabs(a*b*c);

        printf("\n");
        printf("The Received Signal Power at location 5,in dBm, is: %.2f",
                65.76+20*log10(0.02653*x/PaLenOne)+65.76+20*log10(0.02653*
                m/PaLenTwo)-12.60);
        printf("\n\n");
        break;
case 6:printf("Enter the angle of incidence for location 6 along path 1:");
        scanf("%f",&Ang);
        printf("Enter the total PathLength for location 6 along path 1:");
        scanf("%f",&PaLenOne);
        printf("Enter the total PathLength for location 6 along path 2:");
        scanf("%f",&PaLenTwo);
```

```
        Rad = Ang*PI/180;
        g = fabs(sqrt(e-cos(Rad)*cos(Rad)));
        k = (sin(Rad)-g)/(sin(Rad)+g);
        x = fabs(k);

        printf("Enter the first angle of incidence for location 6 along path 2:");
        scanf("%f",&AngOne);

        RadOne = AngOne*PI/180;
        q = fabs(sqrt(e-cos(RadOne)*cos(RadOne)));
        a = (sin(RadOne)-q)/(sin(RadOne)+q);

        printf("Enter the second angle of incidence for location 6 along path 2:");
        scanf("%f",&AngTwo);

        RadTwo = AngTwo*PI/180;
        r = fabs(sqrt(e-cos(RadTwo)*cos(RadTwo)));
        b = (sin(RadTwo)-r)/(sin(RadTwo)+r);

        printf("Enter the third angle of incidence for location 6 along path 2:");
        scanf("%f",&AngThree);

        RadThree = AngThree*PI/180;
        s = fabs(sqrt(e-cos(RadThree)*cos(RadThree)));
        c = (sin(RadThree)-s)/(sin(RadThree)+s);
        m = fabs(a*b*c);

        printf("\n");
        printf("The Received Signal Power at location 6,in dBm, is: %.2f",
                65.76+20*log10(0.02653*x/PaLenOne)+65.76+20*log10(0.02653*
                m/PaLenTwo)-12.60);
        printf("\n\n");
        break;
case 7:printf("Enter the angle of incidence for location 7 along path 1:");
        scanf("%f",&Ang);
        printf("Enter the total PathLength for location 7 along path 1:");
        scanf("%f",&PaLenOne);
        printf("Enter the total PathLength for location 7 along path 2:");
        scanf("%f",&PaLenTwo);

        Rad = Ang*PI/180;
        g = fabs(sqrt(e-cos(Rad)*cos(Rad)));
        k = (sin(Rad)-g)/(sin(Rad)+g);
        x = fabs(k);

        printf("Enter the first angle of incidence for location 7 along path 2:");
```

```
            scanf("%f",&AngOne);

            RadOne = AngOne*PI/180;
            q = fabs(sqrt(e-cos(RadOne)*cos(RadOne)));
            a = (sin(RadOne)-q)/(sin(RadOne)+q);

            printf("Enter the second angle of incidence for location 7 along path 2:");
            scanf("%f",&AngTwo);

            RadTwo = AngTwo*PI/180;
            r = fabs(sqrt(e-cos(RadTwo)*cos(RadTwo)));
            b = (sin(RadTwo)-r)/(sin(RadTwo)+r);

            printf("Enter the third angle of incidence for location 7 along path 2:");
            scanf("%f",&AngThree);

            RadThree = AngThree*PI/180;
            s = fabs(sqrt(e-cos(RadThree)*cos(RadThree)));
            c = (sin(RadThree)-s)/(sin(RadThree)+s);
            m = fabs(a*b*c);

            printf("\n");

            printf("The Received Signal Power at location 7,in dBm, is: %.2f",

      65.76+20*log10(0.02653*x/PaLenOne)+65.76+20*log10(0.02653*

                  m/PaLenTwo)-12.60);

            printf("\n\n");
            break;
            default:printf("Undefined location %d please",location);
            printf("\n\n");
             }
       }
            return 0;
}
```